microRNAs play a role in human embryonic stem cell differentiation into endothelial cells

A thesis submitted by

Zhenling Luo

In fulfillment of the requirements for the degree of Doctor of Philosophy

July 2011

Supervisors:

Professor Wen Wang (Queen Mary, University of London, School of Engineering and Materials Science)

Professor Qingbo Xu, Dr. Qingzhong Xiao (King's College London, University of London, School of Medicine, Cardiovascular division)

ABSTRACT

The past recent years have seen a surge of evidence demonstrating the regulation of microRNAs (miRNAs) in a myriad of vascular biology events such as cardiogenesis. Nevertheless, the missing miRNA-link in controlling pluripotent human embryonic stem cell (hESC) fate in differentiation towards the endothelial lineage is currently undiscovered. Main objectives in this project are determining which miRNAs are involved in endothelial lineage differentiation from hESCs and the further delineation in their underlying mechanisms.

Firstly, undifferentiated hESCs were cultured in differentiating conditions to derive endothelial (ECs) and smooth muscle cells (SMCs). hESC-derived ECs express specific EC markers such as PECAM/CD31, eNOS, and vWF, while hESC-derived SMCs express specific SMC markers such as SMA and SMMHC II. Both hESC-derived cells also displayed functional characteristics upon functional analyses.

Next, five potential miRNAs involved in embryonic EC development were determined and selected from the miRNA array expression profile in differentiating hESCs. Using loss- and gain-of-function gene experiments, it was demonstrated that both miR-150 and miR-200c played an important role in EC differentiation from hESCs. However, miR-1915, 141 and 205 did not display such functions. In addition, epithelial-to-mesenchymal transition (EMT)-activator ZEB1/TCF8 was further identified as an important mRNA target for miR-150* and 200c. Importantly, it was also demonstrated that miR-150* and miR-200c were both involved in the vasculogenesis of *in vivo* chick embryos.

These findings may suggest that during hESCs differentiation, an increase of miR-200c expression contribute to the decline or repression of EMT process. Meanwhile, mir-150* also contributes to the differentiation of hESCs, resulting in the formation of more

differentiated, senescence and less proliferative cells or in this case, mature vascular ECs. These findings illustrate that miR-150* and 200c can regulate the development of ECs from hESCs, providing new targets for modulating vascular formation and creating novel clinical therapies in future cardiovascular disease applications.

Declaration

I, PhD candidate Zhenling Luo, confirm that the majority of the experimental work presented here in this thesis were carried out by me. These include the culture, maintenence and differentiation of all hESCs, molecular biology and protein work, function tests and immunostainings. Apart from experiments pertaining to flow cytometry, the cloning of ZEB1/TCF8 3'UTR and luciferase activity assays, were carried out by Dr Qingzhong Xiao. CD146-positive cell sorting was carried out by a member of staff at the Rayne Institute, Denmark Hill, King's College London. Dr Yanhua Hu performed the *in vivo* matrigel plug implantation into SCID mice and Mr Zhongyi Zhang prepared and stained tissue sections with H&E. Lastly, the *in vivo* transfection of miRNA inhibitors into developing chick embryos using Chorioallantoic membrane assay was performed by Gang Wang.

Acknowlegements

I wish to thank Professor Wen Wang and Professor Qingbo Xu for their invaluable advice and also in giving me this unique opportunity to work in this research field. I also wish to extend my gratitude to Dr Qingzhong Xiao for his daily supervision, crucial guidance, help and advice given throughout the research. I am grateful to all those who have helped me progress in my work. Last but not least, to my family and all my friends who had cheered me on throughout these years. This work was supported by grants from the British Heart Foundation and Oak Foundation.

Table of Contents

List of Figures

List of Tables

List of Abbreviations and Acronyms

2D	2-dimensional
3’UTR	3’untranslated region
AGO	Argonaute family protein
AP	Alkaline phosphatase
ANOVA	One-way analysis of variance
CD144/VECAD	Cluster of Differentiation 144/Vascular Endothelial-Cadherin
CD31/PECAM	Cluster of Differentiation molecule 31 /Platelet Endothelial Cell Adhesion Molecule-1
cDNA	Complementary Deoxyribonucleic acid
Chrdl-1	Chordin-like 1
CM	Choroallantoic membrane
DAPI	4,6-diamidino-2-phenylindole
Dcx	Doublecortin
DGCR8	DiGeorge syndrome critical region gene 8
DH20	Distilled water
Dil-Ac-LDL	Dil-labeled acetylated low density lipoprotein
DMSO	Dimethyl sulfoxide
dNTPs	2'-deoxynucleoside 5'-triphosphate
D-PBS	Phosphate Buffered Saline
EB	Embryoid body
EC	Endothelial Cell
EDTA	Ethylenediaminetetraacetic acid

Egfl-7	Epidermal growth factor like-7
EGM2	Endothelial growth medium
eNOS	Endothelial Nitric Oxide Synthase
FACS	Fluorescence-activated cell sorter analysis
FGF	Fibroblast growth factor
FITC	Fluorescein isothiocyanate
Flk-1	Fetal Liver Kinase-1
GAPDH	Glyceraldehyde 3-phosphate dehydrogenase
HH	Hamburger and Hamilton
hbFGF	human basic Fibroblast Growth Factor-2
hESCs	Human embryonic stem cells
hiPSC	Human iPSCs
HUVECS	Human Umbilical Vein Endothelial Cells
HCL	Hydrochloric acid
miRtrons	Intronic miRNAs
iPSC	Induced pluripotent stem cells
Ig	Immunoglobulin
IGF-1	Insulin-like growth factor 1
IVF	In-vitro fertilisation
KCL	Potassium chloride
Kdr	Kinase-inserted domain containing receptor
KLF4	Kruppel-like factor 4
MACS	Magnetic activated cell sorting
MEF	Mouse Embryonic Fibroblast
mESCs	Mouse embryonic stem cells

MgCl2	Magnesium Chloride
MHE	Mesodermal hematoendothelial
miR-141	MicroRNA-141
miR-150*	MicroRNA-150*
miR-200c	MicroRNA-200c
miR-205	MicroRNA-205
miR-1915	MicroRNA-1915
miRtrons	Intronic miRNAs
miRNAs	microRNAs
NaOH	Sodium hydroxide
NC	Negative control
Oct3/4	Octamer 3/4
PECAM-1	Platelet endothelial cell adhesion molecule-1
PCR	Polymerase Chain Reaction
PDGFR-β	Platelet-derived growth factor receptor-beta
PIK3R2/p85-beta	phosphoinositol-3 kinase regulatory subunit 2
pri-miRNAs	Pimary mRNA transcript
RISC	Ribonucleic acid induced silencing complex
RLU	Relative luciferase unit
RT-qPCR	Real-time quantitative polymerase chain reaction
SCID	Severe combined immunodeficient
SDS	Sodium dodecyl dulfate
SCP1	Small C-terminal domain phosphatase 1
SEM	Standard error of the mean
SM22α	Smooth Muscle 22-alpha

SMA	Smooth muscle alpha-Actin
SM-MHC II	Smooth muscle myosin heavy chain II
Sox 2	SRY (sex determining region Y)-box containing gene 2
SPRED1	Sprouty-related protein
SSEA1	Stage-specific embryonic antigen-1
SSEA4	Stage-specific embryonic antigen-4
SEM	Standard error of the mean
TRBP	human immunodeficiency virus Transactivating response RNA-binding protein
TRITC	Tetramethyl Rhodamine Iso-Thiocyanate
UEA-I	Ulex Europaeus-I
UTR	Untranslated region
VE-cadherin	Vascular Endothelial Cadherin
VEGFR2	Vascular endothelial growth factor receptor 2
VSMCs	Vascular smooth muscle cells
VLA-2	Very late activation antigen 2
VLA-3	Very late activation antigen 3
VSMCs	Vascular smooth muscle cells
ZEB1/TCF8	human Zinc finger E-box-binding homeobox 1/ transcription factor 8

CHAPTER 1

CHAPTER 1

Introduction

1.1 The Vascular system

1.1.1 The physiology and anatomy of the blood vessels

The human vascular system carries out vital transport of nutrients and oxygen to tissues as well as the removal of metabolic waste products. The vascular system comprises of an arterial, a venous, a capillary and a lymphatic compartment that maintains an immune barrier against foreign pathogens.

In the human body, the circulatory system is divided into the pulmonary and systemic circulation. The pulmonary circulation carries deoxygenated blood from the heart to the lungs via the pulmonary arteries and returns oxygenated blood back to the heart through the pulmonary veins. Meanwhile, the systemic circulation carries oxygenated blood away from the heart to the whole body. There are two subtypes of systemic arteries which can be grouped into the muscular and elastic category. The elastic arteries generally have a large lumen with thin walls while the muscular arteries have a smaller lumen and thicker wall. Systemic arteries deliver blood to the arterioles which help regulate blood pressure by contracting their smooth muscle walls. Following which, oxygen-rich blood flows into the capillaries where a fast exchange of nutrients and gases ensues. The thin walls and large surface area of the single endothelial-celled capillaries is a perfect environment for diffusion to occur. Blood returns from the body back to the heart through the low-pressured veins (Fig.1A).

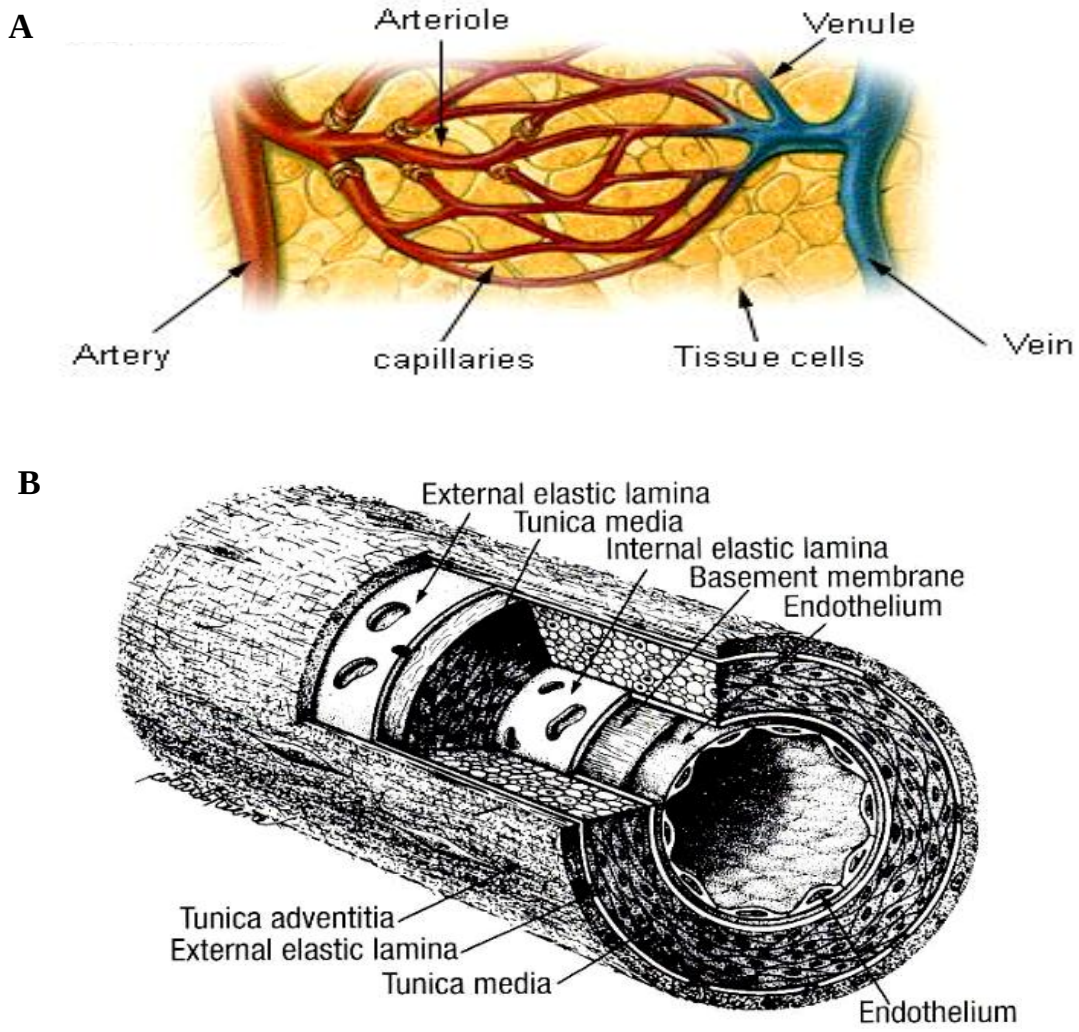

Fig. 1. Blood circulation in the veins and arteries

(A) In the systemic circulation, oxygenated blood is pumped through the heart's aorta which then branches into many smaller arterioles which run throughout the body. Gaseous and metabolic exchange occurs in the capillaries which gather to form small venules. Deoxygenated blood is pumped back into the right atrium of the heart through the vena cava veins [1]. (B) A cross-section of an artery showing the three main layers consisting of the innermost tunica intima, the thick tunica media, and the outermost adventitia [2].

There are three layers in the structure of arteries which are namely the tunica intima, tunica media and tunica adventitia (Fig.1B). The intima is the innermost layer coating the lumen layer and consists of two further layers; the endothelium and a subendothelial layer. Endothelium is a single layer of endothelial cells (ECs) that line the inner lumen of the vessel. As these cells are constantly in need of replacement, the basal lamina that the cells are supported on has a high turn-over rate of 1% daily [3]. Coating the endothelium is the subendothelial layer that contains delicate loose connective tissues with some smooth muscle cells. Separating the subendothelial from the media layer, is an internal elastic lamina made of elastin and fibrous tissue. Concentric layers of vascular smooth muscle cells that synthesize extracellular matrix are arranged helically in the tunica media together with fibrous and elastic tissues. The external elastic lamina separates the media from the outermost adventitia layer which contains elastic and Collagen Type I fibers that form loose connective tissue.

Arteries have thicker walls as compared to veins which are generally thin-walled, contain less elastins and have low distending pressures. Thus veins are stiffer than arteries. There are several different types of arteries depending on their sizes and the extent of the medial layer (Fig.2). In order of descending artery size are the large elastic arteries, smaller muscular arteries, and arterioles. Larger elastic arteries, such as the aorta, help to cushion stroke volume, decrease ventricular work and maintain pressure during diastole [3]. The smaller and more muscular arteries aid in regulating peripheral resistance and blood flow by changing their vascular smooth muscle tone which leads to a change in lumen size.

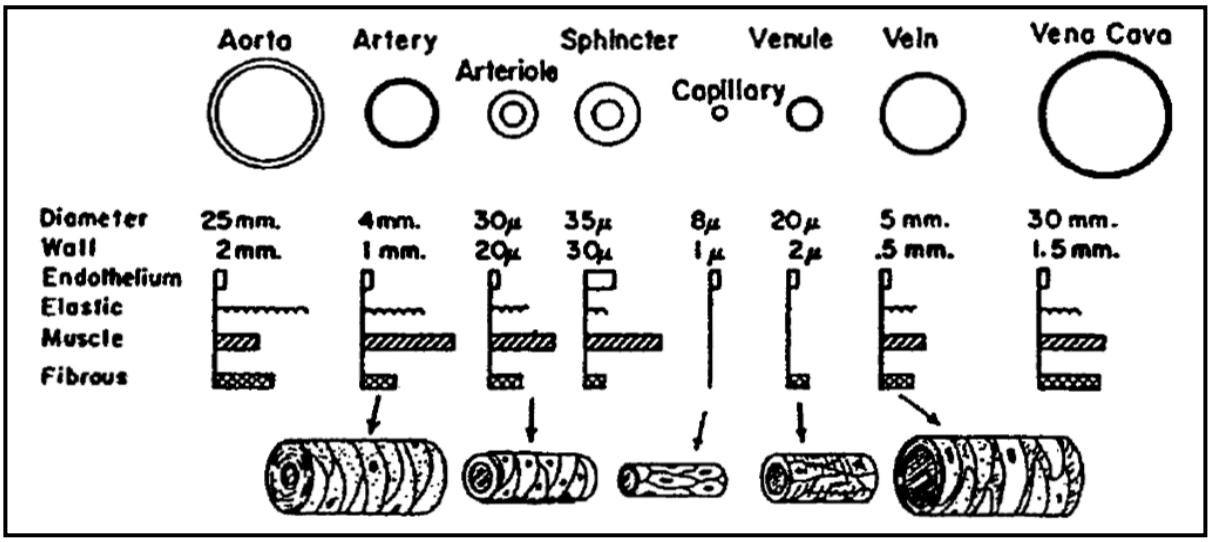

Fig. 2. The different composition and relative sizes of endothelium, elastic, smooth muscle and fibrous tissues in each type of vessel

Larger arteries contain more elastic and fibrous connective tissue, whereas smaller arteries have more smooth muscle in the tunica media. Smooth muscle content in the arteries is more than that of veins. Note that capillaries are the smallest vessel of the system which lack smooth muscle cells [4].

1.1.2 The major building blocks of the blood vessel

1.1.2.1 Endothelial physiology

The endothelium comprises of a thin monolayer of ECs lining the inside of blood vessels in the entire circulatory and organ systems. While the subendothelium that coats the endothelium provides elasticity and support to the structural integrity of the vessels, ECs are the building blocks of blood vessels and a vital inferface between the circulating blood stream and the body tissues. In an adult human body, approximately 10^{12} ECs constitute the inside of the blood vessel lining and cover a total surface area of roughly (5000 m^2) [5(Ref number 5)].

1.1.2.1a Synthesis of Subendothelial Components

ECs are situated on the underlying subendothelium that contains an array of different matrix proteins such as collagen, laminin, thrombospondin, fibronectin, elastin, glycoso-aminoglycans and von Willebrand Factor (vWF) [6, 7] . Collagen is a major constituent of the subendothelium and is capable of either promoting or inhibiting endothelial cell growth. *In-vitro* culture assays have shown that most of these collagens are secreted by the ECs into the culture medium or into their underlying extracellular matrix [8, 9]. Moreover, ECs express Very late activation antigen 2 (VLA-2) and Very late activation antigen 3 (VLA-3) integrins which act as attachment sites for binding collagen and other matrix molecules. In addition, the glycoprotein laminin which is secreted by ECs into the subendothelium, interacts with both integrins VLA-2 and VLA-3. Tissue culture studies have shown that laminin promotes endothelial cell adhesion, growth and tubulogenesis [10]. Also involved in the adhesion function of ECs are fibronectin and thrombospondin. However, both can induce detachment of ECs and facilitate cell movement. Both proteins are produced by ECs and exist as fibrillar meshworks in low amounts in the subendothelium [11, 12].

Elastin is another matrix protein found in the subendothelium and synthesised initially as a single chain soluble protein, the tropoelastin. After secretion, multiple tropoelastin molecules covalently bind together with crosslinking amino acids, desmosine and isodesmosine to form elastin [13]. Last but not least, glycosoaminoglycans can be found in both ECs and subendothelium. The EC membrane contains predominantly heparan sulfate whereas the subendothelium contains members of the glycosoaminoglycans such as heparan sulfate, dermatan sulpfate and chondroitin sulpfate [14, 15]. Heparan sulfate binds to collagen and is involved in EC attachment initiation. It also plays a role in the anticoagulant property of ECs with the activation of anti-thrombin III. Providing a non-thrombogenic surface which inhibits platelet adhesion, blood clot and facilitates blood flow**,** is a vital physiological role of the endothelium.

Nevertheless, when an injury agitates the endothelium and hence exposing the subendothelial, a cascade of coagulation activity follows to stop bleeding. Between these two anticoagulant and procoagulant states, a dynamic equilibrium exists that enables the injured endothelium to return back to its normal quiescent state once the procoagulant stimulant disperse [16]. During the activation of the coagulation cascade, platelets are attracted to the site of injury and soon degranulate. Platelets aggregate in the presence of the exposed subendothelium's collagen types IV, V and microfibrils [17]. It is believed that platelets adhere to the subendothelium via their membrane receptors specific for vWF [18]. ECs synthesise and secrete functionally active large molecular weight vWF multimers which actually consist of an aggregation of smaller 220 kDa vWF subunits [19]. Functional vWF is released from Weibel-Palade bodies of the ECs by thrombin during injury. It can be bound to collagens in the extracellular matrix of the subendothelium or by receptors on the ECs.

Apart from this hemostasis role, ECs also contribute to numerous metabolic functions including thrombolysis, vasomotor property, antigen presentation and synthesis of growth factors and adhesion molecules.

1.1.2.1b Endothelial Derived Growth Factors

Not only do ECs produce a variety of extracellular matrix proteins, they also secrete several regulatory factors such as platelet derived growth factor (PDGF), insulin-like growth factor 1 (IGF-1) and fibroblast growth factor (FGF) which promote cell growth [20, 21]. Other than endothelial cells, smooth muscle cells also secrete PDGF which acts as a major mitogen and chemoattractant [22, 23]. PDGF is a well characterised growth factor which plays a significant role in angiogenesis [24]. It is a dimeric glycoprotein containing four polypeptide chains A, B, C and D which results in the formation of five different dimeric isoforms, the homodimers (AA, BB, CC, DD) and heterodimers (AB). PDGF produced from ECs could stimulate the proliferation of underlying smooth muscle cells [21, 25]. In addition, there seems to be a synergistic relationship between PDGF and IGF-1 whereby PDGF can induce the mitogen IGF-1 expression in ECs which in turn promotes smooth muscle cell growth [26]. Other endothelium derived factors such as endothelin, angiotensin II, nitric oxide, and

oxygen free radicals have also shown to be mitogenic for both endothelial and smooth muscle cells.

1.1.2.1c Adhesion Molecules on Endothelial Cells

ECs express adhesion molecules on their surfaces that aid in cell-cell interactions and adhesion for vessel formation. EC-cell interactions are vital for the maintenance of vascular integrity. Platelet endothelial cell adhesion molecule-1 (PECAM-1) or known as Cluster of Differentiation molecule 31 (CD31), is expressed by all ECs in the adult, whereby its expression is largely concentrated at junctions between adjacent cells [27]. Belonging to the immunoglobulin (Ig) gene superfamily, PECAM-1 is composed of 6 extracellular Ig folds, a transmembrane and a cytoplasmic domain. It has a molecular weight of 130 kDa and is differentially glycosylated involving N-linked and O-linked sites. PECAM-1 promotes cell-cell adhesion at lateral junctions between adjacent ECs [28] by homophilic binding of its ligand [29, 30]. The adhesion of PECAM-1 has been associated with the maintenance of a vascular permeability barrier and migration of endothelial cells, monocytes or neutrophils [31, 32]. Moreover, it was demonstrated that PECAM-1 is involved in the formation of new blood vessels in angiogenesis. Using polyclonal and monoclonal antibodies directed to PECAM-1, resulted in the inhibition of *in-vitro* tube formation [33]. Another EC adhesion molecule, Vascular Endothelial Cadherin (VE-cadherin; also known as cadherin 5) is of dominant importance as an adhesive component of endothelial-specific adherent junctions (AJs). Blocking the adhesive function of VE-cadherin with antibodies has shown to dissociate EC layers [34].

Collectively, EC junctions are a complex network of adhesion proteins that are linked to intracellular cytoskeletal and signalling molecules. Moreover, modulation of the matrix in the subendothelium allows the endothelium to control the activity of the vessel wall structure. This builds a direct relationship between the endothelium and rest of the vasculature system including the underlying vascular smooth muscle cells.

1.1.2.2 Smooth muscle physiology

Smooth muscle is an involuntary non-striated muscle which can be found in different locations of the human body such as the tunica media layer of large and small arteries and veins, the bladder and uterus. In this context, smooth muscle cells residing in the blood vessels are of interest and will be termed vascular smooth muscle cells (VSMCs).

Depending on the type of vascular bed, VSMCs or pericytes cover the outside of the endothelium lined blood vessels, protecting the fragile channels from rupture. VSMCs also contribute to the contraction and relaxation of the vessels, thus altering the luminal diameter to maintain an appropriate blood pressure and control blood flow. VSMCs exhibit an extraordinary capacity to undergo rather profound and reversible phenotypic plasticity or otherwise known as phenotypic modulation at different developmental stages [35]. Unlike other muscle cells, VSMCs are not terminally differentiated in adult organisms [36]. VMSCs can perform both contractile and synthetic functions which represent the two ends of a spectrum of VSMCs with clearly different morphologies, proliferation and migration rates as well as the expression of different protein markers. Generally, contractile VSMCs have an elongated, spindle-shaped morphology whereas synthetic VSMCs have a less elongated and cobblestone morphology which is also referred to as epithelioid [37, 38]. Moreover, synthetic VSMCs contain a large quantity of organelles involved in protein synthesis, whereas these are largely superseded by contractile filaments in contractile VSMCs. Furthermore, synthetic VSMCs exhibit higher growth and migratory activities than contractile VSMCs.

During normal vascular development, dedifferentiated VSMCs are exceedingly proliferative and migratory. Being highly synthetic, they also tend to produce extracellular matrix components of the blood vessel wall such as collagen, elastin, and proteoglycans, while concurrently acquiring contractile capabilities. However, once fully developed, VSMCs differentiate into a contractile phenotype to assume the functions required of the mature arterial wall. A point to note is that apart from the norm, VSMCs can also dedifferentiate and re-enter the cell cycle in response to injury such as atherosclerosis, after

angioplasty, stenting, or bypass surgery. During dedifferentiation, there is a decrease in VSMCs contractile markers expression and are highly proliferative [39, 40].

Many of the smooth muscle cell (SMC) markers commonly used to define SMC phenotypes are involved in SMC contractile ability either as a structural component or as a regulator of contraction. Smooth muscle alpha-Actin (SMA) is the first SMC contractile protein isoform identified [41]. In addition, both smooth muscle-myosin heavy chain (SM-MHC) and smoothelin are currently the best markers to define the phenotype of mature contractile SMC. In embryonic mouse studies, SM-MHC expression is SMC-specific and has never been detected in non-SMCs [42]. Smoothelin expression is more sensitive and complements SM-MHC as a contractile SMC marker. As depicted in a cultured porcine VSMCs study, smoothelin was expressed more uniformly and more rapidly downregulated during phenotypic modulation towards a synthetic state [43]. Other contractile associated protein markers currently used to define the phenotype of VSMCs are calmodulin, h-caldesmon, and calponin, a thin filament-associated protein implicated in the regulation of SMC contraction [35].

1.2 Stem cells

Despite its crucial and essential capability, the vascular system is sometimes fraught with numerous pathologies. Cardiovascular diseases such as coronary heart disease (heart attack) and cerebrovascular disease (stroke) are the number one cause of global morbidity and mortality. These diseases share common features such as the loss or impairment of tissue-specific cells resulting in damaged blood vessels, endothelial dysfunction and ischemic tissues. Furthermore, minimally invasive surgery and organ transplantation that have been carried out increasingly over the years can lead to the loss and dysfunction of the endothelium in cases such as angioplasty-induced restenosis, transplant arteriosclerosis and vein bypass graft atherosclerosis. In seek of therapeutic treatments, the use of stem cells in vascular regeneration has gained immense momentum over the years.

Stem cells have the ability to self renew and the capacity to differentiate into different types of specialized cells. There are currently different sources of stem cells and these are mainly

categorised into adult stem cells, embryonic stem cells and induced pluripotent stem cells (iPSC). Adult stem cells are multipotent and partially lineage-commited. These cells are capable of giving rise to only cells of a given germ layer. Although adult stem cells are autologous, as these cells are harvested from the patient themselves for stem cell therapy, and hence there is an absence of an immunologic barrier, these cells are however limited in quantity, replicative capacity and are lineage restricted.

Unlike adult stem cell, embryonic stem cells can differentiate into any cell type or any organ from the three germ layers. Mouse embryonic stem cells (mESCs) were isolated in 1981 from the inner cell mass of the blastocyst by Sir Martin J. Evans and Matthew Kaufman [44] and independently by Gail R. Martin [45]. Their discoveries have contributed immensely to the study and understanding of pluripotency and differentiation of stem cells. At almost more than a decade later, James Thomson *et al*. reported the first derivation of human embryonic stem cell lines [46]. The availability of human embryonic stem cells (hESCs) has revolutionized science by providing the opportunity to develop stem cell-based therapies for human diseases.

More recently in 2006, Yamanaka *et al.* reprogrammed mouse fibroblasts (somatic cells) into iPSCs by overexpressing four transcription factors Oct3/4, Sox2, c-Myc, and Klf4 [47]. In this case, differentiated adult cells were simply 'transformed' into cells with traits similar to pluripotent embryonic stem cells. Not only do these cells display pluripotent markers, other studies have also demonstrated that iPSCs were capable of forming the three germ layers and subsequently differentiating into adult stem cells [48-51]. Since the first discovery of iPSCs, many advances were made to streamline the reprogramming process such as removing the use of c-Myc and Klf4 during reprogramming [51-53] and the addition of small molecules to enhance the reprogramming progress [54, 55].

The advent of iPSCs has made the availability of patient-specific stem cells possible and besides, these cells are easily obtainable as the patient's skin or hair tissues can be used. Furthermore, iPSCs do not have the immunological barrier that exists in cells derived from embryonic stem cells. In addition, human iPSCs (hiPSC) can be derived from patients with

genetic diseases, and the derived disease-specific cell lines can aid in understanding heritable disorders and thus search for new cures [56, 57]. Despite these advantages, there are a number of concerns regarding the use of iPSCs in clinical application. The use of gene manipulation via retroviruses or lentiviruses in deriving iPSCs, increases the risk of inducing oncogenesis [58, 59]. Another cause of concern is that a significant number of hiPSC lines were found with an abnormal expression of imprinted genes [60] and gene expression profiles [48, 61], which were otherwise found to be stable in hESCs. It also seems that there are functional differences observed between differentiated cells derived from hESCs and iPSC. Cells derived from iPSC had a significantly increased apoptosis, severely limited growth, expansion capability and an early cellular senescence [62]. Although there may be one day that hiPSCs will provide the same theurapeutic potential as hESCs, but until solutions or explainations to these problems are found, the use of iPSC is currently not ideal for clinical applications.

Herein, 'naturally occurring' and genetically unmodified hESCs, still hold the greatest potential in therapeutic applications and the 'gold standard' in terms of pluripotency [59, 63].

1.2.1 Human embryonic stem cells as a therapeutic source for vascular regeneration

Current cell transplantation therapies to treat vascular diseases are hampered by the lack of donor cells and the ability to acquire a vast number of harvested cells. Besides, fully matured ECs isolated from patient's blood vessels have limited proliferation and expansion capabilities. On the other hand, hESCs, which have an unlimited self-renewal capability [46], can offer a plentiful source of ECs for therapeutic revascularization. Hence, human embryonic stem cells (hESCs) are increasingly sought after as the cellular therapy for regenerating damaged areas.

hESCs were initially derived in 1998 by isolating the inner cell mass of pre-implanted 5-6 days old blastocysts via immunosurgery [46]. These cells have an indefinite lifespan and are pluripotent, which refers to their ability to differentiate into the three embryonic germ

layers – the ectoderm, mesoderm and endoderm [64]. In addition, their capability in prolonged self-renewal has sparked enormous interest for their therapeutic applications. These applications include the engineering of artificial blood vessels, repair of damaged vessels and cell transplantation for the replacement of ischemic tissues [65-69]. Another beneficial area of hESCs cells is the creation of a valuable source of human disease model for drug discovery and toxicology *in-vitro* screening studies [70, 71]. Moreover, the availability of hESCs enables the study of the earliest events in human embryogenesis and developmental biology as well as the formation of functional blood vessels during development. This will certainly dismiss the need for using ethically complicated early stage human embryos for *in-vivo* research.

In order to fulfill the potential of hESCs as a platform for treating cardiovascular diseases, the understanding of its roles and functional biology in vasculogenesis is pivotal. As such, the following sections will discuss current vasculogenesis studies focusing hESCs as a model system and the relevant mechanisms that occur during the process.

1.3 Mechanisms of embryonic vasculogenesis and vascular cell differentiation

Both vasculogenesis and angiogenesis take place in the early developing embryo, enabling the establishment of the vascular system. In fact, the cardiovascular system is the first organ formed during early embryogenesis [72]. Moreover, during the early stages of embryogenesis, the endothelium is the first tissue to differentiate. Formation of a functional *de novo* vascular network from embryonic mesoderm via the process of vasculogenesis is crucial for embryonic survival and organogenesis [73].

1.3.1 *Formation of the hemangioblast in embryos and embryonic stem cells*

Vasculogenesis is driven by the invagination of epiblastic cells through the primitive streak to form the mesoderm during gastrulation. *De novo* mesodermal cells gradually organize into different segments such as the axial (notochord), paraxial (somites), intermediate mesoderm (kidney), lateral and extra-embryonic mesoderm (Fig.3) [74]. After the formation of the coelome, the lateral mesoderm divides into two layers attributing to a dorsal sheet

(somatopleural mesoderm) and a ventral sheet (splanchnopleural mesoderm). The extraembryonic mesoderm is situated at the posterior part of the mesoderm. Both lateral and posterior mesoderm which comprises the posterior two thirds of the embryo, were shown by Murray in 1932 to give rise to endothelial as well as hematopoietic cells [75]. Formation of endothelial and hematopoietic cells occurs after migration of the newly formed lateral and posterior mesodermal cells toward the yolk sac where the cells differentiate. Florence Sabin was the first who observed under light microscope that migration leads to the appearance of mesdoderm cell clusters or known as hemangioblastic aggregates during the incubation period in living chick blastoderms [76]. From the second day of incubation, she observed that hemangioblastic aggregates were present at the border of the embryonic and extraembryonic areas, which subsequently matured to blood islands. Cells present at the periphery of these aggregates flatten and differentiate into ECs, while cells in the core of the cluster differentiate into hematopoietic cells (Fig.3). Embryonic ECs aggregate and coalesce to form *de novo* vascular networks via the process of vasculogenesis. Ultimately, both the intra and extra embryonic vessels will form a vascular plexus.

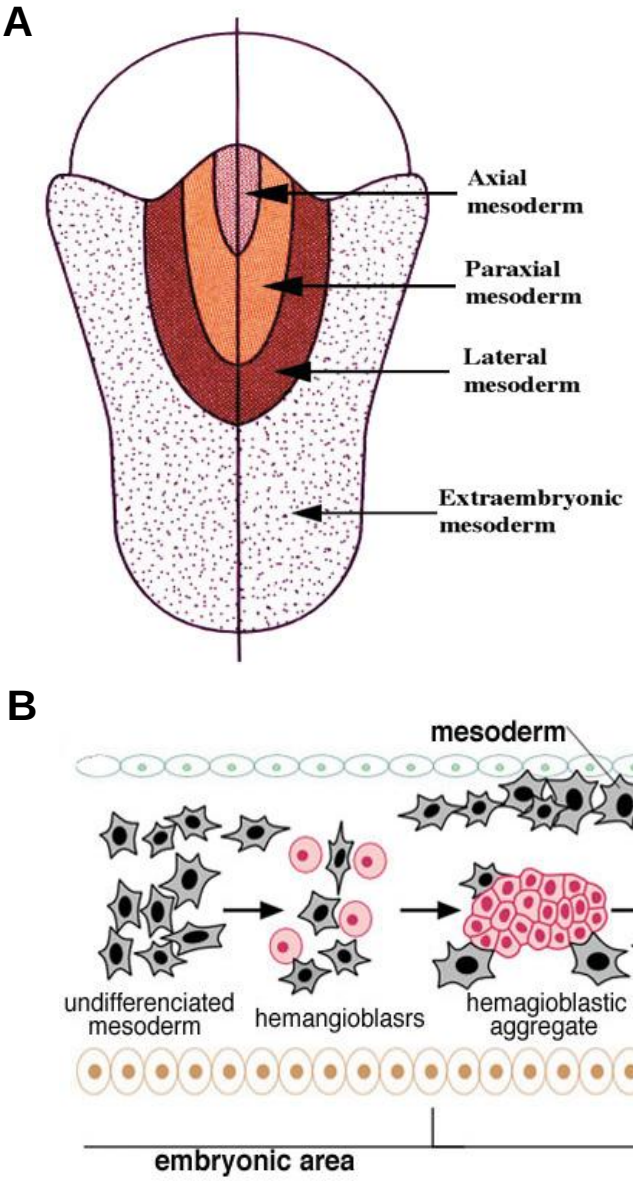

Fig. 3. The origins of the hemangioblast

(A) A schematic map depicting the prospective mesodermal territories of a gastrulating chick embryo [74]. (B) A Schematic drawing of the yolk sac blood island development according to Sabin [76].

1.3.1.1 Derivation of hemangioblasts from hESCs

Since both ECs and hematopoietic cells originate in close proximity during embryonic development, the hypothesis of a common vascular precursor or a hemangioblast was postulated (Fig.4) [75, 76]. The hemangioblast concept was proven initially from studies in differentiating mouse embryonic stem cells (mESCs) [77-79] and later in early developing mouse embryos [80]. These early studies carried out in mouse, have paved the progress for the identification of hemangioblasts in hESCs.

Previously, before the advent of the hESCs model system, the study of early hematopoietic and endothelial precursors during human embryonic development has been impeded. Reasons are due to the scarcity of early human embryos, its associated ethics and the lack of *in-vitro* experimental conditions which can mirror the early-stage human embryonic development. The limited and exclusive number of studies using human embryos showed that hematopoietic cells first arise in the third week of human ontogeny inside yolk sac developing blood vessels and subsequently found one week later from independent origins, within the wall of the embryonic aorta and vitelline artery. Flow cytometry analysis of sorted CD31+/ CD45- or CD34+/CD45- early ECs from the yolk sac and aorta resulted in a yield of blood-forming hemogenic ECs [81]. However, whether these precursor cells display hemangioblast properties remains elusive.

Using hESCs as a culture model system and ultilising a similar technical approach to generate mouse hemangioblasts, Zambidis *et al* achieved both primitive and definitive human hematopoiesis from the formation of human embryoid bodies (hEBs) [82]. The formation of spontaneous hEBs, mimics the early events of human yolk sac blood development, from the differentiation of mesodermal-hemangioblast followed by primitive erythromyeloid hematopoiesis. Without supplemental growth factors or xenogeneic stromal cocultures, hEBs were differentiated in serum-free colony-forming cells assay conditions. After 6-9 days, semi-adherent mesodermal hematoendothelial (MHE) cluster colonies emerged, which contained both adherent and nonadherent cells. The nonadherent cells expressed CD45 and gave rise to hematopoietic colonies whereas the adherent cells from MHE colonies resulted in cells with endothelial morphology, expression of endothelial markers, CD31, VE-cad, vWF, and were capable of Dil-labeled acetylated low density lipoprotein (Dil-Ac-LDL) uptake. To further support the hemangioblast concept, MHE colony derived primitive hematopoietic blasts were also located close to adherent CD31+VE-cadherin+ ECs. However, it is unclear whether MHE colonies are generated from single hESCs as the formation of hEBs in this study were generated from dispase induced hESCs cell clumps. This raised an uncertainty in the relationship between MHE colonies and bipotential hemangioblast.

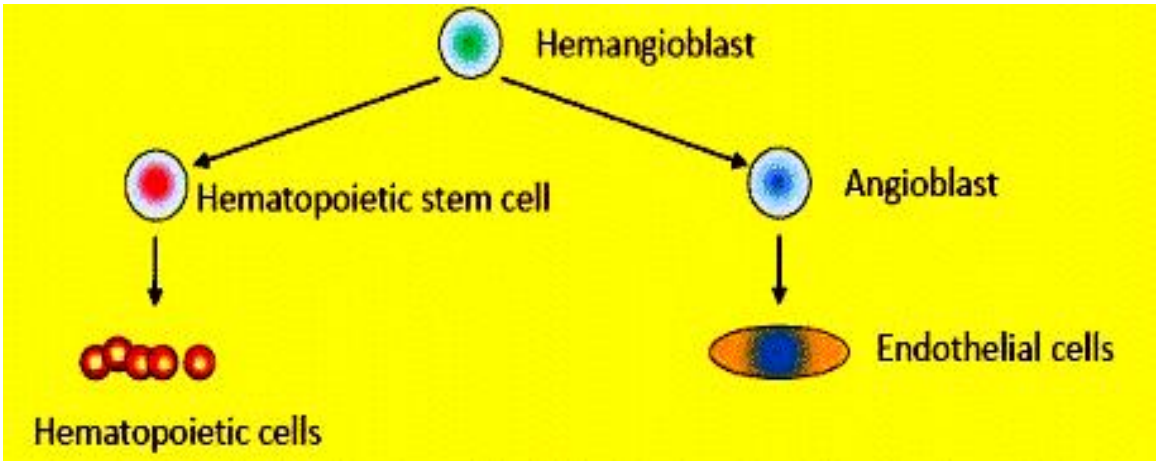

Fig. 4. The origins of ECs and hematopoietic cells

In the developing embryo, both angioblasts and hematopoietic stem cells share a common precursor, the hemangioblast. Angioblasts further differentiate into ECs which line the inside of blood vessels, whereas hematopoietic stem cells can give rise to blood cells [83].

In addition, several *in-vitro* hESCs studies have also shown to support the hypothesis that both hematopoietic and endothelial cells develop from a common precursor, the hemangioblast or from primitive hemogenic endothelial cells [62, 84]. Using serum free medium containing a cocktail of cytokines BMP-4, FGF-2 and VEGF, Kennedy *et al.* have derived hemangioblasts from *in-vitro* hESCs differentiation [85]. These hemangioblasts were identified by the ability to generate blast colonies with hematopoietic and endothelial potential as previously reported in mESCs differentiation studies [77]. However the kinetics of hematopoietic colony formation is different from previous studies [84, 86] which could be because of the different hESC differentiation conditions, growth factors or different hESC lines used. Due to the employment of a variety of different differentiation protocols [82, 84, 85], it is unclear whether the same or different populations of potential bipotent precursors were examined.

Presently there is no standard protocol in generating hESCs-derived hemangioblasts, thus resulting in varying kinetics of hEBs differentiation and expression of hemangioblast-

related markers. An imminent reason is the use of different mixtures of cytokines and batches of fetal bovine serum and hence, contributing to variation between different research groups. The discovery of more specific markers expressing exclusively only on hemangioblast's cell surface and concurrently emerging at specific differentiation time-points as well as function assessments may aid in solving these discrepancies.

1.3.2 *hESCs derived endothelial cells*

The isolation and establishment of EC lines in 1973 was an early achievement in the vascular biology field [87]. However, these cultures do not provide a three-dimensional interaction that comprise of the cultured ECs, the underlying matrix and the adjacent supporting cells, which are crucial in the regulation of vascular processes. In comparison, pluripotent embryonic stem cells are capable of forming EBs wherein vascular development occurs in a myriad of interactions with adjacent non-ECs. Since the first *in-vivo* observation of differentiating ESCs into ECs and subsequent vascular morphogenesis by Doetschman *et al.* [88], a series of ECs differentiation studies were carried out extensively in murine embryogenesis, including maturation steps, molecular events, and growth factor involvement [89-92]. The combinations of assessing multiple endothelial specific markers and functional assays such as Dil-Ac-LDL uptake and vasculogenesis using matrigel assays are classic hallmarks in identifying and characterizing ESC-derived ECs. Microscope examinations determined that ESC-derived ECs also acquire a cobblestone morphology [93]. Expression of PECAM-1, VEGFR2, VE-cad, endothelial nitric oxide synthase (eNOS) and vWF were detected in a time-dependent manner from the early stages of ESCs differentiation to mature vessels via immunofluorescence staining and gene expression analysis in mouse EBs [89]. Vittel *et al*. reported that Fetal Liver Kinase-1 (Flk-1; alternatively known as Vascular endothelial growth factor receptor 2 (VEGFR2) or Kinase-inserted domain containing receptor (Kdr)) mRNA occurred at differentiation day 3 whereas later stage markers such as VE-cad and Tie1 mRNAs were detected at day 5. Flk1 has been regarded as one of the earliest markers to appear during endothelial linage development and has also been reported to appear around day 3-4 of differentiation [91]. On the other hand, expression of VE-cad and vWF are known as late or mature EC markers.

The belief that ESCs must undergo through the EB route to proceed with differentiation was overturned by Nishikawa *et al* [79]. mESCs grown on collagen type IV coated dishes as a monolayer, further differentiated into Flk1+ cells and eventually gave rise to ECs. Using similar methods of differentiation, Yamashita *et al.* showed that isolated Flk1+ cells, which under the influence of $VEGF_{165}$ application, resulted in the formation of ECs [90]. Moreover, treatment of Flk1+ cells with PDGF-BB also formed mural cells, which further demonstrated that Flk1+ cells could give rise to vascular cells. *In-vivo*, these Flk1+ cells could incorporate as endothelial and mural cells and contribute to the developing vasculature in chick embryos [90]. Since then, isolating Flk1+ cells and the inclusion of VEGF into culture systems in differentiating towards EC has been widely utilised in many groups [91, 92]. In an alternative to obtain ECs and VSMCs from differentiating mESCs, Xiao *et al.* isolated stem cell antigen-1 positive (Sca-1+) vascular progenitor cells from mESCs and further differentiated these cells on collagen type IV in the presence of $VEGF_{165}$ and PDGF-BB to derive ECs [94] and VSMCs [95]. Using this method, we achieved a large quantity of functional ECs with flow cytometry analysis depicting that 99% of differentiated cells were positive for CD31/PECAM and 75% were vWF positive. *In-vivo*, these ECs showed the capacity to regenerate the endothelium of denuded vessels and reduced neointimal lesion formation after arterial injury in mice. Moreover, histone deacetylase 3 (HDAC3) which reportedly regulates the structure and function of chromatin [96], was found to play a role in the differentiation process of $Sca\text{-}1^{+}$ progenitor cells towards the endothelial lineage [94].

Advances and findings in early mESCs derived ECs studies have aided in hESCs studies, with the endothelial potential of hESCs being increasingly apparent during the past recent years. Several groups have successfully derived ECs from hESCs, mainly via two approaches, the spontaneous differentiation of EBs, also known as three-dimensional differentiation (3D) [66, 67, 93, 97-100] or two-dimensional differentiation (2D) as monolayers [101-106]. In 2002, a breakthrough in differentiating hESCs to derive ECs was reported by Levenberg *et al*. [67]. During differentiation, endothelial-specific genes were characterized from Ebs to assess their vasculogenic potential. CD31/PECAM-1, CD34 and VE-Cad

mRNA expressions peaked at days 13-15. Subsequently, CD31/PECAM-1+ cells were cell-sorted from day 13 EBs. A yield of 2% CD31/PECAM-1^+ cells was obtained and these cells were expanded in endothelial growth medium. These cells were characterised by analyzing the expression of endothelial-specific genes and proteins. Cells were positive for markers such as CD34, VE-Cad and vWF and capable of Dil-Ac-LDL uptake. *In- vivo* study was carried out by transplanting PECAM-1/$CD31^+$ cells into severe combined immunodeficient (SCID) mice. Further histological examinations on transplanted implants were immunoreactive with human CD31 and CD34. The presence of mouse blood cells in the human positive lumens was indicative of the formation of functional microvessels. However, some questions remain unanswered as blood carrying function of the vessels was not investigated further *in-vivo* and the integration of the implant into the host vasculature was not well defined. Later, some research groups concluded that a population of primitive precursors ($CD31^+Flk1^+CD45^-$) or $CD34^+$ vascular progenitor cells could be obtained from day 10 EBs which upon further selection and differentiation, could give rise to mature and functional ECs [66, 84, 107]. These studies confirmed that the EB is a true event of early human development wherein EC progenitor cells exist and whereby adult ECs could be derived.

In another study using EBs to derive endothelial cells, Kim *et al*. isolated the center region of attached EBs which expressed higher endothelial markers compared to the outgrowth region of the EBs [98]. To obtain cells from the center region of the EB, the group used a two-step enzyme treatment comprised of trypsin-Ethylenediaminetetraacetic acid (EDTA) and cell dissociation buffer. Flow cytometry analysis of cells from the center region revealed a higher level of PECAM/CD31+ cells at 7.39% as compared to Levenberg *et al* [67]. As these cells were further differentiated, they expressed endothelial markers and were capable of tube formation in matrigel assay as well as Dil-Ac-LDL uptake. However, these cells were not conducted *in-vivo* and hence the behavioral function of these hESCs-derived ECs was not fully evaluated. Cho *et al*. took a step further with the cells isolated from the central region of the EBs [93]. After mechanical isolation of the PECAM-1/$CD31^+$ cells in the middle of the EB and further expansion, vWF positive cells were sorted out via FACS. *In-vivo* evaluation was carried out by transplanting the vWF positive cells into the hindlimb of a mouse ischemia model. In the transplanted mice, perfusion blood flow was improved with

enhanced angiogenesis as observed by the increased formation of capillaries and arterioles. There was also an improvement of limb salvage as these cells facilitate postnatal neovascularisation. Moreover, reverse transcription polymerase chain reaction analysis showed that human angiogenic factors such as VEGF, bFGF and Ang1 were expressed only in the transplanted ischemic mouse limbs. Taken together, this study has shown that transplanted hESC-ECs could serve as an alternative cell source for therapeutic angiogenesis to treat peripheral ischemia or other ischemic diseases. Also, improvements during cell transplantation in this study could be made by using a matrix which might enhance the efficacy of cell therapy by facilitating optimal cell transfer and distribution into ischemic sites. However as Cho *et al*. retrieved 41.81% vWF positive cells, it seems that mechanical isolation is a less efficient method compared to the two step enzyme treatment carried out by Kim *et al* who obtained 52.04% of vWF positive cells [98]. Interestingly, both groups used the same hESC line, CHA-3 hESC in their studies. Another probable reason in the differences is the different length of days taken to culture and attach the Ebs prior to isolation (Table 1).

Table 1. Differences in the culture and subsequent attachment of Ebs.

Probable reasons in explaining the different percentages obtained in the derivation of vWF positive hESC-derived ECs from studies carried out by Kim *et al.* and Cho *et al.* Determination and optimisation of the most efficient method will greatly aid in retrieving high numbers of potentially pure hESC-derived ECs for therapeutic therapies.

	% of hESCs-derived vWF +cells isolated	**Medium in which EBs was cultured in**	**No. of days for EB formation**	**Medium in which attached EBs were cultured**	**No. of days EBs was attached prior to isolation of cells in the middle region**
Kim *et al* [98]	52.04%	bFGF-free + DMEM/F12 medium supplemented with 20% serum replacement, 1 mM l-glutamine, 1% nonessential amino acids, 100 mM β-mercaptoethanol	5 days	Not mentioned	10 days

Cho *et al* [93]	41.81%	Same as Kim *et al*	9 days	DMEM + 10% Fetal Bovine Serum	7-9 days

The formation of EBs is believed to be an inefficient method to gain large quantities of pure hESCs-derived ECs as usually an entire colony of hESCs is required for generation of a EB. Hence, the differentiation of hESCs towards the endothelial lineage was achieved in a 2-dimensional (2D) model bypassing the need for EB formation [101, 103]. Gerecht-Nir *et al*. reported the differentiation of hESCs into vascular cells by seeding undifferentiated aggregates of hESCs on collagen-IV coated surface [103]. After 6 days, the cell population was filtered through a 40μm strainer, resulting in a population of filtered cells expressing endothelial progenitor markers such as CD31, CD34 and GATA binding protein 2 (GATA2). Further differentiation of these filtered cells in human $VEGF_{165}$ resulted in the growth of vWF expressing mature ECs, which are capable of Dil-Ac-LDL uptake. Vasculogenesis was observed when the differentiated cells were seeded in 3D collagen type-1 and matrigel culture systems. Nevertheless, the method of isolating vascular progenitor cells using a 40μm filtration may compromise the purity of these isolated cells and is not as specific as to FACS and magnetic activated cell sorting (MACS). The lack of *in-vivo* study also questioned the long-term durability and integration of these differentiated cells in animal models.

Zack *et al.* also used the 2D method to generate hESCs-ECs, by seeding undifferentiated hESCs on mouse embryonic fibroblasts in the presence of FBS but without additional growth factors for 10 days [101]. They obtained ~10% CD34+CD45- cell population and 60-90% CD31+ cells. After two rounds of magnetic bead selection, 80-95% purity of CD34+ cells was achieved and these progenitor cells were further differentiated in endothelial growth medium with VEGF and bFGF. The resultant hESCs-derived ECs contributed to arborized blood vessels after transplantation into SCID mice. The implants successfully formed functional vessels and integrated into the recipient's circulatory system which lasted more than 150 days. Oyamada *et al*. also demonstrated the therapeutic potential of transplanted hESCs-derived hECs. In this study, transplanted hESCs-derived ECs and

mural cells improved vascular regeneration and reduced the infarct area after stroke in mice [104].

There are several reported 2D differentiation studies which also used various feeder layers such as OP9 bone marrow derived mouse stromal cells or methylcellulose to induce the formation of hESCs-derived ECs [82, 104, 108]. However instead of differentiating hESCs using the conventional 3D or 2D method, one particular study utilized genetic manipulation of hESCs to drive the production of ECs. Rufaihah *et al.*, made day 7 hESCs EBs, trypsinised them into single cells and transduced with an adenoviral vector expressing the human $VEGF_{165}$ gene (Ad-$hVEGF_{165}$). For more than 30 days post-transduction, Ad-$hVEGF_{165}$-transduced cells continued secreting high levels of $hVEGF_{165}$ into the culture medium as compared to non-transduced and Ad-null-transduced cells. Immunostaining for hVEGF revealed 90% transduction efficiency. They also assessed the biological activity of the secreted $VEGF_{165}$ by Ad-$hVEGF_{165}$-transduced cells which stimulated an extensive proliferation of human umbilical cord vascular endothelial cells (HUVEC). Real-time PCR showed an upregulation of VEGF, Ang-1, Flt-1, Tie-2, CD34, CD31, CD133 and Flk-1 gene expression in the Ad-$hVEGF_{165}$-transduced cells. Although flow cytometry analysis revealed an approximately 5-fold increase in CD133 marker expression in Ad-hVEGF165-transduced cells as compared to control, other specific endothelial markers such as PECAM-1/CD31 and vWF were not qualitatively assessed. Moreover the function of these derived Ad-$hVEGF_{165}$-transduced cells was not determined in matrigel or Dil-Ac-LDL assays. Hence the vasculogenesis of the derived Ad-$hVEGF_{165}$-transduced cells is questionable as well as its behavior *in-vivo*.

Although ECs present a common set of markers and features, they exhibit certain heterogeneity. For example in structural heterogeneity, ECs from aorta are larger and thicker than those found in capillaries and veins [109]. This heterogeneity also comprises of diversity in different expression of cell surface markers, proteins and mRNA [110, 111]. Hence, challenges still remain to delineate, refine, control, monitor and quantify the kinetics of vascular differentiation, maturation and tissue organization so as to mimic the complex microenvironment where vasculogenesis occurs during embryogenesis.

1.4 MicroRNA and its role in vasculogenesis

The past recent years have seen a surge of evidence illustrating that microRNAs (miRNAs) are involved in various biological processes, such as cardiogenesis and the differentiation of skeletal muscle and hematopoietic lineages [112-114]. Its importance has also been highlighted in the human genome, which has been estimated to encode up to 1000 miRNAs that are predicted to regulate a third of all genes [115]. miRNA was initially studied in model organism such as *Caenorhabditis elegans* where the founding members of miRNAs, lin-4 and let-7 were discovered to regulate crucial roles in its development [116, 117]. With the ever expanding investigations into its function and regulation, the concept of miRNA manipulation to regulate disease-related processes is fast becoming a feasible future therapeutic approach.

1.4.1 microRNA biogenesis

miRNAs are highly conserved, short non-coding RNA molecules of about 22 nucleotides in length. They regulate gene expression at the post-transcriptional level by either repressing target mRNAs through an antisense mechanism or by enhancing the degradation of mRNA, thereby silencing gene expression.

Originally, miRNAs reside in the nucleus as RNA polymerase II primary miRNA (pri-miRNAs) transcripts, which are transcribed from independent miRNA genes (intergenic), polycistronic transcripts that often encode multiple related miRNAs (polycistronic), or introns of protein-coding genes (intronic) (Fig.5) [118]. Once the stem-loop pri-miRNAs are expressed, they are matured and processed in two steps, catalyzed by the ribonuclease III (RNase III) type endonucleases Dicer and Drosha. Within the nucleus, pimary miRNA transcript (pri-miRNAs) are processed by Drosha which form complexes with a double-stranded RNA-binding domain protein, DiGeorge syndrome critical region gene 8 (DGCR8)/Pasha [119, 120]. Eventually the pri-miRNAs are processed into approximately 70-100 nucleotide hairpin-shaped precursors known as pre-miRNAs. The majority of mammalian miRNAs encoded in introns are processed before splicing. But there is a subset of very short intronic miRNAs (miRtrons) that bypass the Drosha pathway [121] and gets

processed into pre-miRNAs by the spliceosome and the debranching enzyme. Both pre-miRNAs and miRtrons are transported to the cytoplasm via an Exportin-5 and Ran-GTP–dependent mechanism [122].

Once in the cytoplasm, the doubled-stranded ribonuclease Dicer, forms a complex with protein (human immunodeficiency virus transactivating response RNA-binding protein) TRBP and cleaves the pre-miRNAs to yield ~20-22 base pair mature miRNA duplexes [123]. After cleavage, one strand of the RNA duplex is incorporated into an Argonaute family protein (AGO) to form the core component of the effector ribonucleic acid induced silencing complex (RISC). Mammals express multiple AGO homologues, which are namely AGO1–AGO4. During loading into the RISC, the RNA duplex is unwound to form a mature single-stranded miRNA (guide strand) and its complementary strand (passenger strand or miRNA*) which is typically degraded [124]. On the other hand, there are instances when the miRNA* strand can also be loaded into the RISC to function as active miRNAs and involve in gene regulation [125-127]. Generally, selection of the active mature strand that associates with the RISC seems to depend on the stability of both ends of the double-stranded RNA [128, 129]. It appears that there is a preference for the strand with lower stability base pairing of the 2–4 nucleotides at the 5' end of the double-stranded RNA duplex [128].

1.4.2 microRNA mode of operation

Mature miRNAs guide the RISC to target mRNAs and binds with Watson–Crick base pairing to the 3'untranslated region (UTR) of specific target mRNAs. Unlike in plants, few mammal miRNAs are highly complementary to their target mRNAs and thus most binds with near-perfect complementary match [130-132]. The 7-8-nucleotide seed sequence spanning from nucleotides 2 to 8 in the 5′ end of the mature miRNA strand is critical for the majority of 3'UTR mRNA target recognition [133, 134]. However, in some rare cases, there are also reports that demonstrated the ability of mature miRNAs which target regions outside the mRNA 3'UTR, such as the amino acid coding sequence and regions in 5'UTR of mRNA targets [135, 136]. Moreover, each miRNA might have up to several hundred mRNA targets, which may be part of a related pathway or process [137].

After recognization by miRNA, this leads to endonucleolytic cleavage and degradation of the target mRNAs and this mechanism applies to small interfering RNAs (siRNAs) and many plant miRNAs. However, since animal miRNAs pair imperfectly with their target mRNAs, this leads to translational repression or deadenylation and decay of mRNAs [138]. Finally, mRNAs which are repressed by deadenylation or during the translation–initiation step, are transported to P-bodies for either degradation or storage [139].

1.4.3 Nomenclature for miRNAs

A standard miRNA nomenclature scheme has been applied since the initial large-scale miRNA discoveries [140-142]. Names are assigned after a submitted manuscript has experimentally confirmed the discovery of the miRNA and before the publication of article [143]. In the nomenclature system, the prefix "mir" is followed by a dash and sequential numerical identifiers that often indicate order of naming (e.g. mir-123 was named and likely discovered prior to mir-456) [144]. Identical miRNAs have the same number, regardless of organism (e.g. hsa-miR-101 in human and mmu-miR-101 in mouse are orthologous). Abbreviated 3-letter prefix is designated to species of origin (e.g. hsa-miR-101 belonged to Homo sapiens). The capitalized "miR-" refers to the mature form of miRNA whereas the uncapitalized "mir-" refers to the pre-miRNA precursors. Mature miRNAs that differ at only one or two nucleotide positions are annotated with an additional lower case letter (e.g. miR-123a would be closely related to miR-123b) [144]. Pre-miRNAs that are located at different loci in the genome but leading to completely identical mature miRNAs have an additional dash-number suffix (e.g. hsa-mir-194-1 and hsa-mir-194-2 are both located in different loci of the genome but lead to an identical mature miRNA hsa-miR-194) [143]. In the instance whereby two different mature miRNAs sequences originate from opposite arms of the same hairpin pre-miRNA precursor, they are assigned with a -3p (3'arm) or -5p (5'arm) suffix. In terms of the levels of miRNA relative expression, an asterisk following the name indicates a miRNA expressed at low levels relative to the miRNA in the opposite arm of a hairpin (e.g. although both miR-123 and miR-123* share a pre-miRNA hairpin, higher levels of miR-123 would be found in the cell) [144].

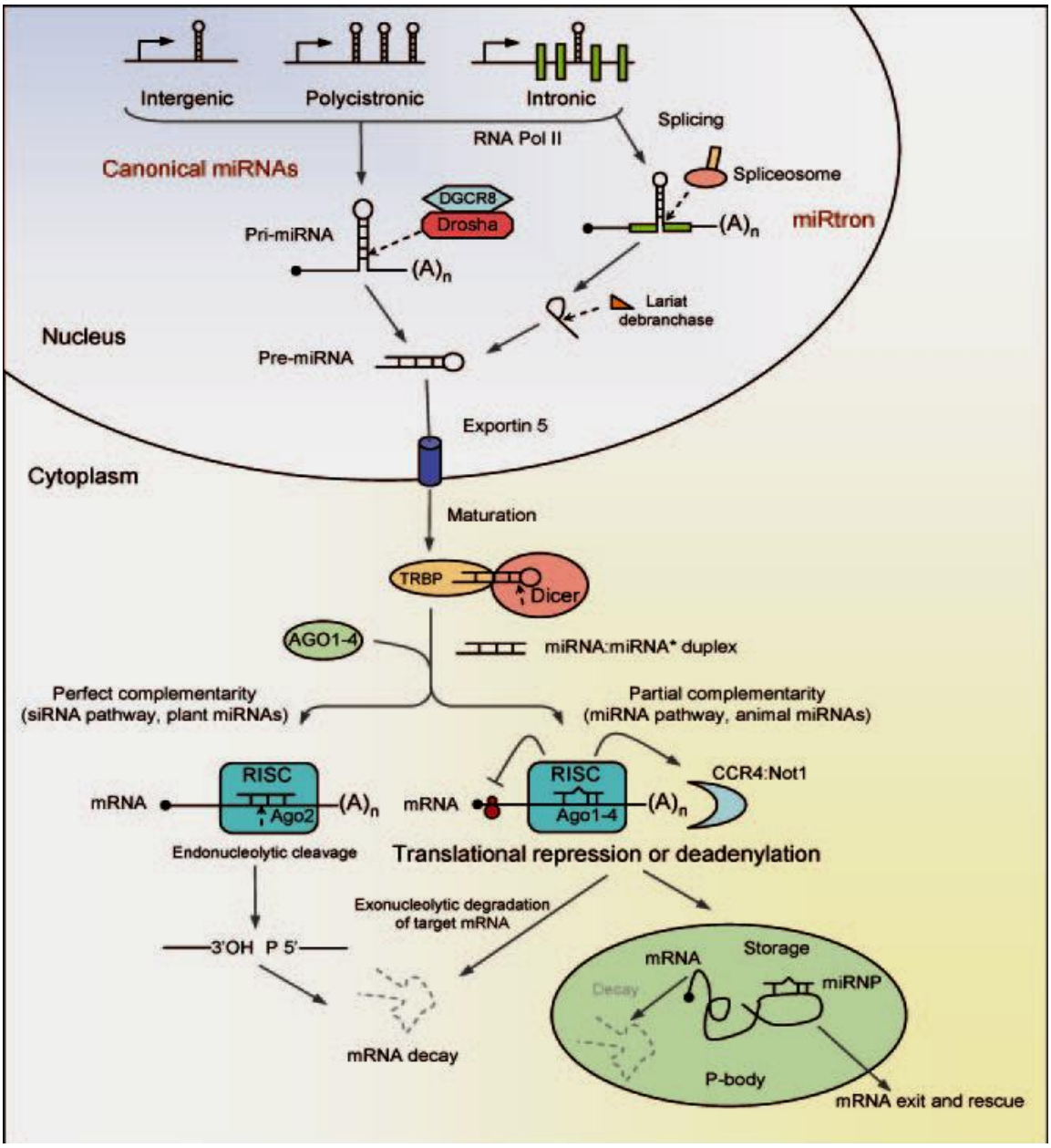

Fig. 5. Process of the formation of miRNAs and their functions

miRNAs are generated in a two step processing pathway (nuclear and cytoplasmic) mediated by enzymes, Dicer and Drosha. Mature miRNAs are incorporated into a RISC complex, which contains components of the Argonaute family (Ago1 to -4). Targeted mRNA is either translational repressed or degraded [145].

1.4.4 microRNA and its regulation in vascular biology

Vascular biology applies to processes affecting blood vessels. It has been increasingly well established that miRNAs play important roles in vascular biology. The first few experiments demonstrating the significance of miRNAs in mammalian vascular biology regulation, involved depleting levels of miRNAs in vascular cells by arresting miRNA biogenesis [146-148]. In an *in-vivo* study involving transgenic mouse lacking the first two exons essential for the function of dicer, homozygous dicer $^{ex1/2}$ mutant mouse did not survive. Majority of E11.5 dicer $^{ex1/2}$ embryos have impaired growth and development and those which survived had a severely compromised blood vasculature formation. Hence this indicates that dicer or miRNAs plays a crucial role in mouse development and its angiogenesis [146]. Moreover, the knockdown of dicer in ECs as shown *in-vitro*, reduced its proliferation and cord formation. In this study, there was an increased expression of FLT/VEGFR and KDR/VEGFR2 suggesting that the VEGF signaling pathway was upregulated to compensate for failed angiogenesis and remodeling [147]. In addition, the silencing of both Dicer and Drosha significantly abated capillary sprouting of ECs and tube formation [147, 148].

Other members of miRNAs were also reported in the regulation of vascular biology and angiogenesis. The activation of angiogenic program in ECs is crucial for normal embryonic development and regenerative therapy such as tissue healing or transplantation. However, uncontrolled and excessive angiogenesis can also lead to pathological discorders such as cancer. In one of the studies that looked into the role of miRNAs in angiogenesis, it was discovered that both miR-221 and miR-222 regulated the expression of c-Kit and its ligand; the stem cell factor. Interaction between miR-221/2 and c-Kit, forms part of a complex, which **inhibits** endothelial cell migration, proliferation, and angiogenesis *in vitro* [149]. In another study, Bonauer *et al.* has identified the miR-17-92 cluster as a negative regulator of angiogenesis. miR-92a, a member of this cluster, inhibits angiogenesis both *in vitro* and *in vivo* [150]. More recently, Sabatel *et al*. discovered that in ECs, miR-21 acts as a negative modulator of angiogenesis by targeting RhoB [151].

Another miRNA integral to angiogenesis and blood vessel formation is miR-126. miR-126 is an endothelial specific miRNA and one of the most abundantly expressed miRNAs in endothelial cells [148, 152] . It is found prominently in the heart and other highly vascularized murine tissues [153-155]. Located in chromosome 9q34.3 within the host gene encoding for epidermal growth factor like-7 (Egfl-7), miR-126 regulates many aspects of endothelial cell biology *in vitro*, including organization of the cytoskeleton and cell migration [155, 156]. Its expression also appears crucial during embryonic development as knockdown studies in zebrafish resulted in hemorrhage and loss of vascular integrity [152]. Moreover, in a mice study, targeted deletion of miR-126 leads to partial embryonic lethality with hemorrhagic defects during development [155]. Nevertheless, those surviving mice in this study exhibit impaired neovascularization and thus show increased mortality after myocardial infarction and inadequate wound healing [155].

Besides, miR-126 was found enriched in ECs derived from mESCs **[152]**. Fish *et al.* further discovered that miR-126 targets the Sprouty-related protein (SPRED1) and phosphoinositol-3 kinase regulatory subunit 2 (PIK3R2/p85-beta) which are negative regulators of the VEGF pathway **[152]**. These findings were further ratified by Spred1 overexpression and VEGF signaling inhibition in zebrafish studies whereby defects similar to miR-126 knockdown were observed [152]. Following reports stating that effects in miR-126 appear to regulate vascular integrity and angiogenesis in mouse and zebrafish models, a recent report has also demonstrated levels of miR-126 being induced in day 10 differentiated hESCs grown in EC differentiaiting conditions [106]. However, no further studies have if miR-126 play a role in hESCs differentiation towards the EC lineage. Moreover, Fish *et al.* were unable to promote differentiation of miR-126 overexpressing pluripotent stem cells towards the EC **lineage [152]**. This indicates that although miR-126 is found enriched in vascular progenitors, it does not control early EC lineage commitment.

To date, present studies have demonstrated the regulation of miRNAs in a myriad of vascular biology events, nevertheless there are still insufficient evidence demonstrating their involvement in early human development of vascular cells, how they control EC fate commitment and their mechanisms involved in these differentiation processes. Hence this project aims to determine and identify miRNAs which are crucial in regulating the

differentiation of hESCs into ECs. Delineation of the mechanisms and signaling pathways involved by these particular vascular-specific miRNAs will greatly aid in understanding the molecular regulation of human vasculogenesis. These findings will also serve to benefit future clinical therapies in cardiovascular disease applications.

1.5 Project objectives

1. Design and develop a differentiation culture model to derive endothelial and smooth muscle cells from undifferentiated hESCs.

2. Isolate pure population of hESC-derived ECs that display EC markers using FACS. Function tests will be assessed on these hESC-derived cells to ensure that these cells display functional characteristics of vascular EC cells.

3. Determine and identify which selected enriched miRNAs are crucial in regulating the differentiation of hESCs into ECs, microRNA array analysis will be carried out.

4. Determine if selected miRNAs also play a role *in vivo* developing chick embryos

5. Delineate the underlying mechanisms of EC differentiation from hESCs mediated by the selected miRNAs. Target mRNA will be determined using gain-of-function and loss-of-function tests. Luciferase assay will then be used to verify the miRNA target sites.

Hypothesis
miRNA may play a role in early human endothelial cell development.

CHAPTER 2

CHAPTER 2

Materials and Methods

2.1 Maintaining the human embryonic stem cells

2.1.1 Making stocks of 25ug/ml Mitomycin C

Two milligram of Mitomycin C (Sigma-Aldrich) was dissolved in 1ml of Mouse Embryonic Fibroblast (MEF) medium containing Dulbecco's Modified Eagle Medium (DMEM; Gibco, Invitrogen) with 15%**v/v** Foetal Bovine Serum (FBS; ATCC, Manassas, VA), vortexed and spun down. The dissolved Mitomycin C was topped up with MEF medium to make a concentration of 25µg/ml and sterile filtered through a 0.2µm filter (Whatman). The prepared 25µg/ml Mitomycin C stocks were aliquoted and stored at -20ºC. A final concentration of 8µg/ml of Mitomycin C was used to inactivate MEFs.

2.1.2 Making stocks of 100 mg/ml Collagenase type IV

Reconstitiute 1g of the lyophilized enzyme Collagenase type IV (CIV; Gibco, Invitrogen) with 10ml of DMEM / F-12 1:1, (1X) containing 15 mM HEPES (Stem Cell technology). The solution was mixed well and filtered using a 0.2µm filter (Whatman). Aliquots of the 100mg/ml CIV stock solution were stored at -20ºC. CIV was further diluted with DMEM/F12 to a concentration of 0.5mg/ml prior to use.

2.1.3 Making stocks of human basic Fibroblast Growth Factor-2

Fifty microgram of human basic Fibroblast Growth Factor-2 (hbFGF; Miltenyi Biotec Inc, Auburn, USA) was reconstituted with 1ml of 0.1%**v/v** Bovine Serum Albumin (Sigma-

Aldrich). 50µg/ml of the prepared hbFGF was further diluted to 10µg/ml and aliquoted into smaller volumes of 100-200 µl for long-term storage at -20ºC. 4ng/ml of hbFGF was used in maintaining hESCs.

2.1.4 Inactivating MEFs and preparing feeders for hESCs passaging

MEFs (CF-1 strain, ATCC, Manassas, VA) were grown to approximately 80% confluency prior to inactivation. Spent medium was aspirated and cells were washed once with Dulbecco's Phosphate Buffered Saline (D-PBS; Sigma-Aldich). 8µg/ml of Mitomycin C was added to the flask and incubated for 2 hours in a 37ºC incubator. After which, Mitomycin C was removed and cells were washed once with D-PBS before incubating with trypsin (Gibco, Invitrogen) for 3 minutes at 37ºC. An equal volume of MEF medium was added to neutralise the trypsin. Cells were collected into a 15ml tube and centrifuged at 270g for 5 minutes. The cells were resuspended in 2ml of MEF medium, counted using the hematocytometer and plated at 350,000 cells per 25cm^2 gelatinised flasks. The MEFs were allowed to settle overnight at 37ºC before plating hESCs. For the optimal maintenance of hESCs, MEFS were only used from passages 3 to 5.

2.1.5 Preparation of soda lime 3mm glass beads

hESCs were passaged using either Pasteur pipettes (Scientific Laboratory Supplies Limited, Nottingham, UK) or soda lime glass beads (Sigma-Aldrich) after treatment with 0.5mg/ml CIV. The glass beads were prepared and sterilised before use. Firstly, the beads were incubated with concentrated 3.8M Hydrochloric acid (HCL) overnight. The next day, equal amounts of 3.8M Sodium hydroxide (NaOH) was added and incubated for 10 minutes to neutralise the HCL. The mixture was discarded and tap water was allowed to run into the beaker containing the glass beads for a couple of hours. After rinsing, the glass beads were washed 4 times with distilled water (dH_20). dH_20 was left with the glass beads to soak overnight. The following day, the glass beads were washed twice with dH_20,

autoclaved and dried. Approximately 15-20 glass beads were filled into capped cryovials (Greiner Bio-One) and subsequently autoclaved and dried for use in hESCs passaging.

2.1.6 Thawing vitrified hESCs onto feeders

Inactivated MEFs were prepared and seeded onto gelatinised In-vitro fertilisation (IVF) dishes (Corning, NY) at a cell density of 50,000/dish prior to thawing hESCs. On the day of thawing, MEF medium in which the MEFs were seeded in was replaced with hESC medium after washing once with D-PBS and placed in the 37ºC incubator for at least half an hour. hESC medium contained knockout DMEM and supplemented with 20%**v/v** Knockout Serum Replacement (KoSR), 1% **v/v** Non-essential amino acid, 1mM Glutamax, 0.1mM β-mercaptoethanol (Gibco, Invitrogen) and 4ng/ml hbFGF. Warm hESC medium was also aliquoted onto 1-2 wells of a 24-well plate where vitrified hESCs were thawed into and left in the incubator for 5 minutes. The thawed pieces of hESCs in the 24-well plate were immediately transferred onto the previously prepared MEF feeders in IVF dishes. The freshly thawed cells were allowed to settle overnight in the 37ºC incubator and medium was changed the day after next. During the routine maintenance of hESCs, medium was changed daily and cells were passaged onto new MEF feeders every 3-4 days. hbFGF was added to the medium fresh daily.

2.1.7 Passaging hESCs onto fresh MEFs

The Shef-3 human embryonic stem cell line was obtained from the United Kingdom Stem Cell Bank (UKSCB, Hertfordshire, UK). Prior to passaging hESCs, the MEF medium in the freshly prepared 25cm^2 MEFs flask was replaced with hESC medium after washing once with D-PBS and kept in the 37ºC incubator. hESCs were treated with 0.5mg/ml CIV after the removal of spent medium and incubated for 5 minutes at 37ºC. CIV was removed and hESC medium was added to the flask. hESCs were then either mechanically passaged at a ratio of 1:2 using pasteur pipettes under the dissection microscope (Nikon, Japan) or

glass beads and transferred to the freshly prepared MEFs. The cells were allowed to settle and attach overnight in the 37ºC incubator and the hESC medium was only changed the day after next.

2.1.8 Freezing stocks of hESCs with 10% Dimethyl sulfoxide

Spent medium was removed from flask and hESCs were incubated with CIV for 30 minutes until the edges of hESCs colonies start to curl. After the replacement of CIV with hESC medium, undifferentiated hESC colonies were passaged into larger than usual sized clumps using the pasteur pipette. The passaged cells were collected and spun at 50g for 5 minutes. The cell pellet was washed once with D-PBS and centrifuged again. The supernatant was removed and the cell pellet was resuspended in cold freezing medium consisting of 10% **v/v** Dimethyl sulfoxide (DMSO; BDH) and FBS. The hESCs suspension was split into cryovials at a ratio of 1:3, placed into a freezing container (NUNC) and stored at -80^{o}C freezer overnight. Next day, the cryovials were transferred into liquid nitrogen for long-term storage.

2.1.9 Thawing hESCs from frozen cryovials onto MEFs

Upon immediate retrieval of the frozen cryovials from liquid nitrogen, hESCs in the vials were thawed in a 37 ºC water bath. The thawed hESCs suspension was added slowly to pre-warmed MEF medium. The thawed cell mixture was centrifuged at 50g for 5 minutes and the supernatant was subsequently removed. The cell pellet was gently resuspended in pre-warmed hESC medium and seeded onto freshly prepared MEF flasks. Medium was changed only the day after next. Freshly thawed hESCs might take 1 week for colonies to surface.

2.2 Differentiating hESCs into vascular cells

2.2.1 Differentiation of hESCs towards the endothelial lineage

Matrigel™ Basement Membrane Matrix (BD Biosciences, Bedford, MA) was diluted at 1:50 and coated on 75cm^2 flasks for 3 hours at 37ºC. Meanwhile, undifferentiated hESCs were passaged as previously mentioned using pasteur pipettes except that each of the pieces were cut smaller than usual at approximately 200-300 cells. The passaged hESCs were collected and centrifuged at 50g for 5 minutes. The supernatant was removed and the cell pellet was resuspended in complete Endothelial Growth Medium-2 (EGM-2; Lonza, Walkersville, MD). hESCs were counted using the hematocytometer and seeded onto the prepared Matrigel™ coated flasks containing EGM-2. Cells were seeded at densities of 1.3 x 10^6, 1.0 x 10^6, 8 x 10^5, 8 x 10^5 and 6 x 10^5 per 75 cm^2 for differentiation days 3, 5, 6, 7, 9 respectively. During differentiation, the medium was changed every other day

2.2.2 Differentiation of hESCs towards the smooth muscle lineage

75cm^2 flasks were coated with 10µg/ml of Collagen type IV (BD Biosciences, Bedford, MA) for 3 hours. Undifferentiated hESCs were collected via mechanical scraping using pasteur pipettes after 5 minutes incubation with Collagenase IV. hESCs were passged to obtain small colonies of 200-300 cells each. Before seeding, cells were collected and centrifuged at 50g for 5 minutes. Supernatant was removed and cells were resuspended in differentiation medium containing α-Minimum Essential medium (Gibco, Invitrogen), 0.05mM β-mercaptoethanol (Gibco, Invitrogen) and 10%v/v Fetal Bovine Serum (Gibco, Invitrogen). hESCs were counted using the hematocytometer and were seeded at densities of 1.3 x 10^6, 1.0 x 10^6, 8 x 10^5, 8 x 10^5 and 6 x 10^5 per 75 cm^2 for differentiation days 3, 5, 6, 7, 9 respectively. During differentiation, the medium was changed every other day.

2.3 Real-time quantitative-Polymerase Chain Reaction (RT-qPCR) analysis

2.3.1 Extraction of Ribonucleic acid from samples

Cell scrappers were sterilised in 70% Ethanol for a few minutes and rinsed in cold 1X PBS. Medium from 75cm^2 flasks where cells were grown in were discarded and the flask was washed once with 1X PBS to remove any remaining dead cells. Cells were scrapped in cold PBS as most enzymes were active at room temperature. The cells were collected into 15ml tubes and centrifuged at 1000 rpm for 5 minutes. Supernatant was discarded and the cell pellet was either stored at -80 ºC or followed with RNA extraction.

All work involved with Ribonucleic acid (RNA) was carried out in a sterile or RNase free manner. Prior to carrying out RNA extraction, the work area was first disinfected using 70% Ethanol. Sterile and autoclaved pipette tips and eppendorf tubes were used to prevent RNA degradation. RNA was extracted using RNeasy Mini Kit (Qiagen, Valencia, CA). The cell pellet was loosened by vortexing. 500µl of Buffer RLT was added to lyse the cells and vortexed to mix. Each sample was transferred into a QIAshredder spin column placed in a 2 ml collection tube, and centrifuge for 1.5 minutes at 13.2 revolutions per minute (rpm), room temperature. 500µl of 70% Ethanol was added to the collected supernatant to precipitate the RNA. The mixture was pipetted for at least 25-27 times and precipitation was observed. 700µl of each sample was transferred into RNeasy Spin Column and centrifuged for 0.5 minute for 13.2 rpm. This step was repeated until all remaining individual samples were centrifuged through the column. 700µl of wash Buffer RW1 was added to each RNeasy spin column and spun at 13.2 rpm for 30 seconds. A new collection tube was changed for each column. 500µl of Buffer RPE was added to each RNeasy spin column and centrifuged for 0.5 minutes at 13.2 rpm. The flow-through was discarded. Another 500µl of Buffer RPE was added into each column and spun for 2 minutes at 13.2 rpm. Flow-through was discarded and each RNeasy spin column was transferred to a new 2ml collection tube. 45µl of RNase-free water was aliquoted to the center of the column

and left to incubate for 1 minute. The tubes were spun for 2 minutes for 13.2 rpm and the RNA samples were stored -80 ºC

2.3.2 Reverse Transcription-Polymerase Chain Reaction

RNA samples were thawed in ice after retrieval from -80 ºC and mixed by vortexing. Prior to measuring the RNA concentration, 5µl of RNA sample was diluted to 500µl with RNase-free water (1:100 dilution). The RNA concentration was determined using the spectrometer (Bio-rad). 2.5µg of RNA was diluted with RNase-free water to make a total volume of 8µl before adding 2µl of Random Primers (50ng/µl, Promega, Madison, WI, USA). The mixture was vortexed to mix and incubated for 5 minutes at 70ºC in a heating block (Techne, Staffordshire, UK) which destabilised mRNA secondary structures and enhanced primer binding to mRNA. After heating, the mixture was quickly placed on ice for 5 minutes. Meanwhile, the master mix for the reverse transcription reaction was prepared. The master mix of one reaction contained 19µl of RNase-free water, 2µl of 25mM 2'-deoxynucleoside 5'-triphosphate (dNTPs; Invitrogen), 10µl of 5X Reaction Buffer, 6µl of 25mM Magnesium Chloride ($MgCl_2$), 2µl of ImProm-II reverse transcriptase and 1µl of RNasin Plus RNase Inhibitor (Promega, Madison, WI, USA). The master mix was mixed and aliquoted at 40µl into each tube of the prepared RNA sample. The samples were placed into the thermal block of a Thermal Cycler (Techne, Staffordshire, UK) which has a programme set at 25ºC for 5 minutes for annealing to occur and followed by an extension at 42 ºC for 90 minutes. The reaction was stopped by denaturing the enzyme at 70ºC for 15 minutes. The final concentration of each synthesised complementary Deoxyribonucleic acid (cDNA) samples was 50ng/µl. Samples were stored at -20 ºC.

2.3.3 Real-time Polymerase Chain Reaction (qPCR)

Real-time PCR also known as quantitative-PCR, was carried out on ice at all times. The work area was disinfected with 70% Ethanol and autoclaved pipette tips and eppendorf tubes were used. cDNA samples were thawed from -20ºC and diluted with RNase-free water to a working concentration of 10ng/µl. The master mix for one reaction of a real-time PCR was made using 7.5µl RNase-free water, 12.5µl SYBR® Green PCR Master mix (Applied Biosystems), 1.5µl of 2µmol forward primer and 1.5µl of 2µmol reverse primer (Primer sequences are listed below in Table 2). The master mix was mixed by vortexing and aliquoted at 23µl for each reaction in a well of a MicroAmp® Optical 96-well Reaction Plate (Applied Biosystems). Each sample was carried out in duplicates. 2µl of 10ng/µl sample cDNA was added last to its respective wells. The 96-well plate was sealed with a cover film and centrifuged at 700g for 1 minute to collect all reaction mixtures at the bottom of the plate. ABI Prism 7000 (Applied Biosystems) was used to run the PCR reaction with one cycle programmed to run at at 50ºC for 2 minutes, 95ºC for 10 minutes and 40 cycles each of 95ºC for 15 seconds and 60ºC for 1 minute. The real-time PCR programme was run after the 96-well plate was inserted into the plate holding area. After the reaction has completed, the real-time PCR result was analysed with the ABI Prism 7000 SDS software. Housekeeping gene 18S was used as normalisation control.

Table 2. Primer sequences used in real-time PCR.

human CD144	Forward: ATGAGAATGACAATGCCCCG
	Reverse: TGTCTATTGCGGAGATCTGCAG
human CD146	Forward: TTCCACTGCCAGTCCTCATACC
	Reverse: CACACAATCACAGCCACGATG
human vWF	Forward: TGCGAAGTACCTTGGTTACCCA
	Reverse: TAATCGTCAGTACATGCCCCG

human Kdr	Forward: TGCGAAGTACCTTGGTTACCCA
	Reverse: TAATCGTCAGTACATGCCCCG
hu Nanog	Forward: AAGGTCCCGGTCAAGAAACAG
	Reverse: GCTGGAGGCTGAGGTATTTCTG
human SMA	Forward: TGAGCGTGGCTATTCCTTCGT
	Reverse: GCAGTGGCCATCTCATTTTCAA
human SM Calponin	Forward: ATTTTTGAGGCCAACGACCTG
	Reverse: CCCACGTTCACCTTGTTTCCT
human MYH11-SM2	Forward: AACTTCGCAGTGATGCACCAG
	Reverse: CCATTGAAGTCTGCGTCTCGA
human PDGFR-beta	Forward: GCAATGTGACGGAGAGTGTGAA
	Reverse: AGCAAATTGTAGTGTGCCCACC
human 18S	Forward: CCCAGTAAGTGCGGGTCATAA
	Reverse: CCGAGGGCCTCACTAAACC

2.4 Protein expression analysis

2.4.1 Staining hESCs to determine their pluripotent or differentiated states

2.4.1.1 Immunofluorescence staining for pluripotency markers in undifferentiated hESCs

For staining undifferentiated colonies of hESCs were cultured for 4-5 days on mouse feeders grown in 8-wells chamber slides (NUNC, Rochester, NY, USA). Spent medium was aspirated and hESCs were fixed in 4%v/v paraformaldehyde (Sigma-Aldrich) for 15 minutes at room temperature. After fixing, cells were washed twice for 5 minutes with 1X PBS. 0.1%v/v Triton X-100 in 1× PBS (Sigma-Aldrich) was used to permeabilise hESCs for 10 minutes at room temperature. Cells were washed twice for 5 minutes with 1X PBS and blocked with either 4% normal rabbit or swine serum (Dako, Denmark). After blocking for 30 minutes at room temperature, cells were incubated with primary antibodies diluted in blocking solution. The primary antibodies used were directed against Stage-specific embryonic antigen-4 (SSEA4; 1:50), TRA-1-60 (1:50), TRA-1-81 (1:50), SRY-box containing gene 2 (Sox 2; 1:800), Stage-specific embryonic antigen-1 (SSEA1; 1:100; all five antibodies were from Chemicon), Octamer 3/4 (Oct3/4; 1:50; Santa Cruz Biotechnology, CA), VEGFR1 (1:50) and VEGFR2 (1:50), both from Abcam, Cambridge, UK) for an hour. Following incubation with primary antibodies at room temperature, cells were washed thrice for 5 minutes. Cells were later incubated for another hour at room temperature with secondary antibodies diluted in 1X PBS. The secondary antibodies used were Polyclonal Rabbit Anti-Mouse Immunoglobulins Tetramethyl Rhodamine Iso-Thiocyanate (TRITC), Polyclonal Swine Anti-Rabbit Immunoglobulins TRITC and Polyclonal Swine Anti-Rabbit Immunoglobulins Fluorescein isothiocyanate (FITC; all secondary antibodies used were from Dako, Denmark). These isotype IgG antibodies were substituted as primary antibodies for negative controls. Cells were washed thrice for 5 minutes with 1X PBS and stained with 4,6-diamidino-2-phenylindole (DAPI; 1:1000; Sigma-Aldrich) for 3 minutes. After two further washes with 1X PBS, cells were mounted using Fluorescence Mounting Medium (Dako, Denmark). Fluorescence images were viewed using fluorescent microscope (Axioplan 2 imaging; Zeiss).

2.4.1.2 Determining alkaline phosphatase activity in undifferentiated hESCs

hESCs were fixed with a 4%v/v paraformaldehyde for 1-2 minutes, aspirated and rinsed once with PBS. Alkaline phosphatase reagents (Chemicon) were prepared by mixing Fast Red Violet with Naphthol phosphate solution and water in a 2:1:1 ratio. This staining solution was incubated with hESCs in the dark at room temperature for 15 minutes. Staining solution was removed, rinsed with PBS and cells were covered with PBS to prevent drying. Alkaline phosphatase (AP) activity in hESCs was observed under a microscope.

2.4.1.3 Immunofluorescence staining to detect vascular markers in differentiated hESCs

For derivation of endothelial cell lineage, undifferentiated hESCs were seeded in 8-wells chamber slides (NUNC, Rochester, NY, USA) and differentiated for 9 days while cultured in their differentiation medium as mentioned previously. The immunostaining procedure was carried out as previously mentioned in section 2.4.1.1. Most of the staining was carried out via the indirect method whereby 0.1%v/v Triton X-100 was used to permeabilise cells. Only cells to be stained with markers CD31/PECAM (1:20; Santa Cruz Biotechnology, CA), CD146 (1:300), CD144/VE-cad (1:20) and VEGFR2/Kdr (1:50; all three were from Abcam, Cambridge, UK), do not require the permeabilisation step (Direct method). The remaining endothelial markers used were vWF (1:60; Abcam, Cambridge, UK) and endothelial Nitric Oxide Synthase (eNOS; 1:200; Sigma-Aldrich). Markers used to stain for smooth muscle cells were Smooth Muscle α-Actin (1:100; Sigma-Aldrich), Smooth Muscle Myosin Heavy Chain II (SM MHC; 1:100; AbD Serotec, Oxford, UK) and Calponin (1:600; Abcam, Cambridge, UK).

2.4.2 Western blot and immunodetection

Prior to carrying out western blot, proteins were extracted from cell samples on ice. Cell pellets were collected from scrapping cells grown in 75cm^2 flasks using cell scrapers. The cell pellets were either stored at -80^{o}C or continued with protein extraction. The cell pellet

was mixed with 100µl of lysis buffer and sonicated at 4^{o}C to disrupt cell membranes which resulted in the release of protein contents. After which, the lysates were left on a rotator and incubated for 40 minutes at 4^{o}C to lyse. Samples were centrifugated at 4^{0}C, 13.2rpm for 9 minutes to remove cell debris and 100µl of protein supernatant was collected into pre-cooled microtubes. Concentrations of proteins were measured in duplicates using the BIORAD Protean assay solution (Bio-rad, Herts, UK) diluted at 1:5. 2µl of each protein sample was added to 998µl of the diluted BIORAD Protean assay solution (1:500 dilution). The mixtures were vortexed and incubated for 10 minutes. Protein contents were measured using the spectrophotometer (Bio-rad, Herts, UK) which has a Bradford standard protein curve readings already stored in the machine. Lysis buffer and 5X sodium dodecyl dulfate (SDS) loading dye were then added into each sample.

Protein samples were either stored at -80ºC or continued with electrophoresis. Prior to loading wells of a 4-12% NuPAGE® Novex Bis-Tris Mini Gel (Invitrogen), samples were denatured at 96 ^{O}C for 7 minutes, vortexed and centrifuged. After setting up the XCell SureLock™ Mini-Cell (Invitrogen) electrophoresis apparatus and gel, 40µg of each protein sample as well as a Precision Plus Protein™ Protein Standard marker (Bio-rad) was loaded into the wells of the gel. The distance migrated through the gel is strictly dependent upon the molecular weight of the protein. The gel was run at 160V for 2 hours in running buffer. After which, the proteins were transferred from the gel onto nitrocellulose membranes (GE Healthcare) using the XCell II™ Blot Module (Invitrogen) blotting apparatus. Blotting pads, filter papers and membranes were pre-soaked in transfer buffer and assembled as shown in Fig.6. The surface of the gel was also wetted with transfer buffer and all trapped air bubbles in the setup were removed by rolling over the surface with a roller. The proteins were electrotransferred in transfer buffer for 3 hours at 25V, 400mA.

Fig. 6. A pictorial representation of setting up a western blot transfer assembly

The negatively charged molecules will migrate out from the gel and move towards the positive electrode which gets deposited on the nitrocellulose membrane.

XCell II™ Blot Module Manual, Invitrogen

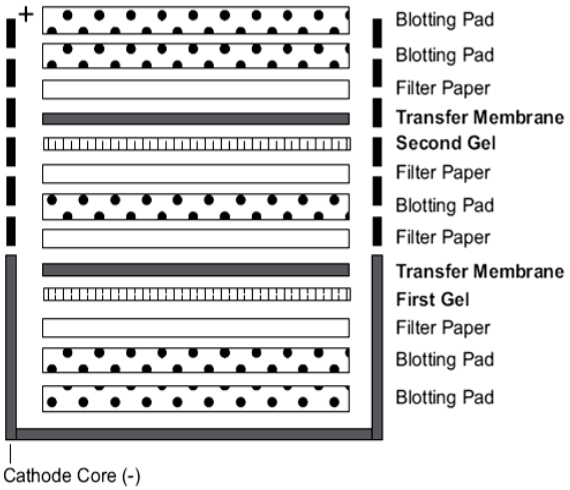

After electrotransfer, the nitrocellulose membrane was blocked with the proteins facing upwards, in 5%**w/v** milk (Marvel) in PBST on a three-dimensional rocker. After 1 hour, the membrane was incubated with the respective primary antibodies on the slow rocker overnight at 4ºC. Endothelial markers and their respective concentration used were CD31/PECAM (1:200), CD144/VE-cad (1:200; both from Santa Cruz Biotechnology, CA), eNOS (1:2000; Sigma-Aldrich) and CD146 (1:1000), vWF (1:1000), Kdr (1:500; all three were from Abcam, Cambridge, UK). Markers used for detecting smooth muscle cell proteins were Smooth Muscle α-Actin (1:2000; Sigma-Aldrich), Smooth Muscle Myosin Heavy Chain II (1: 150; AbD Serotec, Oxford, UK). Glyceraldehyde 3-phosphate dehydrogenase (GAPDH) was used as a housekeeping protein (1:500; Santa Cruz Biotechnology, CA). The next day, the membrane was washed 3 times with PBST for 10 minutes each wash. Secondary horseradish peroxide conjugated antibodies were incubated with the membrane at room temperature on the rocker. After 1 hour, the membrane was washed again 3 times with PBST for 10 minutes each wash. Finally, the membranes were exposed for 2 minutes with ECL-Plus reagents (Amersham Biosciences, Stockholm, Sweden) which aid in detecting proteins in the presence of the secondary horseradish peroxide conjugated antibodies. The excess reagent was removed from the membrane, wrapped in plastic film and secured in an autoradiographic cassette. In the dark room, membranes were exposed to Hyperfilm ECL (GE Healthcare) for normally 2-10 minutes

(depending on signal strength) and the protein bands were developed using the developer machine (Xograph healthcare, UK).

2.4.3 Flow cytometry

Flow cytometry was carried out either using the direct or indirect method depending on the antibody of interest. For both methods, cells were detached by incubating with Collagenase IV for 10 minutes followed by trypsin-EDTA (Gibco, Invitrogen) for another 10 minutes. The number of cells was counted and centrifuged at 1000 rpm for 5 minutes. Cell pellet was washed once with cold PBS and spun again to remove supernatant. 5ml of cold 4% Paraformaldehyde was added and incubated on ice for 20 minutes. The mixture was centrifuged at 1000 rpm for 5 minutes to remove supernatant. Only for intracellular markers detection, 5ml of cold permeabilisation buffer containing 0.1% Triton X-100 in PBS was added to the cell pellet, vortexed and incubated for 15 minutes on ice. Removal of permeabilisation buffer was carried out by centrifugation at 1500 rpm for 5 minutes. Cells were resuspended in 10% FBS to adjust the cell concentration to 1x 10^7 per ml and incubated on ice for 20 minutes to block non-specific antibody binding. Cell suspension was aliquoted into individual glass tubes with each to stain for a different fluorochrome-conjugated antibody. Endothelial markers used were CD146 (1:1000), VEGFR2/Kdr (1:250), vWF (1:400; all three obtained from Abcam, Cambridge, UK), and CD31/PECAM (1:40), CD144/VE-cad (1:40) (both from Santa Cruz Biotechnology, CA). Markers used to stain for smooth muscle cells were Smooth Muscle α-Actin (1:50; Sigma-Aldrich) and SM MHC (1:50; AbD Serotec, Oxford, UK). Isotype IgG negative controls and/or additional negative control which do not require any addition of primary antibodies were also included. The cells and antibody mix were vortexed and incubated at room temperature in the dark. After 1 hour, 2ml of cold PBS was added to the mixture, vortexed and centrifudged at 1500 rpm for 5 minutes. Supernatant was aspirated and removal of any residual liquid from the cell pellet was achieved by dabbing glass tubes onto paper napkins. Appropriate secondary antibodies (1:50~100; Sigma-Aldrich and DAKO) resuspended in 100 µl of cold 10%**v/v** FBS were added into respective cell pellets and incubated for 30 minutes at room temperature in the dark. 1.5ml of cold PBS was added to each tube, mixed

and centrifudged at 1500 rpm for 5 minutes. Cell pellet was resuspended in 500µl of 1% Paraformaldehyde and analyzed with a flow cytometer (Becton Dickinson Immunocytometry Systems, Mountain View, CA). Flow cytometry analysis was carried out using the CellQuest software (Becton Dickinson Immunocytometry Systems, Mountain View, CA).

2.5 Fluorescence-activated cell sorter analysis (FACS)

Cells that had been differentiated for 12 days were detached by incubating with Collagenase IV for 5 minutes followed by trypsin-EDTA (Gibco, Invitrogen) for another 5 minutes. The number of cells was counted using haematocytometer and centrifudged at 50g for 5 minutes. Cell pellet was washed once with cold PBS and spun again to remove supernatant. Each staining reaction contain 1 x 10^6 cells which were resuspended in 100µl of PBS contaning 10% FBS and 0.1mM EDTA and incubated on ice for 20 minutes to block non-specific antibody binding. 1-1.5µg of the respective fluorochrome-conjugated antibody was added to each glass tube containing cells. Endothelial markers used were CD146 and vWF (Abcam, Cambridge, UK). Isotype IgG negative controls and additional negative control which do not require any addition of primary antibodies were also included. The mixture was vortexed and incubated on ice in the dark. After an hour, 500µl of cold PBS was added to each staining reaction and vortexed. The supernatant was removed after centrifudging each staining reaction at 50g for 5minutes. Next, the cell pellet was resuspended in 100µl of PBS contaning 10% FBS and 0.1mM EDTA. 2µl of secondary antibodies (1:50; Sigma-Aldrich) were added into each tube and incubateed for 30 minutes on ice in the dark. After which, cells were washed with 1xPBS and centrifuged to obtain cell pellet. The stained cell pellets were resuspended in PBS, filtered using 40µm cell strainers (BD Biosciences, Bedford, MA) and centrifuged again. The cells were resuspended in 500µl of PBS contaning 1% FBS and 0.1mM EDTA prior to using the cell sorter (Becton Dickinson Immunocytometry Systems, Mountain View, CA). Cells which were sorted using FACS were resuspended in EGM-2 medium containing an additional 12% FBS and seeded onto Collagen I coated wells to settle overnight.

2.6 Endothelial function tests

2.6.1 In-vitro EC function test

2.6.1.1 Formation of vascular structures using Matrigel™

Pre-chilled 24-well plates were coated with 100µl of Matrigel™ Basement Membrane Matrix (BD Biosciences, Bedford, MA) per well and incubated for 30 minutes at 37°C [94]. 3 x 10^5 CD146+ sorted cells were counted and plated into each well. These cells were allowed to settle for another 30 minutes in the incubator at 37°C. Thereafter, 400µl of EGM-2 medium (Walkersville, MD) were added to the settled cells and the formation of tubes was observed 24 hours later under a conventional microscope (Nikon, Japan).

2.6.1.2 Dil-labeled acetylated low density lipoprotein uptake and lectin staining

One day prior to staining, 8 x 10^4 CD146+ cells were seeded into each well of a collagen-I coated, 8-well glass-bottomed chamber slide (NUNC, Rochester, NY, USA) and allowed to settle overnight [94]. On the day of staining, culture medium was aspirated and the cells were washed once with D-PBS. 2.4µg of Dil-Ac-LDL (AbD Serotec, Oxford, UK) was dissolved in serum-free DMEM and added to the cells for an hour incubation at 37°C. The mixture was aspirated, and the cells were washed with D-PBS twice to remove any remaining Dil-Ac-LDL. The cells were fixed with 4%**v/v** formalin for 10 minutes and followed by one wash with D-PBS. Next, the cells were further incubated with 10 µg/ml of FITC conjugated Lectin from *Ulex europaeus* (Sigma-Aldrich) at 37°C. After an hour, the mixture was removed and the cells were washed with D-PBS. The cells were subsequently stained with DAPI (1:1000) and the slide was mounted. The stained cells were observed under a fluorescent microscope (Axioplan 2 imaging; Zeiss) and images were taken.

2.6.2 In-vivo EC function test

2.6.2.1 Labelling cells with PKH26 red fluorescent cell linker

Adherent CD146 cells were washed with D-PBS and trypsinised. After 4-5 minutes, the cells were washed once with DMEM (Gibco, Invitrogen), collected into a 50-ml tube and the total number of cells was determined using a haematocytometer. A DMEM mixture containing 3.5 x 10^6 cells was aliquoted into a seperate tube and centrifuged at 400x *g* for 5 minutes. In the meantime, 4 x 10^{-3}mM of PKH26 dye (Sigma, U.S.A) was prepared using Diluent C (PKH26 Red Fluorescent Cell Linker Kit; Sigma, U.S.A). PKH26 is a stable fluorescent dye with long aliphatic tails which incoroporates into the lipid regions of cell membrane [157]. Diluent C is an iso-osomotic aqueous solution designed to maintain cell viability while maximizing dye solubility and staining efficiency. The supernatant was aspirated and the cells were resuspended with 175µl of Diluent C. 175µl of the prepared PKH24 dye was immediately added to the resuspended CD146 cells, mixed by pipetting and incubated at 25 ^oC for 5 minutes. The staining reaction was stopped by adding an equal volume (350µl) of FBS (ATCC, Manassas, VA) and incubated for 1 minute. Next, the serum-stopped mixture was diluted with another equal volume (700µl) of complete medium containing DMEM with 15% FBS. The cells were centrifuged at 400x *g* for 10 minutes to remove staining solution. Supernatant was removed and the cell pellet was transferred to a new tube for three more washes. In each washing step, 10ml of complete medium was used to wash the cell pellet and centrifuged. Finally, the cell pellet was resuspended with 50µl of EGM-2 medium .

2.6.2.2 *In vivo* angiogenesis

PKH26 labeled cells (10^6 in 50µl) were mixed with 50µl of Matrigel (Becton Dickinson Labware) at 4°C, and subcutaneously injected into SCID mice. After 7 days, mice were sacrificed and the implants (Matrigel plugs) were harvested, frozen in liquid nitrogen and

prepared for H&E staining or used for detection of cell markers by immunofluorescent staining. All animal experiments were performed according to protocols approved by the Institutional Committee for Use and Care of Laboratory Animals. Project licence number 7016458.

2.7 microRNA analysis

2.7.1 microRNAs (miRNAs) isolation from samples

Adherent cells were scraped and the collected pellet was snap-frozen in liquid nitrogen for storage at -80ºC prior to miRNA isolation. The extraction of miRNA was achieved using mirVana™ Protein and RNA Isolation System™ Kit (Applied Biosystems, Ambion Inc). As miRNA is susceptible to degradation, the work area was disinfected with 70% Ethanol and RNase-free pipette tips and eppendorf tubes were used. Cell pellets were thawed and 625µl of ice-cold cell disruption buffer was added. Samples were vortexed to lyse the cells completely and to obtain a homogenous lysate. An equal volume of 2X denaturing solution at room temperature was immediately added to the lysate to prevent RNA degradation. After mixing, 1250µl of Acid-Phenol:Chloroform was added to the mixture and vortexed for 1 minute to mix. To separate the mixture into aqueous (upper) and organic (lower) phases, the mixture was centrifuged for 5 minutes at 13,000 rpm at room temperature. The upper aqueous phase was carefully removed and transferred into a fresh centrifuge tube. The volume of 100% ethanol (room temperature) to add to the aqueous phase was 1.25 times the volume of recovered aqueous phase. Each lysate/ethanol sample was mixed thoroughly and aliquoted onto a filter cartridge placed into one of the collection tubes. The mixture was centrifuged at 13,000 rpm for 30 seconds. The flow through was discarded and centrifugation was repeated until all of the lysate/ethanol samples had filtered through the cartridge. 700µl of miRNA Wash Solution 1 was added to the filter cartridge and centrifuged for 30 seconds. The flow through was discarded and the filter cartridge was washed with 500 µl Wash Solution 2/3. A repeat wash with 500µl Wash Solution 2/3 was carried out and flow through was discarded. Residual fluid was removed from the filter

cartridge by centrifuging the assembly for 1 minute. The filter cartridge was transferred into a fresh collection tube and 100µl of 95ºC preheated Elution Solution was aliquoted to the center of the filter. The miRNA eluate was recovered by centrifugation for 30 seconds and the concentration of miRNA in each sample was determined using the spectrophotometer. The samples were either stored at -80ºC or further processed.

2.7.2 cDNA synthesis and qPCR analysis of miRNAs

The NCode™ VILO™ miRNA cDNA Synthesis Kit (Invitrogen) was used to synthesise poly (A) tails of all the miRNAs followed by cDNA synthesis from the tailed population in a single reaction. Each single reaction contained 8µl of 5X Reaction Mix, 4µl of 10X SuperScript® Enzyme Mix, 2µg of microRNA and topped up to 40µl with DEPC-treated water. The contents were vortexed to mix and centrifuged briefly. The samples were placed into a PCR Thermal Cycler which has a programme set at 37ºC for 60 minutes, followed by termination of reaction at 95ºC for 5 minutes and the reaction was held at 4ºC until further use. The 50ng/µl cDNA was diluted to a working concentration of 10ng/µl and stored at -20ºC.

Quantitative real-time PCR was carried out as mentioned previously, except that each master mix reaction contained 10µl EXPRESS SYBR® GreenER™ qPCR SuperMix Universal, 1.5µl of 2µM/L miRNA-specific forward primer, 1.5µl of 2 µM/L Universal qPCR Primer (Primer sequences are listed in Table 3), 0.4µl of 25µM ROX Reference Dye and 4.6µl DEPC-treated water. The master mix was mixed by vortexing and aliquoted at 18µl for each reaction in a well of a MicroAmp® Optical 96-well Reaction Plate (Applied Biosystems). Each sample was carried out in duplicates. 2µl of 10ng/µl sample cDNA was added last to its respective wells. The 96-well plate was sealed with a cover film and briefly centrifuged. ABI Prism 7000 (Applied Biosystems) was used to run the PCR reaction with one cycle programmed to run at 50ºC for 2 minutes, 95ºC for 10 minutes and 40 cycles each of 95ºC for 15 seconds and 60ºC for 1 minute. After the reaction has

completed, the real-time PCR result was analysed with the ABI Prism 7000 SDS software. Housekeeping gene **5.8S** was used as normalisation control.

Table 3. Primer sequences used in miRNA qPCR.

human 5.8s	Forward: AGGACACATTGATCATCGACACTTCGA
has-mir-141	Forward: GCTAACACTGTCTGGTAAAGATGG
has-mir-205	Forward: CTTCATTCCACCGGAGTCTG
has-mir-150*	Forward: AGGCCTGGGGGACAGAA
has-mir-200c	Forward: CTGCCGGGTAATGATGGA
has-mir-1915	Forward: CGACGCGGCGGGAAA
pmiR-Luc-hZEB1	Forward: GACGACACGCGTGACTCAGAGAGCAACAATAC
	Rerverse: CTCCACAAGCTTGTTAGCACGGGTTGGAACTAC

2.7.3 Transfection of miRNA precursors or inhibitors into hESCs derived ECs

Transfection is the introduction of foreign DNA into a eukaryotic cell and an important tool for studying the regulation of gene and protein expression as well as function. Before the preparation of transfection complexes, day-6 of differentiating hESCs were trypsinised, filtered and counted. Cells were centrifuged, resuspended in EGM-2 medium and separated into three tubes, one to be prepared for 24 hours post transfection, 48 hours post transfection and the other for 72 hours post transfection. The cell density required per well of a 6-well plate was $2x10^5$ cells for 24 and 48 hours and $1.5\ x10^5$ cells for 72 hours. The prepared cell suspension was placed in 37 ºC incubator while preparing the transfection

complexes. Either miRNAs inhibitors or precursors and miRNA negative controls were transfected into differentiating hESCs using siPORT^{TM} NeoFX^{TM} transfection agent (Ambion, Applied Biosystems). For each reaction, 95µl of warm Opti-MEM (Gibco, Invitrogen) was mixed with 5µl of warm siPORT^{TM} NeoFX^{TM} agent by pipetting and incubated for 10 minutes at room temperature. While incubating, each miRNA inhibitors or precursors and miRNA negative controls (10µM/L, Ambion, Applied Biosystems) were diluted by adding 92.5µl Opti-MEM to 7.5µl 10µM miRNA inhibitors, precursors or negative controls per reaction. After incubating for 10 minutes, an equal volume of diluted siPORT^{TM} NeoFX^{TM} Transfection Agent was combined with an equal volume of the diluted miRNA. The mixtures were mixed by pipetting and incubated for 10 minutes at room temperature to allow transfection complexes to form. 200µl of transfection complexes were added in each well, followed by the addition of 2.3ml of prepared cells. The plates were gently tilted back and forth to evenly distribute the complexes and cells in the wells. Analysis of miRNAs inhibition or overexpression was carried out in 24, 48 and 72 hours post transfection and the collected samples were subjected to cDNA synthesis and real-time PCR detection as described previously.

2.7.4 Human ZEB1/TCF8 3'UTR vector

Reporter vector harboring sequences of the human Zinc finger E-box-binding homeobox 1 (ZEB1), or alternatively known as transcription factor 8 (TCF8), were created using human genomic DNA from 6-day pre-differentiated hESCs. The 3'-flanking untranslation region (3731bp/3993bp) of human ZEB1 gene was amplified by PCR with primers shown in Table 3 and cloned into the pmiR-reporter-basic vector (Ambion, Applied Biosystems), designated as pmiR-Luc-hZEB1. The vector was verified by DNA sequencing.

2.7.5 Luciferase activity assay

hESC-derived CD146-positive cells (40,000 cells per well of a 24-well plate) were co-transfected with pRenilla (25ng/well), pmiR-Luc-hZEB1 (150ng/well), and negative

control miR precursor, miR-200c precursor or miR-150* precursor (20nM), by using siPORT^{TM} NeoFX^{TM} transfection agent (Ambion, Applied Biosystems) according to the manufacturer's instructions. The cells were then cultured on collagen-I-coated 24-well plate for 48 and 72 hours. Luciferase and *Renilla* activities were detected after transfection using a standard protocol. Relative luciferase unit (RLU) was defined as the ratio of Firefly versus Renilla with that of the control set as 1.0. At least, three independent transfections were performed in triplicates.

2.7.6 In vivo transfection of miRNA inhibitors into developing chick embryos using Chorioallantoic membrane assay

Fertilized chick eggs were obtained from Joyce and Hill Farm and incubated at 38.5°C in a humidified incubator. Hamburger and Hamilton (HH) staging was applied throughout the experiment [158].

Before the start of the experiment, the eggs were incubated until around HH10. After sterilising the surface of the egg shell with 70% ethanol, a window was opened at the side of the egg with a blade. As described previously (in section 2.7.3), transfection complexes containing siPORT NeoFX Transfection Agent and miRNA miR200c inhibitor or control were made prior to the administration of the complexes. Using a microinjector, 100µl of miR200c inhibitor or control was injected beneath the the right hand side of the choroallantoic membrane (CM). The eggs were then sealed tight with tape and placed back into the 38.5°C incubator slowly, window side up. The eggs were incubated for the next few days until HH20. Photos were taken using Nikon stereomicroscope SMZ800 after exposing the CM. Then the left hemisphere of CM and right hemisphere of CM (the anterior/posterior omphalomesenteric vein is regarded as the middle line) were harvested separately for total RNA extraction for miRNA and mRNA identification. **Using a grayscale program in Adobe Photoshop, the area of observed blood vessels at both sides of the chick embryo were analysed.**

2.8 Contractililty assay for assessing smooth muscle cell function

Day 9 hESCs derived SMCs were cultured on collagen type IV coated 48-well plate and washed once with PBS prior to stimulation with the agonist. Potassium Chloride (KCl; BDH, AnalaR, Poole, England) was used as an agonist to assess the contractility ability of SMCs. A serial dilution of KCL in differentiation medium was used at 20mM/L, 40mM/L, 60mM/L and 80mM/L. Using the microscope camera (Nikon, Japan), images of the same field were captured prior to stimulation and during different time points of agonist-induction at 5 minutes, 15 minutes and 25 minutes.

2.9 Statistical analysis

All statistic analyses were carried out using GraphPad Prism 4.00 software (CA, USA). Data were presented as mean $\pm$ Standard error of the mean (SEM). Statistical significance was determined using statistical tests such as Student t test and One-way analysis of variance (Anova). P-values less than 0.05 were considered statistically significant.

CHAPTER 3

CHAPTER 3

Results

3.1 Undifferentiated hESCs express pluripotent markers

It is crucial to maintain and characterize the undifferentiated status of hESCs prior to undergoing any further experiments. To this end, the pluripotency of undifferentiated hESCs cultures was first determined by carrying out alkaline phosphatase (AP) and immunocytochemistry staining on undifferentiated hESCs grown on mouse embryonic feeders (MEFs). All hESCs colonies appeared reddish-purple after staining with the AP reagent, indicating that these colonies were positive for AP activity (Fig.7) which is one of the fundamental characteristics of undifferentiated hESCs. Moreover, a range of human ES cell-specific pluripotent surface markers such as SSEA4, TRA-1-60 and TRA-1-81, in addition with transcription factors OCT3/4 and SOX2, were also strongly expressed in undifferentiated hESCs cultures as demonstrated by immunofluorescence staining with the respective specific antibodies (Fig.8A). However, immunocytochemistry staining with the differentiated marker SSEA1 appeared negative (Fig.8B). These findings demonstrated that hESCs cultured using the current cell culture system is effective in maintaining pluripotent and undifferentiated hESCs. Hence, it also shows that these hESCs are suitable for further use in vascular cell lineage differentiation.

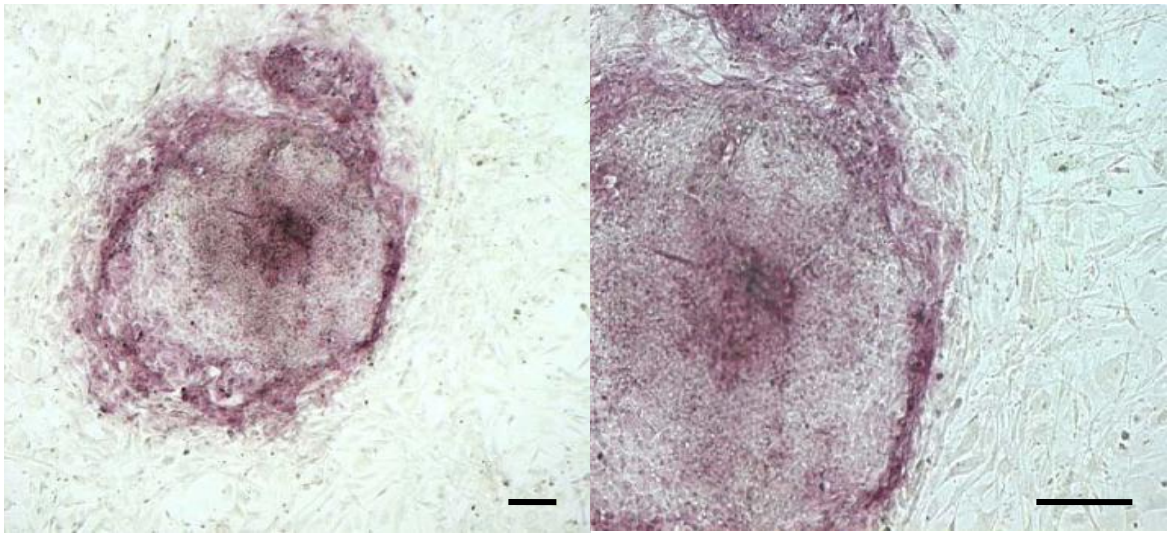

Fig. 7. AP activity in undifferentiated hESCs.

Undifferentiated hESCs colonies were grown on MEF monolayer for 5 days and stained with AP reagents. Images were taken under a conventional microscope. Bar = 100 μm

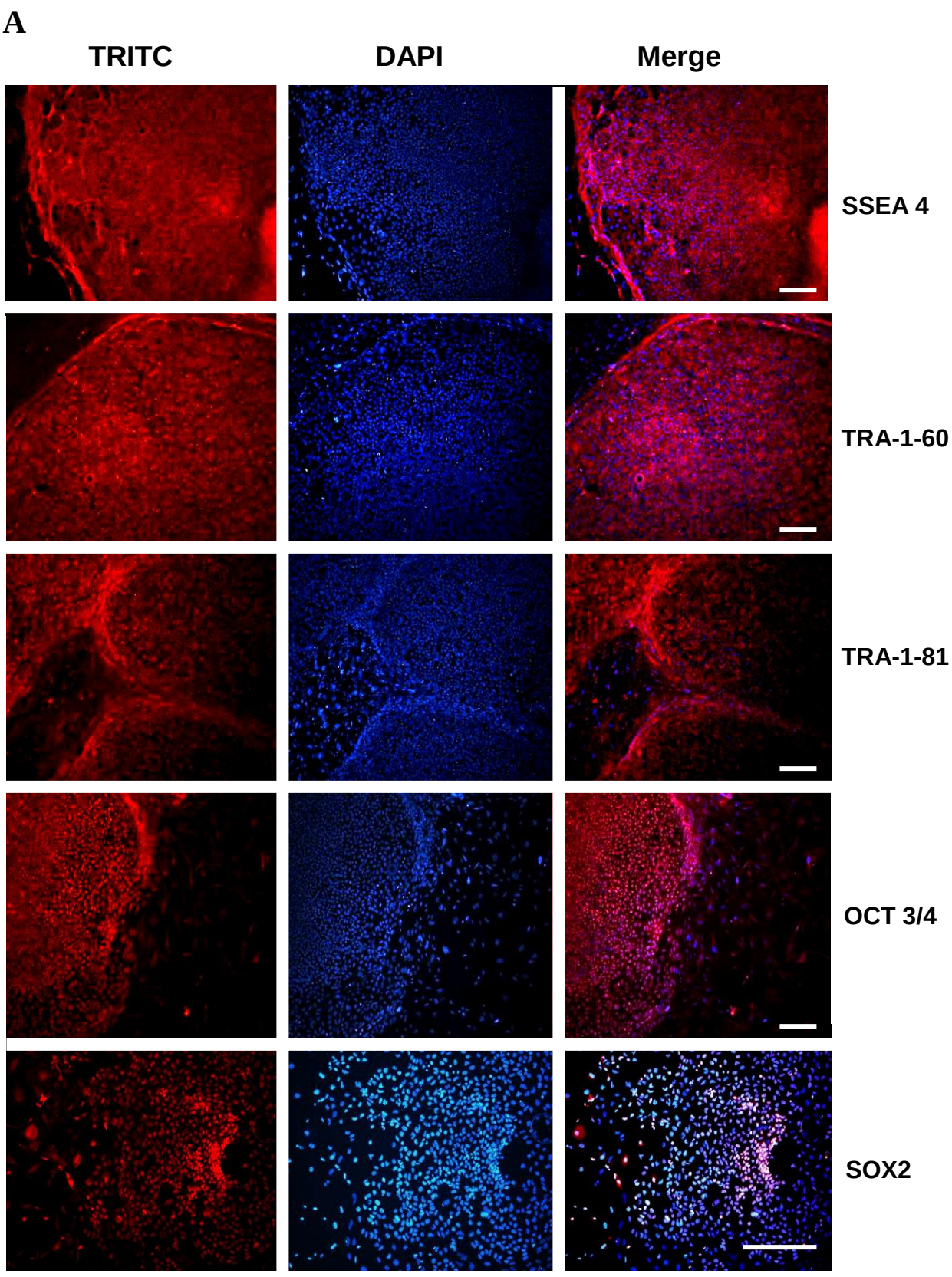
A
TRITC
DAPI
Merge
SSEA 4
TRA-1-60
TRA-1-81
OCT 3/4
SOX2

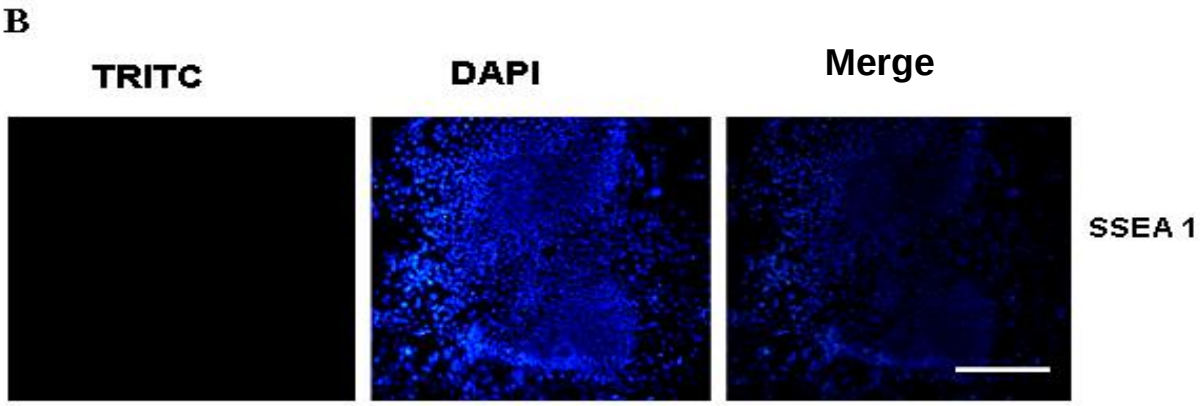

Fig. 8. Pluripotency status in undifferentiated hESCs culture.

(A) Undifferentiated hESCs were grown for 4 days on MEFs in the presence of human basic FGF-2 and immunostained with pluripotent markers (from *Top* to *Bottom*) SSEA4, TRA-1-60, TRA-1-81, OCT3/4 and SOX2. (B) Undifferentiated hESCs were also stained with SSEA1 (*left*) and counterstained with DAPI (*middle*). All images were taken under a fluorescent microscope. Bar = 150 μm.

3.2 hESCs differentiate towards the endothelial lineage

Pluripotent hESCs have the capability to differentiate into three germ layers, namely the ectoderm, endoderm and mesoderm. Based on this theory, undifferentiated hESCs were further cultured in EC differentiation medium (EGM-2) to derive ECs. During the 9 days period of differentiating hESCs towards the endothelial lineage, expression of EC markers was analysed to determine whether the differentiation protocol was successful in deriving ECs. A set of EC markers was analysed using real-time PCR (Figs 9-13), western blot (Fig.14), immunocytochemistry (Figs 15-20) and flow cytometry (Fig.21).

3.2.1 Endothelial-specific genes were upregulated in differentiating hESCs during different differentiation time points

To drive endothelial cell differentiation from hESCs, undifferentiated hESCs were plated onto Matrigel^{TM} Basement Membrane Matrix (BD Biosciences, Bedford, MA) coated dishes or plates and cultured in EGM-2 medium for the indicated experimental time-points. Total RNA and protein were extracted and subjected to RT-PCR and western blot analysis, respectively. Majority of the real-time RT-PCR analysis of mRNA levels in EC gene marker expression revealed a trend in increasing levels of CD144/VE-cad (Fig.9), vWF (Fig.11) and Kdr (Fig.12) as the period of differentiation increased. Gene expressions of CD144/VE-cad, vWF and Kdr at day 9 were significantly elevated as compared to expression at day 0 control levels (Figs. 9, 11, 12). mRNA level of CD146 expression however, was significantly increased at day 3, and declined at days 5, 7 and 9 (Fig.10.) In contrast, expression levels of undifferentiated marker Nanog were significantly decreased at days 5, 7, and 9 as compared to day 0 (Fig.13.). Taken togther, these data demonstrated an increase in the expression of several EC genes during hESCs differentiation, mostly reaching maximum levels at around day 9.

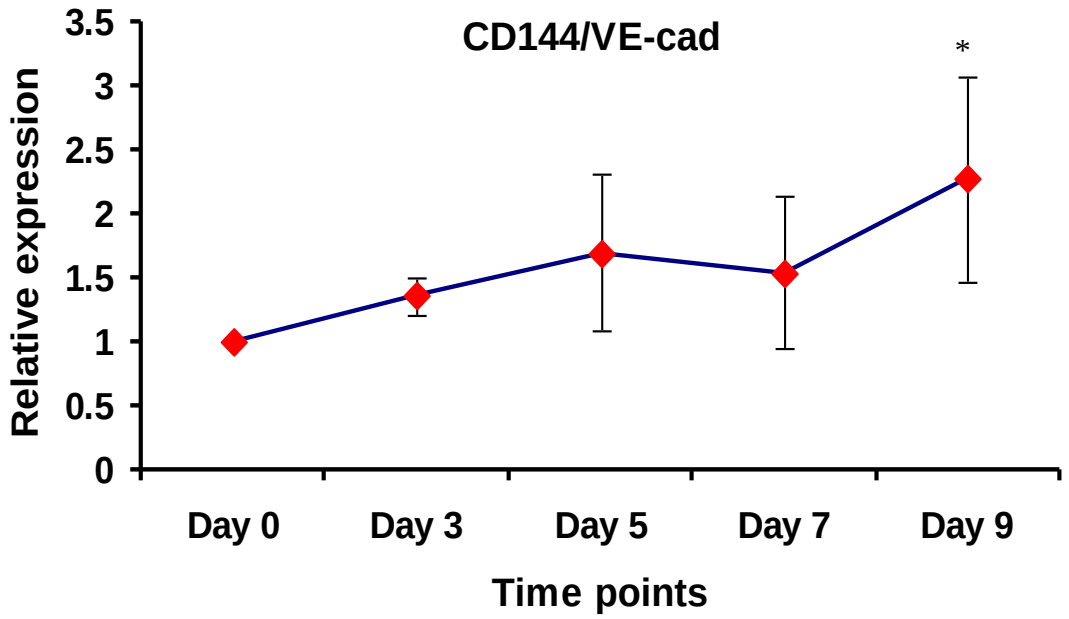

Fig. 9. Gene expression of CD144/VE-cad in differentiating hESCs over a period of 9 days.

Clumps of undifferentiated hESCs colonies were seeded on matrigel and cultured in EGM-2 medium for 3, 5, 7 and 9 days. During each respective time-point, RNA was extracted, reversed transcribed to cDNA as previously described and subjected to real-time PCR analysis. Day 0 (control) samples were obtained from undifferentiated hESCs. Data represent mean $\pm$ SEM of three independent experiments (n=3). Data normalized to 18S and presented relative to day 0 expression.* Relative expression of CD144/VE-cad at day 9 was significantly different from day 0; $p < 0.05$, One-way analysis of variance (Anova) followed by Bonferroni's Multiple Comparison Test.

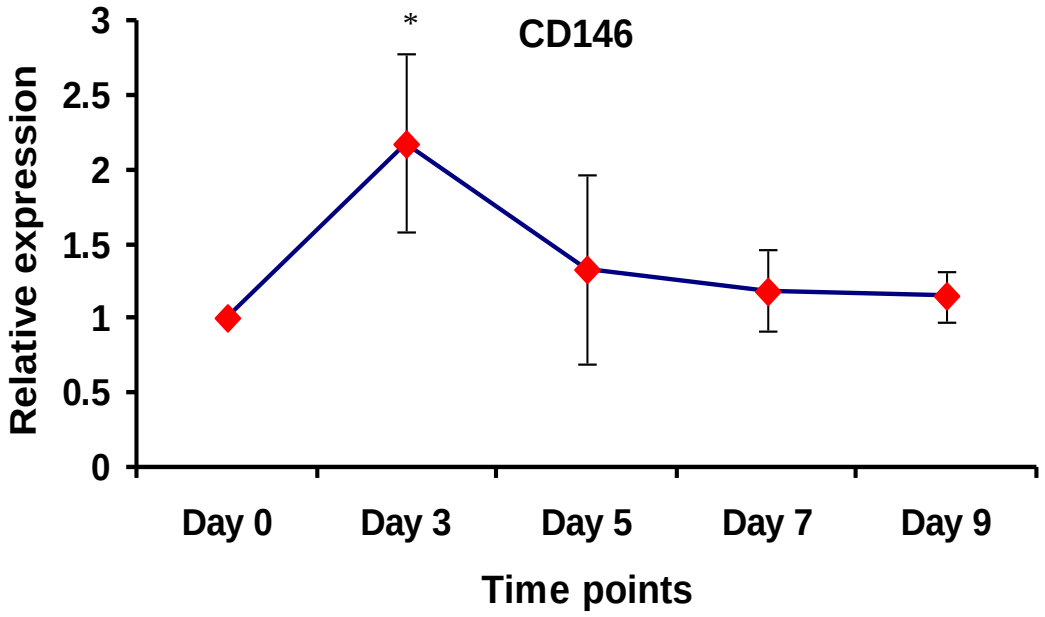

Fig. 10. Gene expression of CD146 in differentiating hESCs over a period of 9 days.

Data represent mean ± SEM of three independent experiments (n=3). Data normalized to 18S and presented relative to day 0 expression.* Relative expression of CD146 at day 3 was significantly different from day 0; $p < 0.05$, Paired t-test followed by one tailed test.

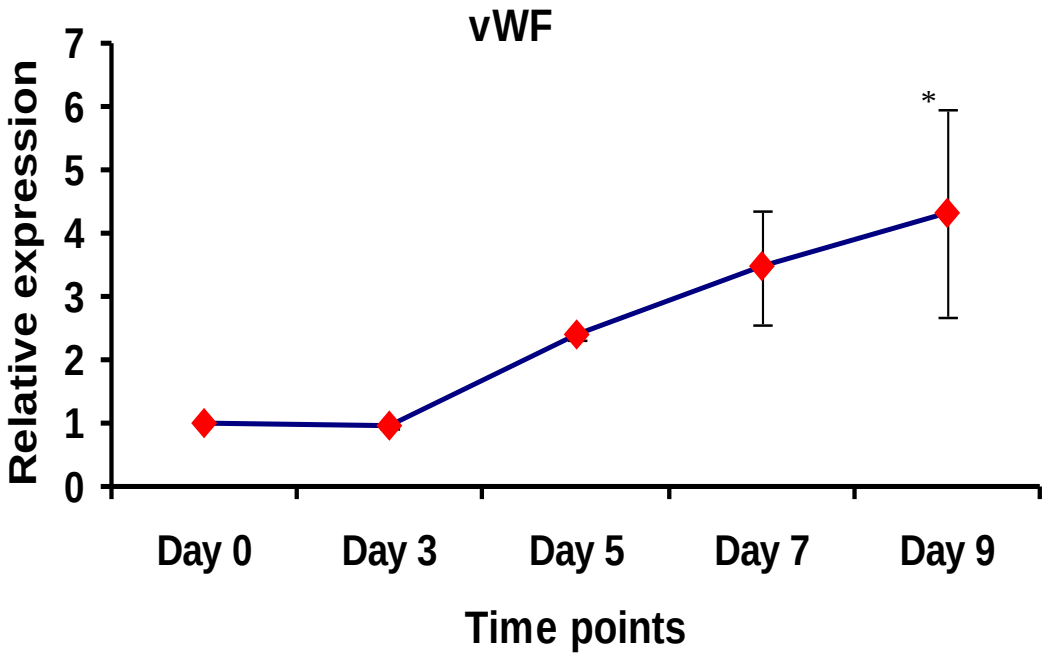

Fig. 11. Gene expression of vWF in differentiating hESCs over a period of 9 days.

Data represent mean ± SEM of three independent experiments (n=3). Data normalized to 18S and presented relative to day 0 expression. * Relative expression of vWF at day 9 was significantly different from day 0; $p < 0.05$, Paired t-test followed by one tailed test.

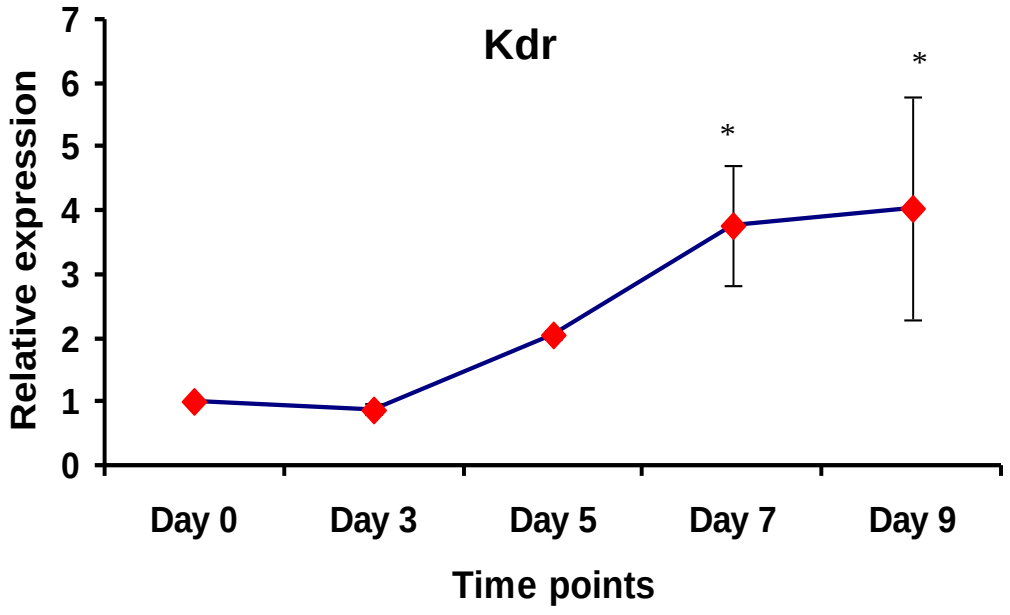

Fig. 12. Gene expression of Kdr in differentiating hESCs over a period of 9 days.

Data represent mean ± SEM of three independent experiments (n=3). Data normalized to 18S and presented relative to day 0 expression. * Relative expression of Kdr at days 7 and 9 were significantly different from day 0; $p < 0.05$, Paired t-test followed by one tailed test.

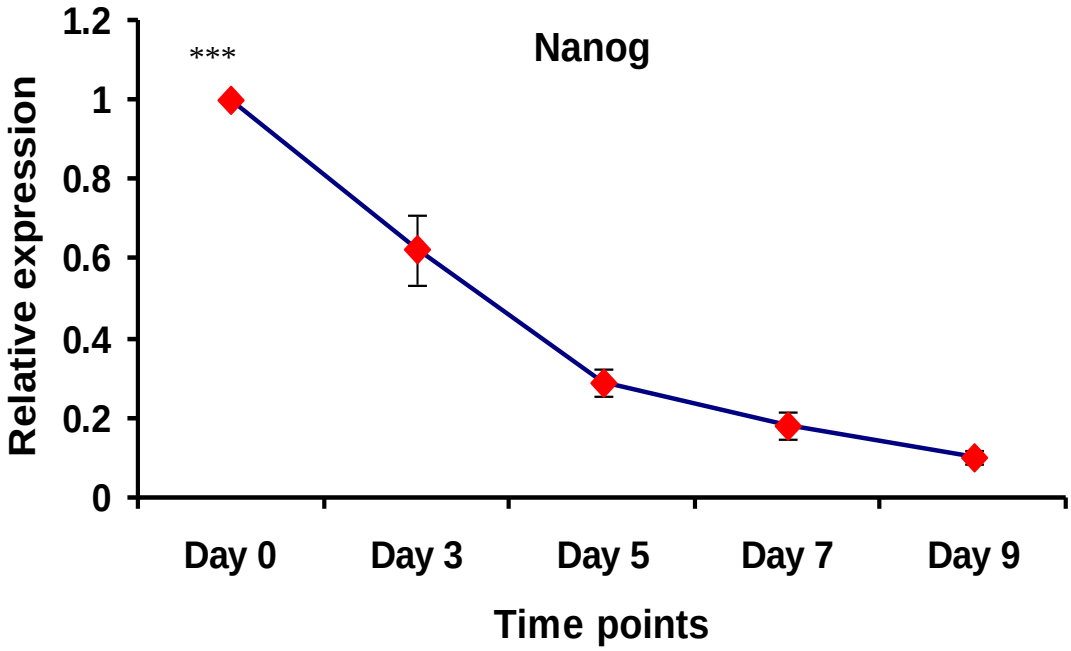

Fig. 13. Gene expression of Nanog in differentiating hESCs over a period of 9 days.

Data represent mean ± SEM of three independent experiments (n=3). Data normalized to 18S and presented relative to day 0 expression. *** Relative expression of Nanog at days 5, 7 and 9 were significantly different from day 0; $p < 0.001$, One-way Anova, followed by Bonferroni's Multiple Comparison Test.

3.2.2 Western blot analysis of endothelial-specific marker expression in differentiating hESCs during different time points

Since gene expression usually results in the subsequent formation of functional proteins, western blotting was carried out to determine the synthesis of each endothelial specific gene expression product. The majority of endothelial protein markers were expressed in an increasing trend as the period of differentiation lengthened (Fig.14). The mature endothelial

marker vWF has a molecular weight of 300kDa and was detected at days 5-9. The protein expressions of functional endothelial marker eNOS and two endothelial cell surface markers (CD31 and CD146), appeared at day 3 and increased gradually till day 9. However, a distinct band with a molecular weight of 130 kDa for CD144/VE-cad appeared later only at day 9. Taken together, the data strongly suggest that the endothelial cell lineage can be successful differentiated from hESCs. Importantly, all of the above mentioned EC markers were undetectable in control day 0 samples, which further confirm its undifferentiated state of human ES cells.

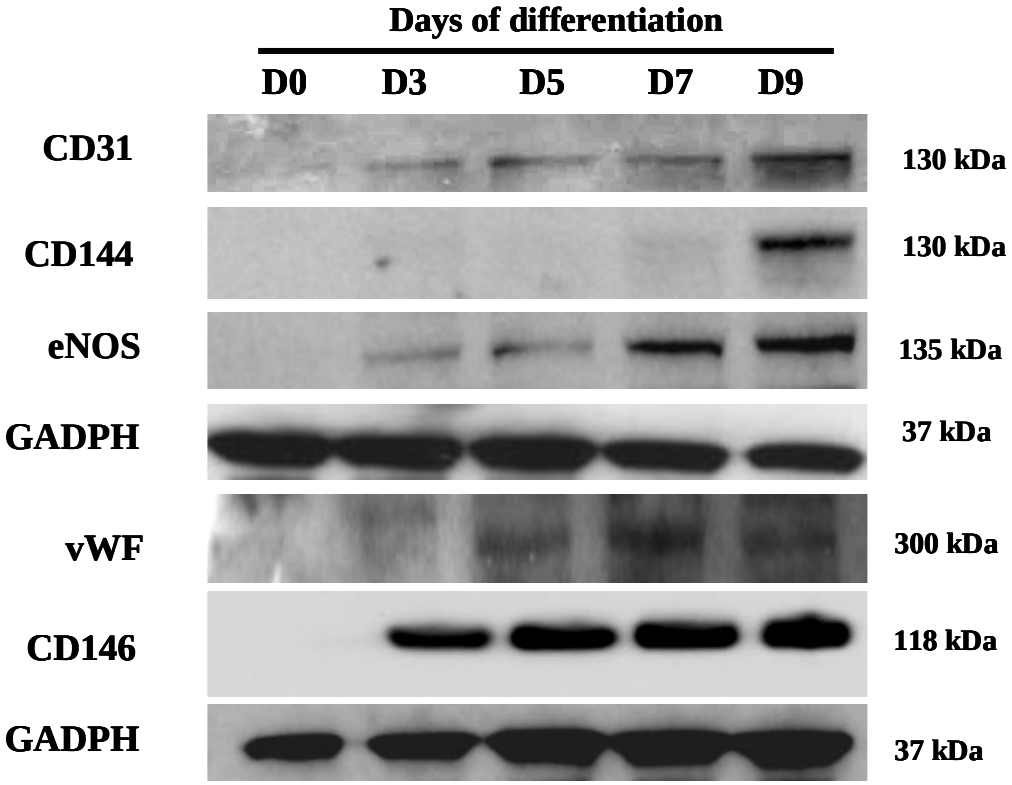

Fig. 14. Western blot analysis of hESCs derived ECs over a 9 day differentiation period.

Undifferentiated hESCs were differentiated in EGM-2 medium and grown over a period of 9 days. As previously described, protein samples were extracted from differentiating hESCs during days 3, 5, 7 and 9. 40μg of each protein sample was loaded into each well, blotted

and probed with endothelial specific antibodies CD31/PECAM-1, CD144/VE-cad, eNOS, vWF and CD146 (*Top* to *Bottom*). Each immunoblot was again reprobed with GADPH, a housekeeping protein to show the total sample loading in each well (*Lower panel*). Day 0 samples were obtained from undifferentiated hESCs. (n=3)

3.2.3 Immunocytochemistry staining on day 9 hESCs derived endothelial cells

In this study, data from RT-PCR and western blot analysis have showed upregulation of mRNA and protein levels of endothelial cell lineage-specific markers in the mixed population of differentiating hESCs under this culture condition. However, the visual localisation of these proteins and their expression patterns in individual cells were still unclear. To achieve this aim, immunocytochemistry was carried out in day 9 hESCs differentiated cells when most of the EC markers were maximally expressed as compared to day 0 control (Fig.9-14) with antibodies against endothelial cell lineage-specific markers. As expected, CD31/PECAM-1 was found distributed at the intercellular clefts (Fig.15) and CD144/VE-cad (Fig.16) as well as CD146 were localised at cell-cell adhesion sites (Fig.17). One of the mature EC marker, eNOS which regulates vascular tone, was found expressed in the cytoplasm compartment (Fig.18). Kdr was also detected on cell surfaces (Fig.19). Another mature marker vWF was found localised as large granules in the cytoplasm (Fig.20). In conclusion, day 9 hESCs derived ECs displayed the proper organisation of protein endothelial junctions.

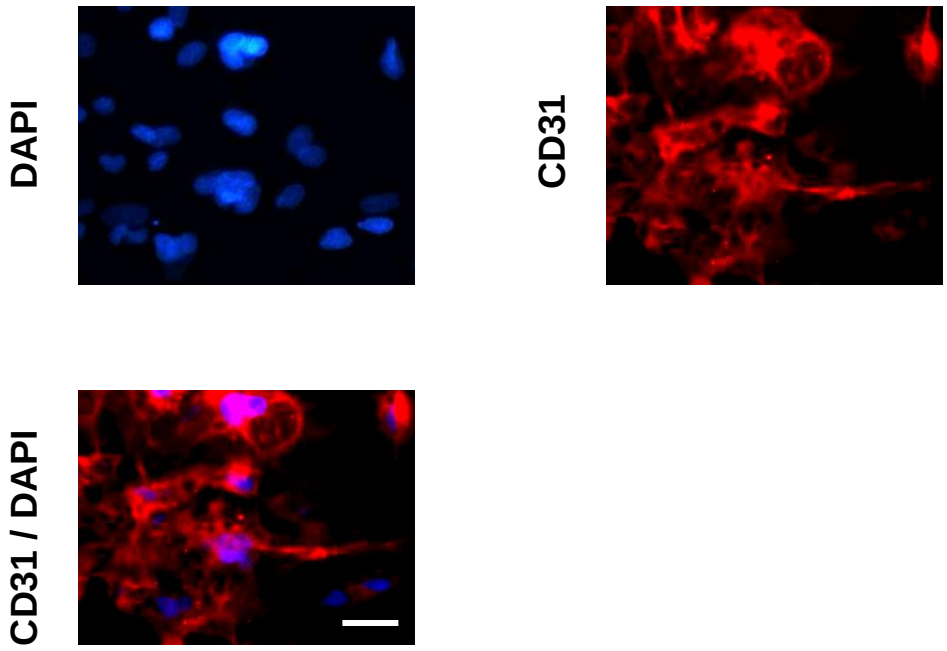

Fig. 15. Expression of CD31/PECAM-1 in hESCs-derived ECs.

Day 9 differentiated hESCs grown in EGM2 were probed with CD31/PECAM-1 primary antibody followed by polyclonal rabbit anti-goat IgG immunoglobulins TRITC. *Anti-clockwise from upper right.* Fluorescent images were captured on CD31/PECAM positive cells (upper right), nucleic acid stains (DAPI) in individual cell (upper left) and an overlapped image depicting the localisation of both CD31/PECAM-1 and DAPI. Bar = 20 µm.

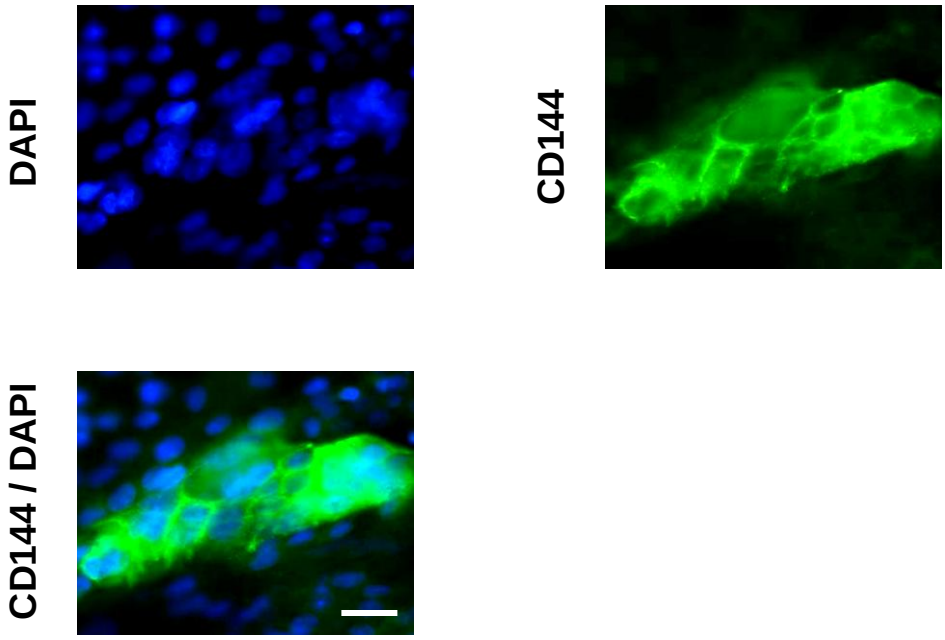

Fig. 16. Expression of CD144/VE-Cad in hESCs-derived ECs.

Day 9 differentiated hESCs grown in EGM2 were probed with CD144/VE-cad primary antibody followed by polyclonal goat anti-mouse IgG immunoglobulins FITC. *Anti-clockwise from upper right.* Fluorescent images were captured on CD144/VE-cad positive cells (upper right), nucleic acid stains (DAPI) in individual cell (upper left) and an overlapped image depicting the localisation of both CD144/VE-cad and DAPI. Bar = 20 µm.

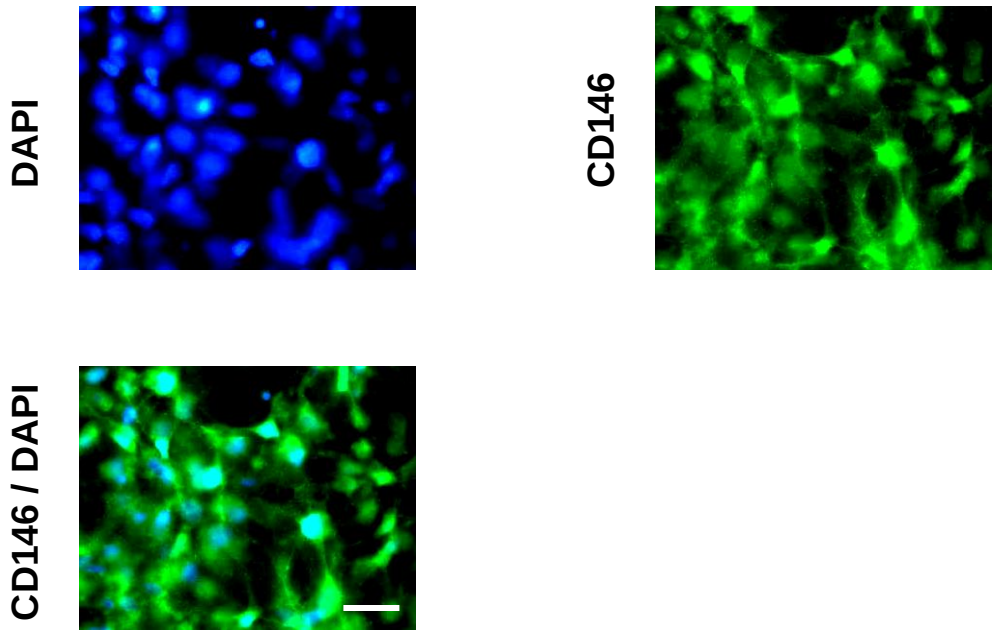

Fig. 17. Expression of CD146 in hESCs-derived ECs.

Day 9 differentiated hESCs grown in EGM2 were probed with CD146 primary antibody followed by polyclonal goat anti-mouse IgG immunoglobulins FITC. *Anti-clockwise from upper right*. Fluorescent images were captured on CD146 positive cells (upper right), nucleic acid stains (DAPI) in individual cell (upper left) and an overlapped image depicting the localisation of both CD146 and DAPI. Bar = 20 µm

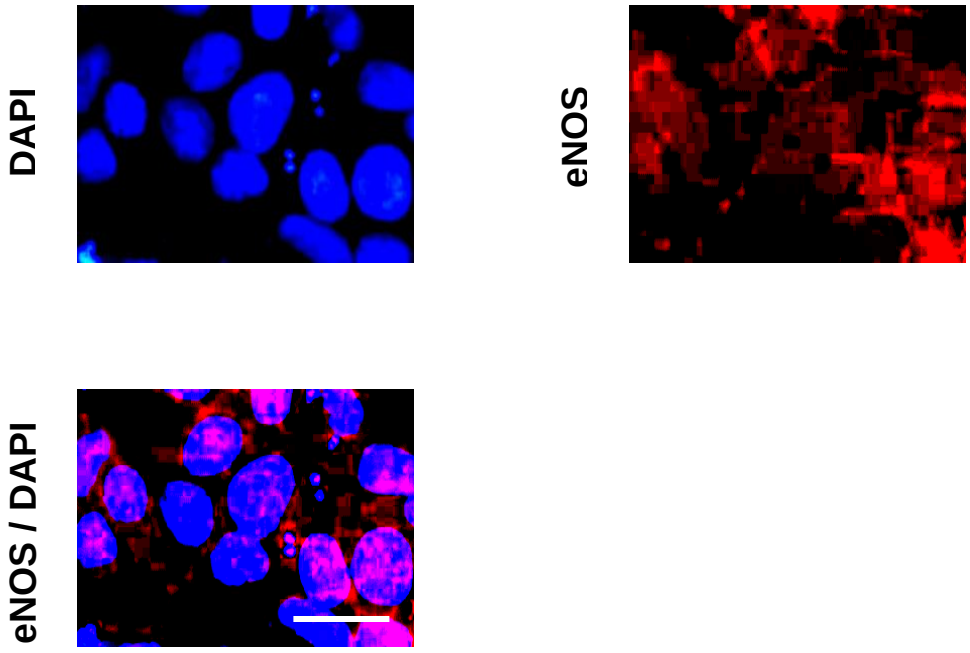

Fig. 18. Expression of eNOS in hESCs-derived ECs.

Day 9 differentiated hESCs grown in EGM2 were probed with eNOS primary antibody followed by polyclonal goat anti-Rabbit IgG immunoglobulins TRITC. *Anti-clockwise from upper right.* Fluorescent images were captured on eNOS positive cells (upper right), nucleic acid stains (DAPI) in individual cell (upper left) and an overlapped image depicting the localisation of both eNOS and DAPI. Bar = 20 µm

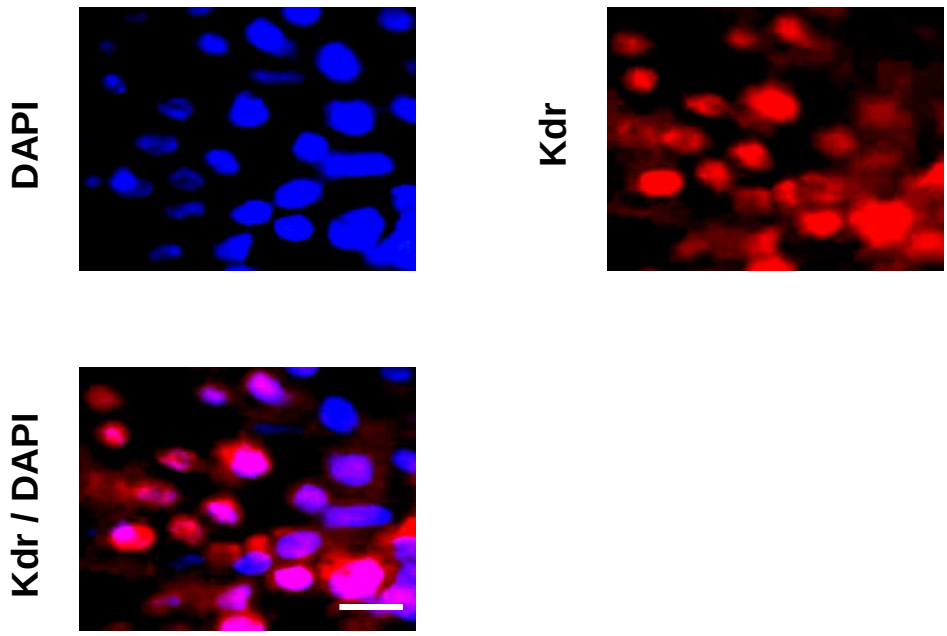

Fig. 19. Expression of Kdr in hESCs-derived ECs.

Day 9 differentiated hESCs grown in EGM2 were probed with Kdr primary antibody followed by polyclonal goat anti-Rabbit IgG immunoglobulins TRITC. *Anti-clockwise from upper right.* Fluorescent images were captured on Kdr positive cells (upper right), nucleic acid stains (DAPI) in individual cell (upper left) and an overlapped image depicting the localisation of both Kdr and DAPI. Bar = 20 µm.

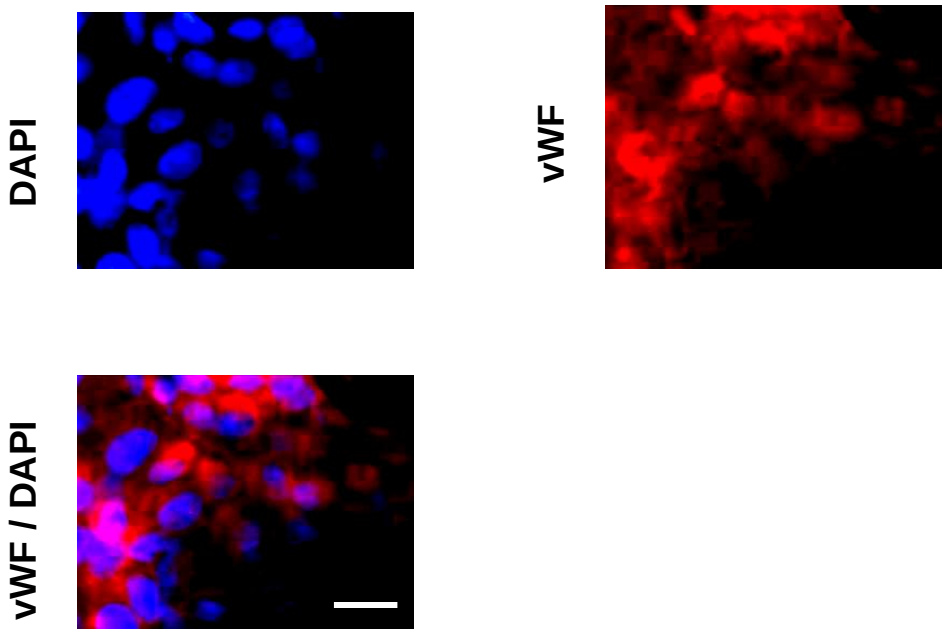

Fig. 20 Expression of vWF in hESCs-derived ECs.

Day 9 differentiated hESCs grown in EGM2 were probed with vWF primary antibody followed by polyclonal goat anti-Rabbit IgG immunoglobulins TRITC. *Anti-clockwise from upper right.* Fluorescent images were captured on vWF positive cells (upper right), nucleic acid stains (DAPI) in individual cell (upper left) and an overlapped image depicting the localisation of both vWF and DAPI. Bar = 20 µm.

3.2.4 Flow cytometry analysis of endothelial-specific proteins during hESCs differentiation towards the endothelial lineage and cell sorting

As a heterogeneous population of cells was observed in this EC differentiating culture condition, the isolation of pure EC population is a critical requirement for *in vivo* cell therapy. It is important to further quantify, analyse and characterise the differentiating heterogeneous hESC population grown in endothelial differentiating conditions with flow cytometry analysis. Moreover, differentiated cells expressing endothelial surface markers will be subjected to cell sorting from this mixed population and flow cytometry analysis will aid in selecting the best marker and the most suitable differentiation day to proceed with cell sorting.

At differentiation day 7, flow cytometry analysis indicated that 16.4% of the cell population expressed CD146 (Fig.21A *Top*). It subsequently increased approximately two-fold at 34.1% at day 17 (Fig.21A *Bottom*). Only 12.7% of cells expressed vWF at day 13 (Fig.21B). Determination of the accuracy and functionality of the antibodies used was analysed on a different cell population, human umbilical vascular endothelial cells (HUVECS). HUVECS express EC markers and widely used as an EC positive control in experiments. In the flow cytometry analysis, 97.3% of HUVECs expressed CD31/PECAM-1 (Fig.21C), 86% expressed CD146 and more than half of the population expressed vWF at 69% (Fig.21C). The ability of the antibodies to detect protein markers in HUVECs indicated that previous flow cytometry analyses on differentiating hESCs were true observations.

Next, the heterogeneous population of differentiating hESCs was subjected to cell sorting to obtain pure population of CD146+ cells. The percentage of CD146+ cells obtained during cell sorting was 96.5% (Fig.22A & B). These CD146+ sorted cell population was further cultured and expanded *in vitro*.

A

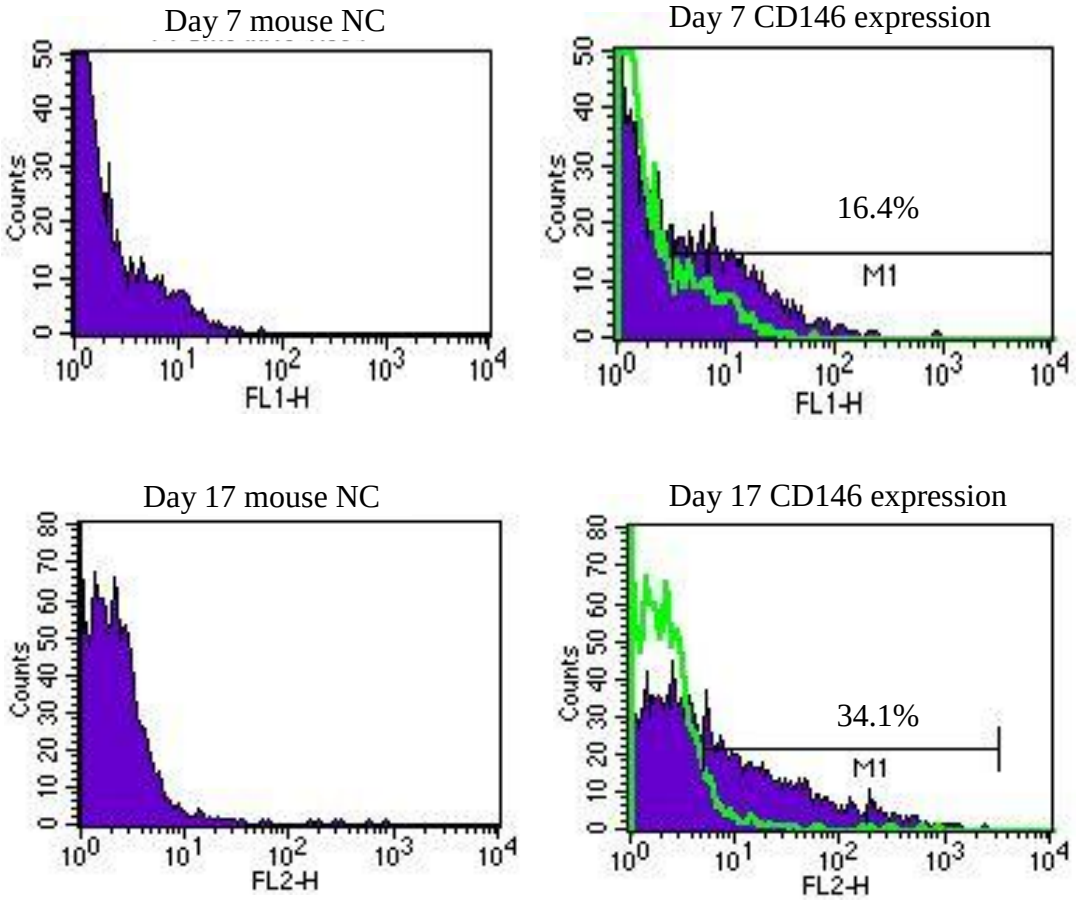
Day 7 mouse NC
Day 7 CD146 expression
16.4%
M1
Counts
FL1-H
Day 17 mouse NC
Day 17 CD146 expression
34.1%
M1
Counts
FL2-H

B

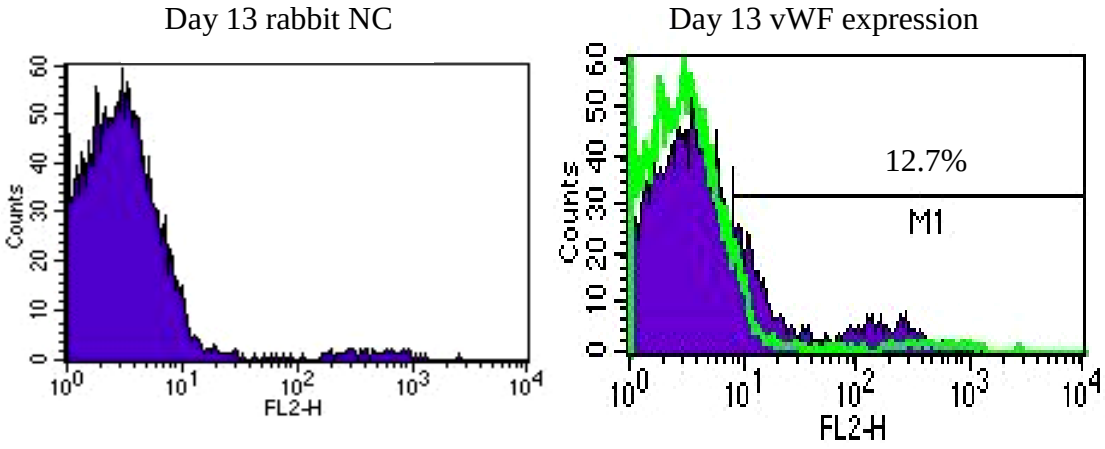
Day 13 rabbit NC
Day 13 vWF expression
12.7%
M1
Counts
FL2-H

C

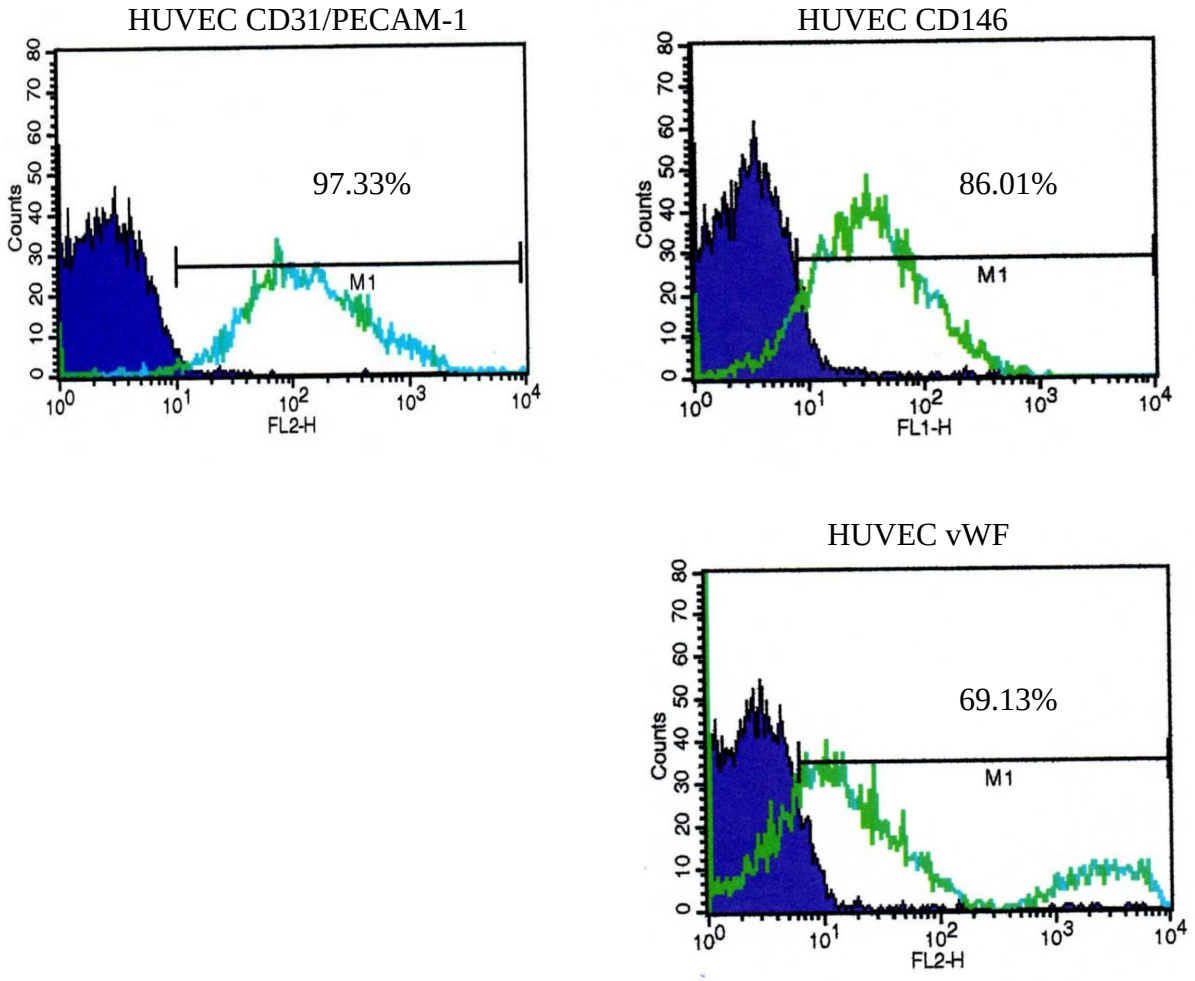

Fig. 21. Flow cytometry analysis of endothelial markers in differentiating hESCs towards the endothelial lineage and HUVECS

Clumps of undifferentiated hESCs were seeded on Matrigel^{TM} coated T75cm^2 flasks in EGM-2 medium and grown for a period of 7, 13 and 17 days respectively. (A) Cells were then used for flow cytometry analysis for CD146 marker. (B) Cells were differenatiated at day 13 subjected to flow cytometry analysis for vWF expressions. *Left.* Histogram of IgG isotype negative controls (NC) used in the experiments. *Right*. Blue histogram depicting the flow cytometry analysis of CD146 or vWF expressing cells. Green histogram represents the same IgG isotype negative controls (NC) from the left-hand side. (C) HUVECS were also subjected to flow analysis to demonstrate the expression of EC protein markers. *Anti-*

clockwise Green histogram depicts the percentage of CD31/PECAM-1 positive HUVECS, followed by the percentage of CD146 and vWF positive HUVECS. Blue histogram represents IgG isotype NC.

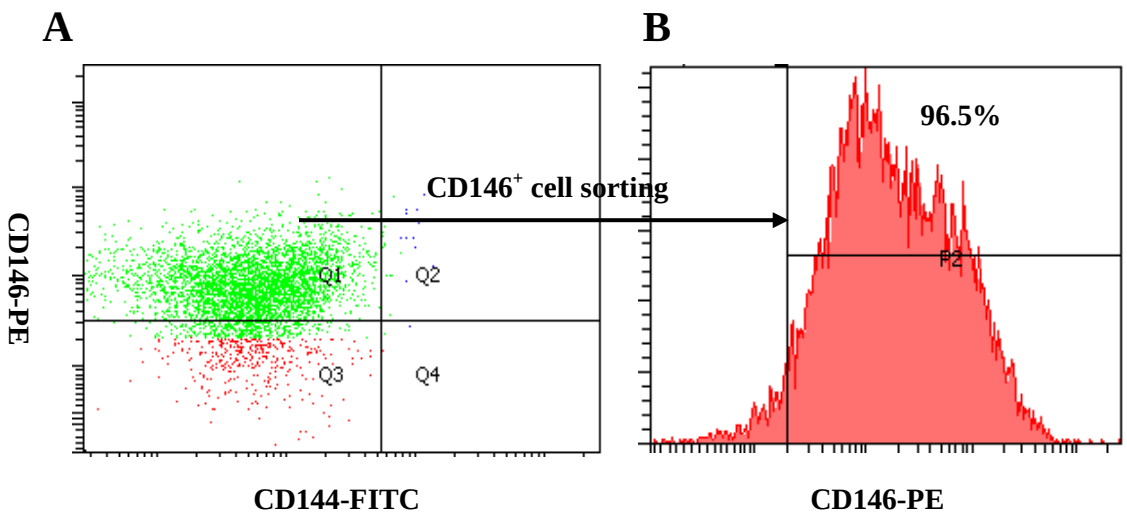

Fig. 22 The percentage of CD146 positive cells obtained during cell sorting.

Clumps of undifferentiated hESCs were seeded on Matrigel™ coated flasks and grown for a period of time. (A) Cells were then analysed for CD146 expressions. (B) A FACS histogram analysis of the percentage of CD146+ cells which were cell sorted from the heterogeneous differentiated hESCs.

3.3 Characterisation of CD146+ cells indicate that these cells are capable of displaying EC features

As part of the characterization study, endothelial function tests were carried out on *in vitro* derived endothelial cells from hESCs after *in vitro* expansion to ensure that these cells behave like their mature endothelial counterparts. A variety of *in vitro* endothelial function tests include investigating endothelial cell surface marker expression such as vWF, Dil-Ac-LDL uptake, lectin binding and the ability to form vascular structures using matrigel assays.

3.3.1 Cell morphology, immunocytochemistry and flow cytometry analyses of expanded CD146+ cells in-vitro

CD146+ cells isolated from the heterogeneous differentiated endothelial cell population were expanded *in vitro*. Early microscopic examinations of cell sorted CD146+ cells grown in EGM-2 medium revealed that 2 different cell phenotypes were observed (Fig.23A). Both cobblestone and spindle-shaped, fibroblast or SMC-like cells were present in passage 4 CD146+ cell culture. However, as the passage number of the cell culture increased, the spindle-shaped, fibroblast or SMC-like cells were absent and only a population of cells with cobbled-stone morphology was observed (Fig.23B). Immunocytochemistry analysis showed that these cells were positive for EC specific markers such as vWF (Fig.24A), eNOS (Fig.24B), CD31/PECAM-1 (Fig.24C) and CD144/VECAD (Fig.24D). Flow cytometry was also carried out to analyse EC markers on *in vitro* expanded CD146+ cells. As shown in Fig.25, the percentage of cell postive for CD146, vWF, CD144 and CD31 cultured in the first passage were found to be at 71.6%, 21%, 11.9% and 5.5% respectively (Fig.25) and which subsequently increased to 75.6%, 29.4%, 15.6% and 6.9% at passage 5.

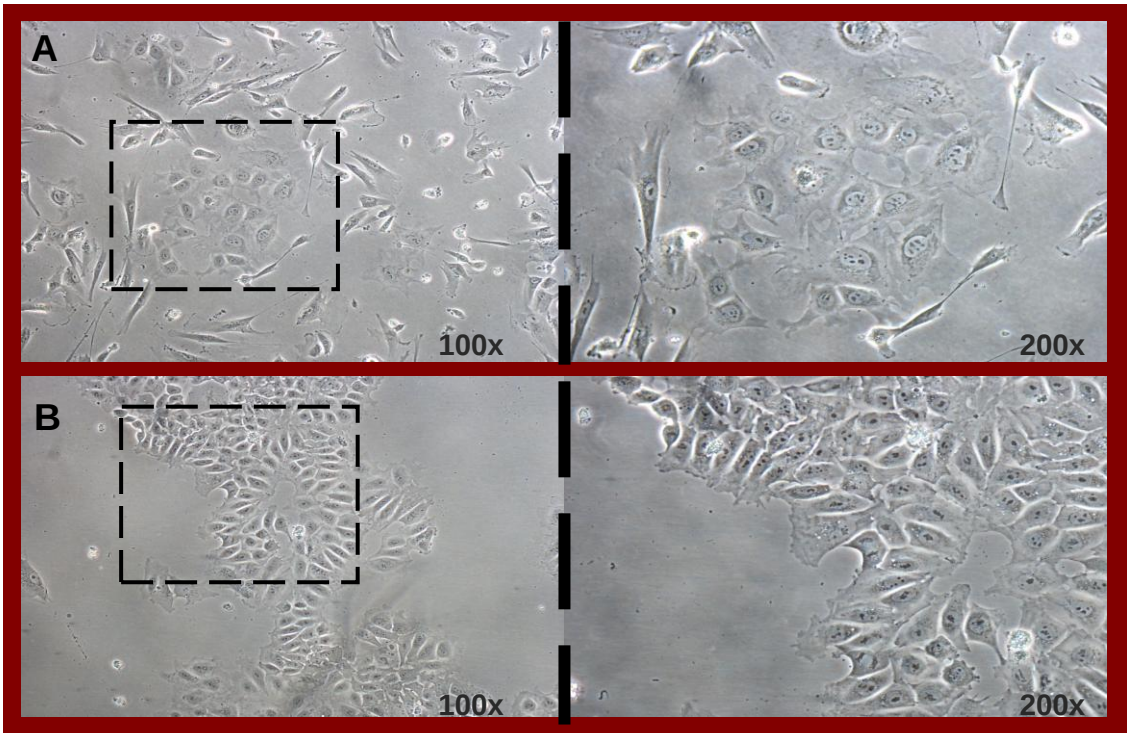

Fig. 23. A bright-field microscopic morphology of CD146+ sorted cells in-vitro culture

CD146+ cells were cultured on 5µg/ml Collagen I coated flask and in the presence of EGM-2 medium. Cells were passaged twice a week and medium was changed every 2 days. (A) *Left* Cell sorted population of CD146+ cells were expanded *in vitro*. After 4 passages, 2 different cell phenotypes were observed in the cell culture. *Right* A higher magnified view of the same population of cells. (B) *Left* At passage 9, only a population of cells with cobbled-stone morphology was observed. *Right* A higher magnified view. Note the columnar arrangement of cells.

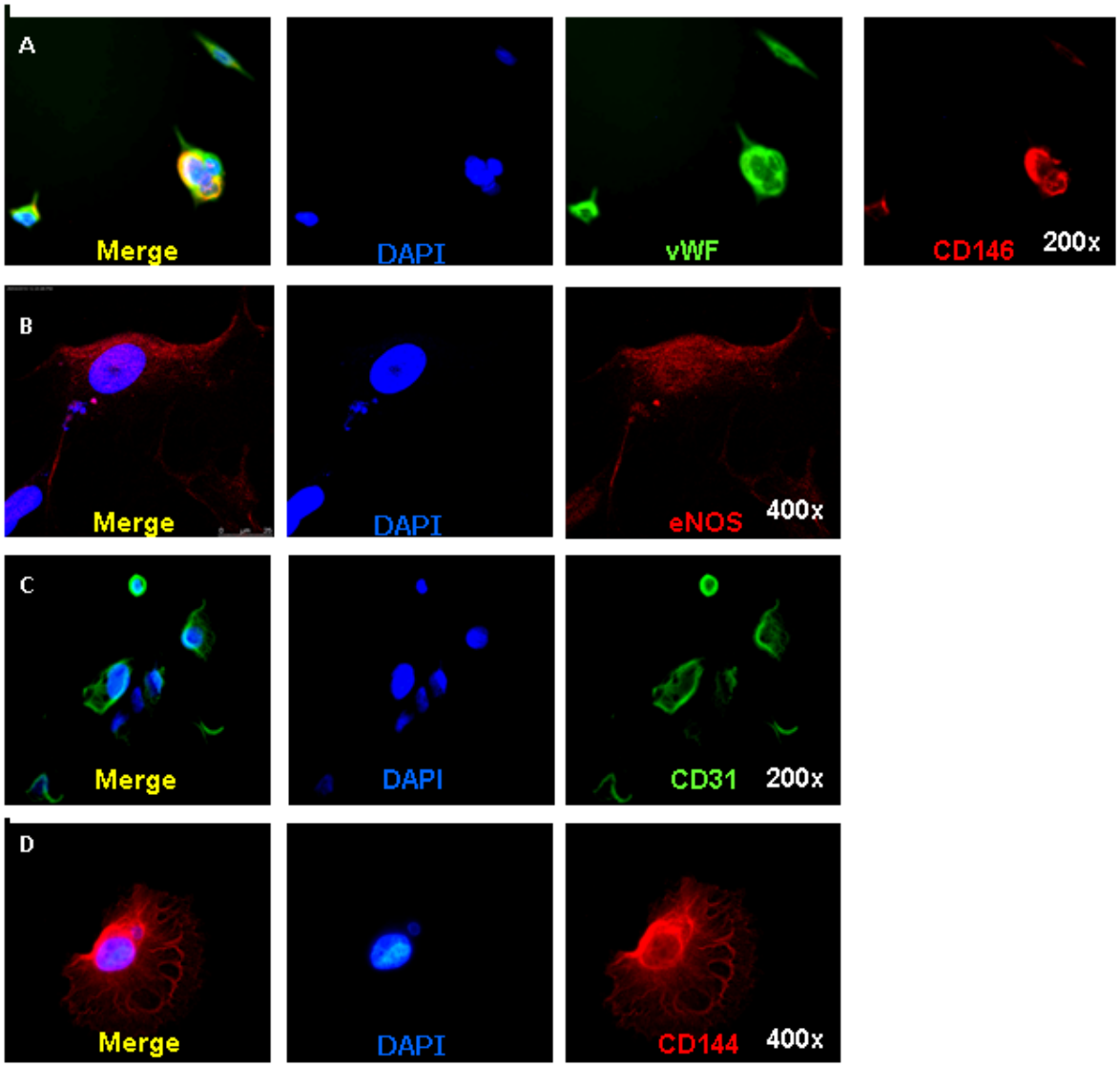

Fig. 24 Expression of EC markers in CD146+ sorted cells

Immunocytochemistry staining was carried out in isolated CD146+ passage 10 sorted cells and their fluorescent images were captured. (A) Cells were co-stained with CD146 and vWF. These CD146+ cells were also stained with other EC markers such as eNOS (B), CD31/PECAM-1 (C) and CD144/VECAD (D). To localise nucleic acid, each individual cell was also stained with DAPI.

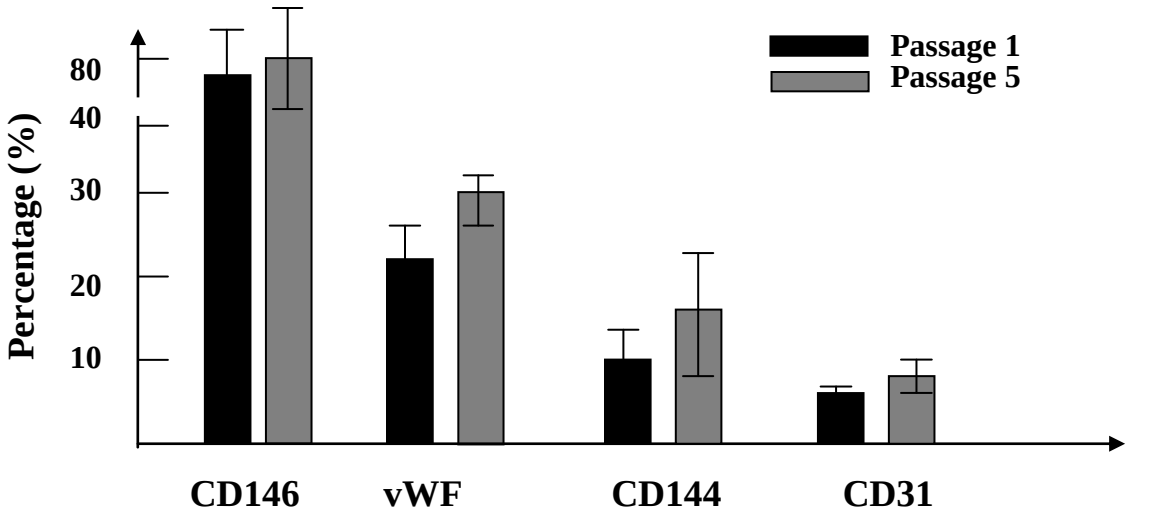

Fig. 25. Flow cytometery analysis of CD146+ cells after cell sorting.

After cell sorting, CD146+ cells were grown in EGM-2 and seeded onto Collagen I coated wells. These cells were expanded *in vitro* and subjected to flow analysis to determine the expression of EC protein markers. Here a bar graph depicts the expression levels of EC markers after CD146+ cells sorting at passages1 and 5.

3.3.2 CD146+ cells display functional EC properties in vitro and in vivo

To further characterize these CD146+ cells, function tests such as Dil-Ac-LDL uptake, lectin binding and *in vitro/vivo* vasculogenesis using matrigel assays were later carried out on *in-vitro* expanded CD146+ cells. As expected, these expanded CD146+ cell population were capable of Dil-Ac-LDL uptake, lectin binding (Fig.26), as well as forming vascular structures in Matrigel™ *in vitro* (Fig.27A) and *in vivo* (Fig.27B). The combination of all these tests demonstrated that the CD146+ cell population could function as mature endothelial cells *in vitro* and *in vivo*.

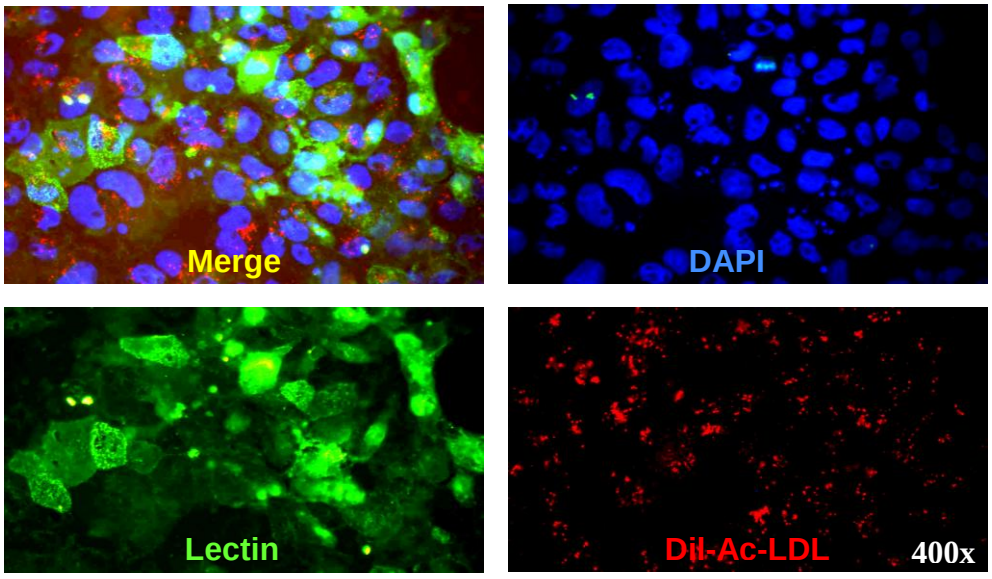

Fig. 26. *In vitro* expanded CD146+ cells display Dil-Ac-LDL uptake and lectin binding

Function tests such as Dil-Ac-LDL uptake and lectin binding stainings were carried out on *in vitro* expanded CD146+ cells. Clockwise: *Upper Left* An overlapped image depicting the localisation of lectin, DAPI and Dil-Ac-LDL. Images for individual localisation for DAPI (nuclear) upper right, Dil-Ac-LDL *lower right* and lectin *lower left* were also captured.

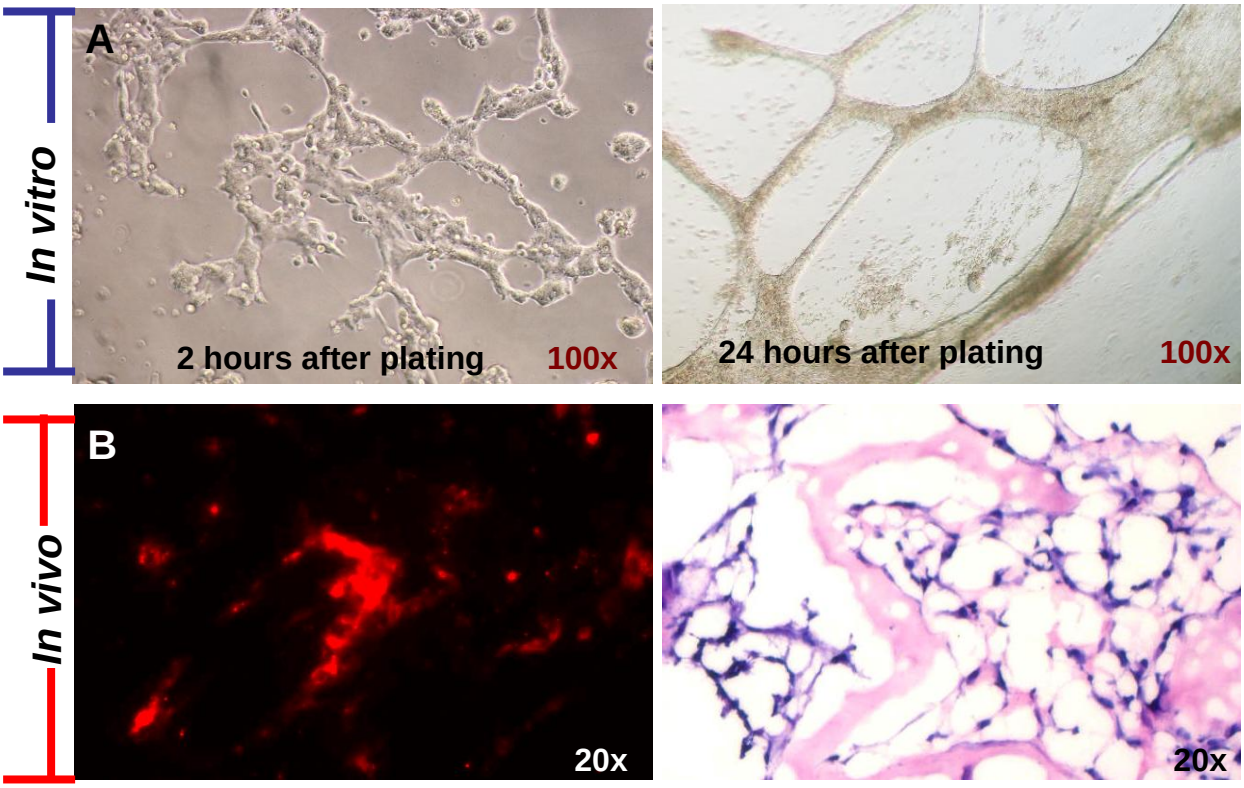

Fig. 27. Formation of vascular structures using Matrigel™ assays

The ability of CD146+ cells to form vascular network *in vitro* and *in vivo*, was assessed by using Matrigel™. (A) *Left* Expanded CD146+ cells were seeded onto a Matrigel™-coated surface and 2 hours later, an early formation of a network was observed using bright-field microscopy, *Right* 24 hours since plating, vascular networks were observed. (B) *In vivo* Matrigel™ plug assay was carried out in SCID mice using CD146+ cells labeled with red fluorescent dye (PKH26) and assessed 1 week later. *Left* From a section of the implanted Matrigel™ plug, red fluorescent labeled CD146+ cells were incorporated within a vascular structure. *Right* H&E staining of a section of the implanted Matrigel™ plug which showed a complex vascular network which had formed in the presence of the transplanted CD146+ cells.

3.4 Identification of miRNAs involved in hESCs differentiation towards the EC lineage

As previously mentioned, miRNAs play various physiological and pathological roles in the cardiovascular system, such as cardiovascular system development and cell differentiation [112, 146-149, 152] . We therefore hypothesize that one or more miRNAs may be involved in endothelial cell differentiation from hESCs. Potential miRNAs involved during endothelial differentiation were selected using miRNA array analysis (Fig.28). Their biological functions were further analysed by inhibiting or enhancing their expression and determining if these influence the expression of EC levels (Figs. 30-31).

3.4.1 Screening for potential miRNAs during differentiation towards the EC lineage

To determine which miRNAs were enriched during the differentiation of hESCs into ECs, miRNA array expression profiling (miRXplore™ Microarrays) was carried out on samples collected during the 9-day differentiation period by the RNA expression experts from Miltenyi Biotec GmbH (Germany). Five potential upregulated miRNAs were selected from the miRNA array analysis and further validated using quantitative real-time PCR. These miRNAs are miR-150*, miR-1915, (Fig.28A) and miR-200 family members, miR-141, miR-205 and miR-200c (Fig.28B). All five miRNAs were selected as they were enriched and displayed a time-dependent increase in expression during the differentiation of hESCs towards the EC lineage **(Fig.28C)**. Expression of miR-150* at day 9 was increased nearly 2-fold as compared to day 0 (control) undifferentiated hESCs (Fig.28A *Left*). Whereas expressions of miR-1915 (Fig.28A *Right*) and the miR-200 family members, miR-141 (Fig.22B *Right*) and miR-200c (Fig.28B *Middle*) were increased nearly 3-fold at day 9 compared to day 0. A 4.5-fold increase in miR-205 (Fig.28B *Right*) expression at day 9 was the highest observation among the miRNAs.

A

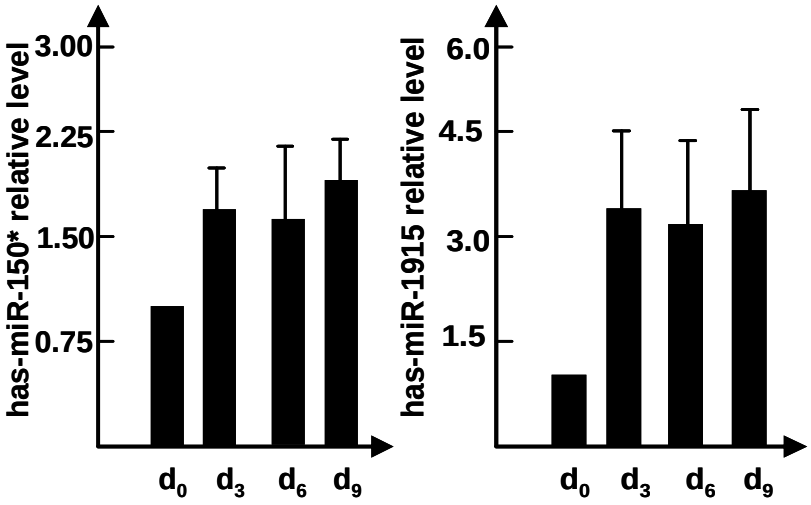

B

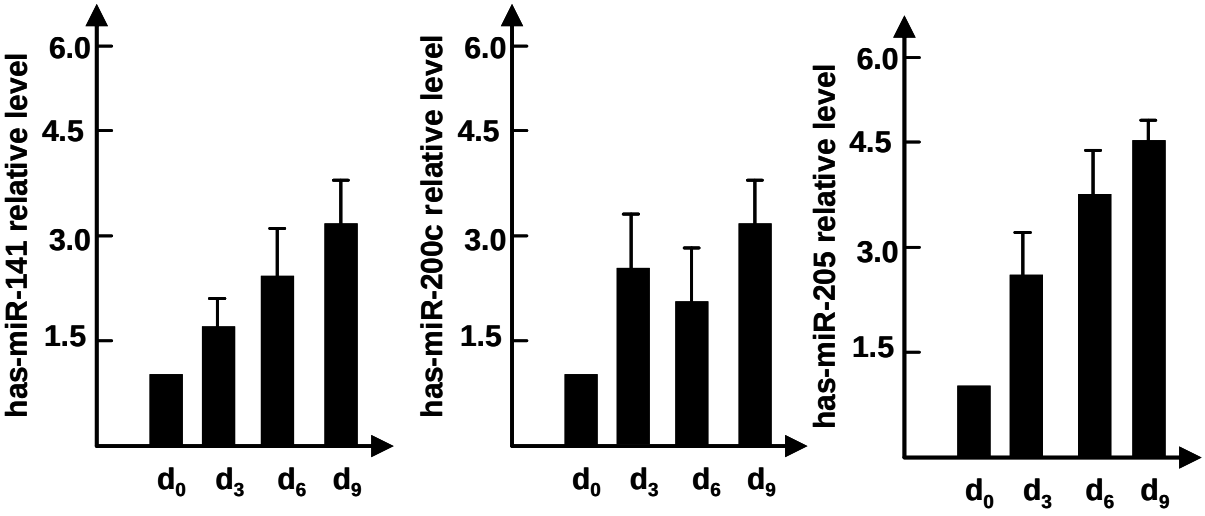

C

miRNA name	Day 3	Day 6	Day 9
hsa-miR-141	1.61627	1.648101	2.495403
hsa-miR-205	1.939123	2.332433	3.234446
hsa-miR-150*	1.986847	2.812245	4.209275
hsa-miR-200c	2.576935	2.507951	3.607276
hsa-miR-1915	5.408016	8.339838	18.133837
Angiogenesis			
hsa-miR-126	ND	ND	1.249804
hsa-miR-210	ND	ND	1.241585

hsa-miR-130a	0.906145	0.945844	1.271549
Anti-Angiogenesis			
hsa-miR-221	0.612299	0.58712	0.572099
Differentiation			
hsa-miR-145	ND	ND	1.746961

Fig. 28. The expression patterns of a set of five enriched miRNAs chosen from the miRNA array analysis.

Undifferentiated hESCs were differentiated towards the endothelial lineage for 9 days as previously described. During differentiation, miRNAs were isolated from each time points of days 3, 6, and 9. Day 0 (control) samples were obtained from undifferentiated hESCs. All miRNA samples were sent for miRNA array analysis. After which, 5 potential upregulated miRNAs were selected from the analysis and the data was collated into histograms. (A) Histograms showing the expression patterns of miR-150* *Left*, miR-1915 *Right*. (B) Histograms showing the expression patterns of the miRNA 200 family members miR-141 *Left* and miR-200c *Middle* and miR-205 *Right*. The histograms represent an average of three independent experiments with standard deviations. Data normalized to 5.8s and presented relative to day 0 expression, which was set as 1.0. (C) A summary list of miRNAs selected from the miRNA array analysis. (ND=Not detected)

3.4.2 miRNA transfection efficiency

Examination into which of the selected potential miRNAs are involved in hESCs differentiation to ECs, was achieved by inhibiting or enhancing their expression and then analysing whether these effects would affect EC expression in the differentiated cells. To achieve this, transfections with miRNA inhibitors or precursors were carried out in day 6

differentiating hESCs using siPORT NeoFX Transfection Agent. An important step prior to carrying out transfection assays is to determine the success rate of the transfection experiment. This was carried out by transfecting differentiated hESCs with Cy3-labeled Anti-miR Negative Control (Ambion, Applied Biosystems) to monitor transfection efficiency. It was observed that after 48 hours transfection with Cy3-labeled Anti-miR Negative Control, 87.41% (Fig.29A) of the transfected cells were Cy3-labeled and at 72 hours post transfection, 83.27% of the transfected cells were positively labeled with Cy3 (Fig.29B).

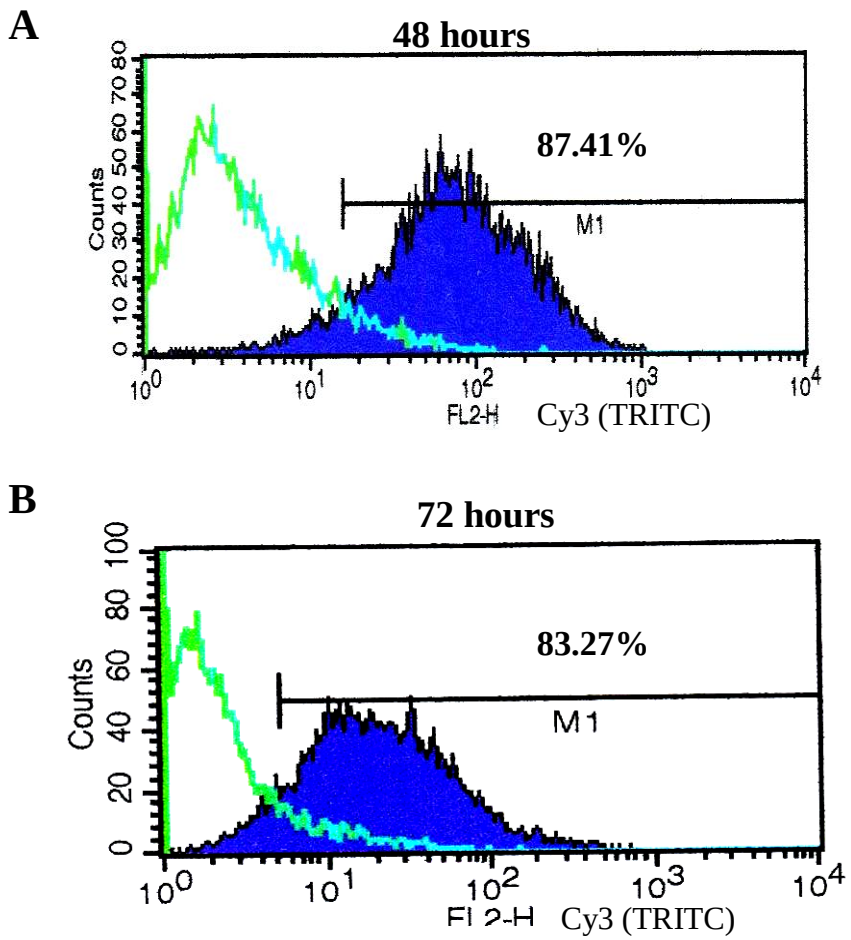

Fig. 29. Determination of transfection efficiency using FACS

Day 6 differentiated hESCs grown in EC conditions were transfected with Cy3-labeled Anti-miR Negative Control (Ambion, Applied Biosystems). These cells were assessed

using flow cytometry 48 and 72 hours post transfection. (A) A flow cytometry histogram showing 48 hours post transfection with Cy3-labelled miRNA inhibitor. (B) A flow cytometry histogram showing 72 hours post transfection with Cy3-labelled miRNA inhibitor. Green histogram depicts controls which were non-transfected day 6 hESCs.

3.4.3 Expression of EC markers (RNA and Protein) in miR-150 and 200c inhibition and over expression studies*

The previous determination of optimal parameters for carrying out miRNA transfection assays will facilitate the subsequent inhibition and overexpression assays for the selected miRNAs. Real-time PCR results in inhibition studies showed that the expression levels of miR-150* and 200c were significantly decreased after 24 hours tranfection as shown in Fig.30A i and ii as compared to control. To determine if these miRNAs are related to EC differentiation from hESCs, further analyses in the expression levels of specific endothelial markers from the same samples were carried out using real-time PCR and western blotting.

In miR-150* inhibition, the mRNA expression levels of EC markers such as vWF, Kdr, CD144 and CD146 were significantly downregulated as compared to control (Fig.30Ai). As expected, inhibition of miR-200c also significantly downregulated mRNA levels of vWF, CD144, Kdr and CD146 (Fig.30Aii) as compared to control. In order to determine if the protein levels of the EC markers were also influenced by the inhibition of miR-150* and 200c in hESCs differentiation, western blot analysis was carried out. It was demonstrated that as compared to control, the protein expression levels of CD146 and CD144 were significantly downregulated by the inhibition of miR-150* and 200c (Fig.30B).

Next, overexpression studies with miRNA precursors were carried out to validate the above mentioned results achieved in the inhibition studies on miR-150* and 200c. mRNA expression levels of miR-150* was significantly increased compared to control (Fig.31Ai). Importantly, the overexpression of miR-150* precursor into the cells significantly upregulated mRNA levels of specific EC markers such as vWF, Kdr, CD144 and CD146 as compared to control (Fig.31Ai). Similar results were also obtained from miR-200c

overexpression experiments (Fig.31Aii). Western blot analysis of samples transfected using the same treatments in Fig.31A showed that similar results were obtained. Protein levels of EC markers such as CD146, CD144 and vWF were significantly upregulated as compared to controls in miR-150* overexpression assays (Fig.31B). Whereas in miR-200c overexpression assays, protein levels of CD144 and CD146 were upregulated (Fig.31B). Taken together, miR-150* and 200c might play a role in hESCs differentiation towards the EC lineage.

A, i

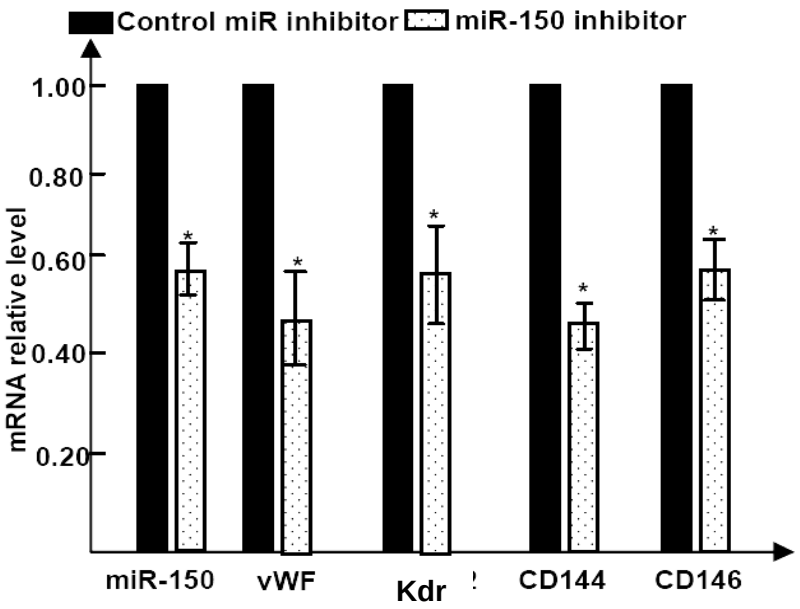

A, ii

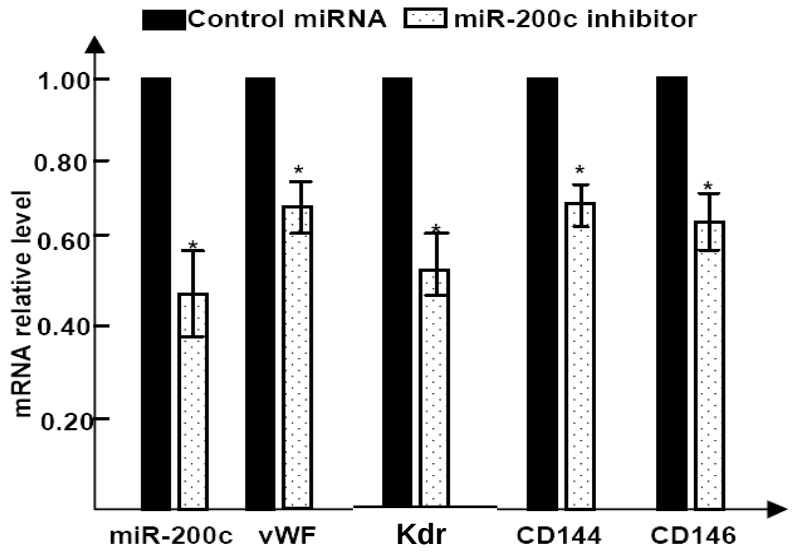

B.

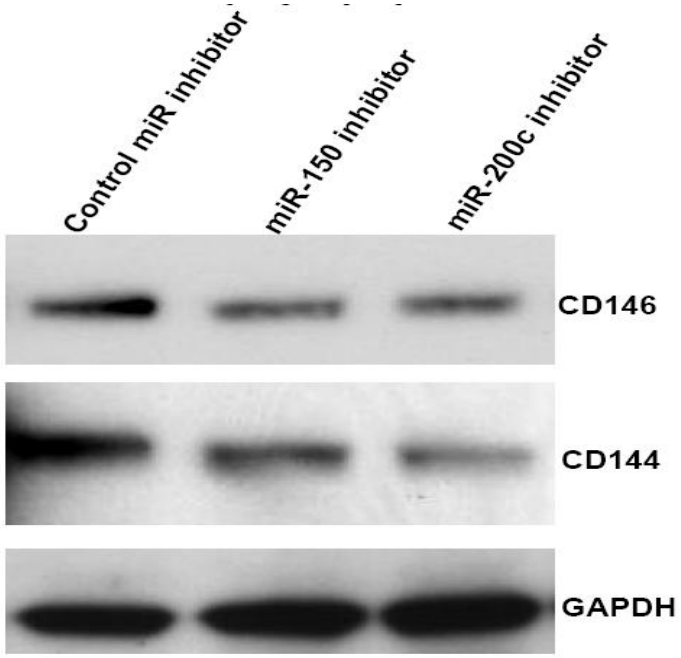

Fig. 30. miR-150* and 200c inhibition downregulate the expression of EC markers in day 6 differentiating hESCs

(A) Real-time PCR analysis of EC expression markers after miR-150* and miR-200c inhibition. i) Day 6 differentiating hESCs were transfected with miR-150* inhibitor and Anti-miR Negative Control. EC mRNA expression levels were analysed at 24 hours post transfection using real-time PCR as previously described in methods. Each column represent mean $\pm$ SEM of three independent experiments (n=3). Data normalized to 5.8s and presented relative to control expression. * $p < 0.05$ (vesus control), Paired t-test followed by two tailed test. ii) Day 6 differentiating hESCs were transfected with miR-200c inhibitor and Anti-miR Negative Control. EC mRNA expression levels were analysed at 24 hours post transfection using real-time PCR as described in methods. Each column represent mean $\pm$ SEM of three independent experiments (n=3). Data normalized to 5.8s and presented relative to control expression. * $p < 0.05$ (versus control), Paired t-test followed by two tailed test.

(B) Protein analysis of EC expression levels in differentiated hESCs after 24 hours inhibitor post transfection. Day 6 differentiating hESCs were transfected with miR-150* and miR-200c inhibitors as well as Anti-miR Negative Control. After 24 hours post transfection, protein samples were extracted and subjected to western blot as previously described. 40µg of each protein sample was loaded into each well, blotted and probed with endothelial specific antibodies CD146 and CD144/VE-cad. GADPH, a housekeeping protein was included to show the total sample loading in each well.

A, i).

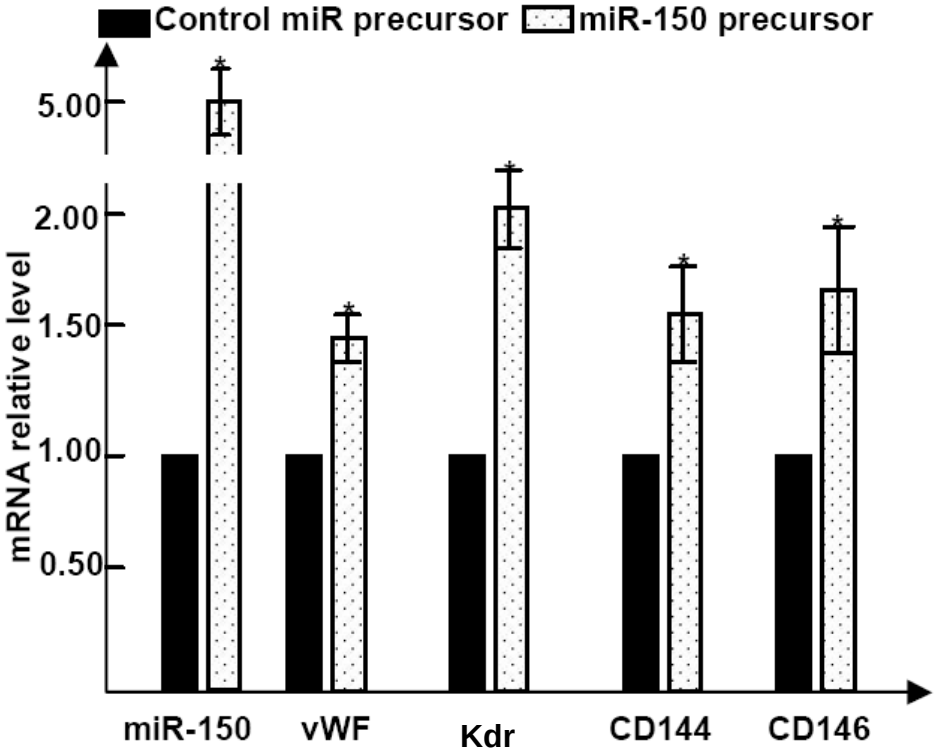

A, ii).

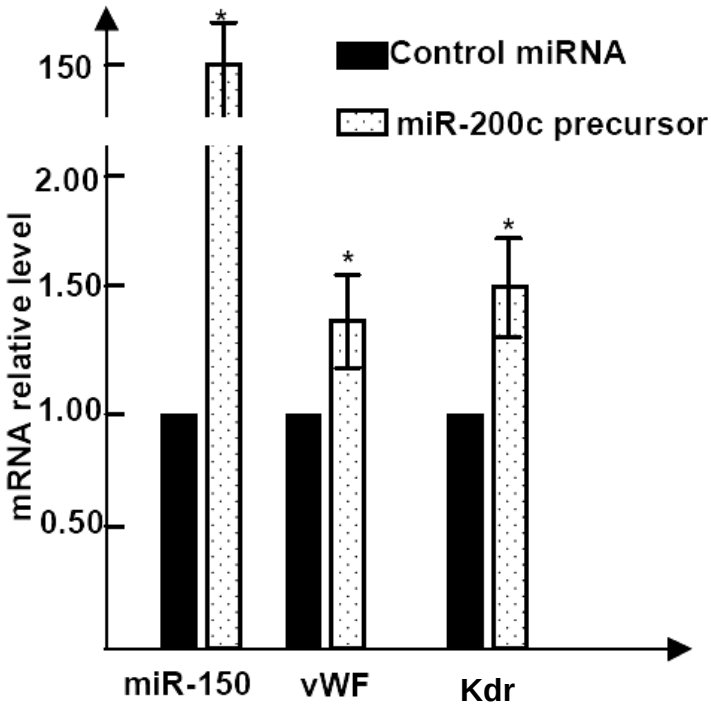
Control miRNA
miR-200c precursor
mRNA relative level
150
2.00
1.50
1.00
0.50
*
*
*
miR-150
vWF
Kdr

B,

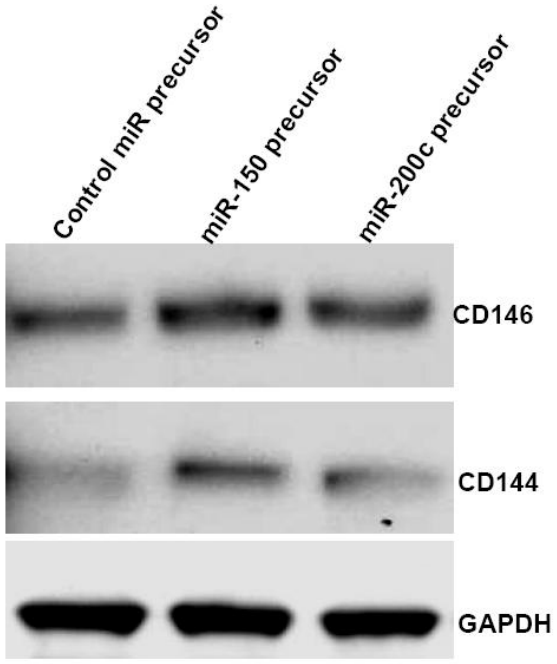
Control miR precursor
miR-150 precursor
miR-200c precursor
CD146
CD144
GAPDH

Fig. 31 mirRNAs 150* and 200c overexpression upregulate the expression of EC markers in day 6 differentiating hESCs

(A) Real-time PCR analysis of EC expression markers after miR-150* and miR-200c overexpression. i) Day 6 differentiating hESCs were transfected with miR-150* precursor and Pre-miR miRNA Precursor Negative Control. EC mRNA expression levels were analysed at 24 hours post transfection using real-time PCR as previously described in methods. Each column represent mean $\pm$ SEM of three independent experiments (n=3). Data normalized to 5.8s and presented relative to control expression. $P < 0.05$ (versus control), paired t test followed by one-tail test. ii) Day 6 differentiating hESCs were transfected with miR-200c precursor and Pre-miR miRNA Precursor Negative Control. EC mRNA expression levels were analysed at 24 hours post transfection using real-time PCR as described in methods. Each column represent mean $\pm$ SEM of three independent experiments (n=3). Data normalized to 5.8s and presented relative to control expression. * $P < 0.05$ (versus control), paired t test followed by one-tail test.

(B) Protein analysis of EC expression levels in differentiated hESCs after 24 or 48 hours overexpression post transfection. Day 6 differentiating hESCs were transfected with miR-150* and miR-200c precursor as well as Pre-miR miRNA Precursor Negative Control. After 24 hours post transfection, protein samples were extracted and subjected to western blot as previously described. 40μg of each protein sample was loaded into each well, blotted and probed with endothelial specific antibodies CD146 and CD144/VE-cad. GADPH was included as internal control to show the total sample loading in each well.

3.4.4 miR-1915, 141 and 205 inhibition did not affect the expression of EC markers in hESCs differentiation

Inhibition studies were also carried out to determine the functional involvement of the remaining three potential miRNAs (miR-1915, 141 and 205), whose expressions were also upregulated during hESCs differentiation towards the EC lineage. Unlike miR-150* and 200c, these miRNAs did not inhibit mRNA expression of EC markers after 24, 48 and 72 hours transfection (Fig.32 A-C), indicating that these miRNAs play no major role in EC differentiation from hESCs.

A

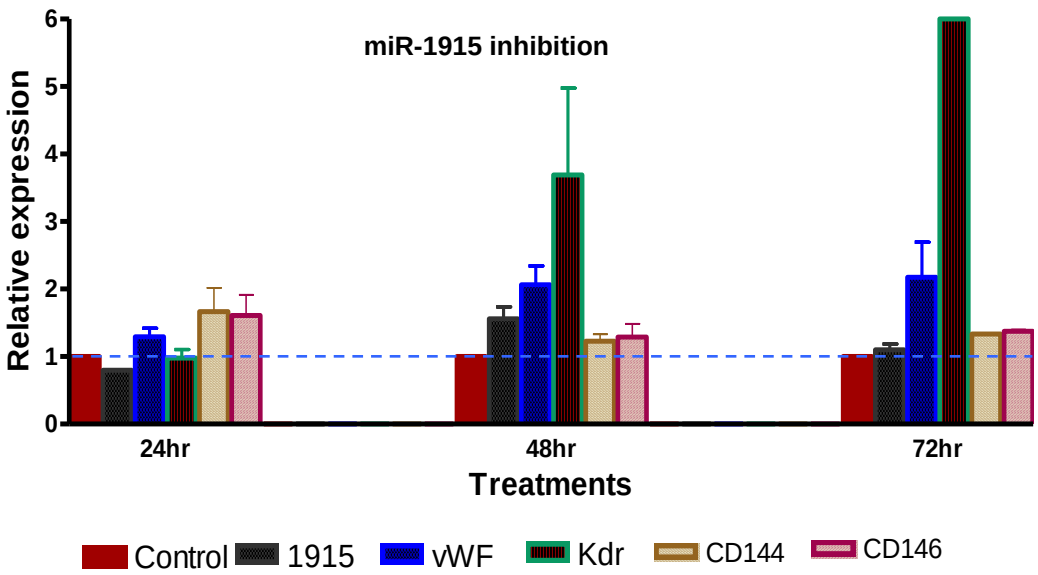

B

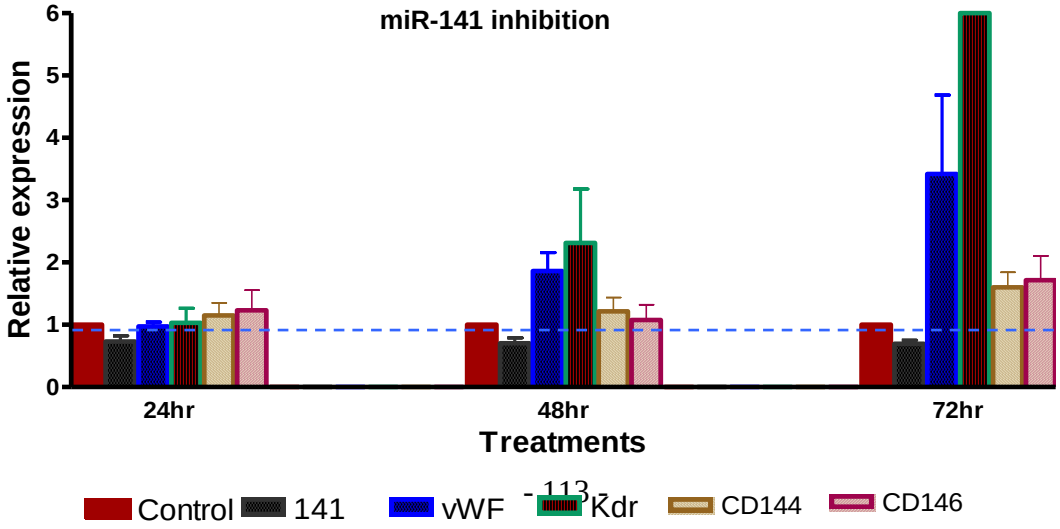

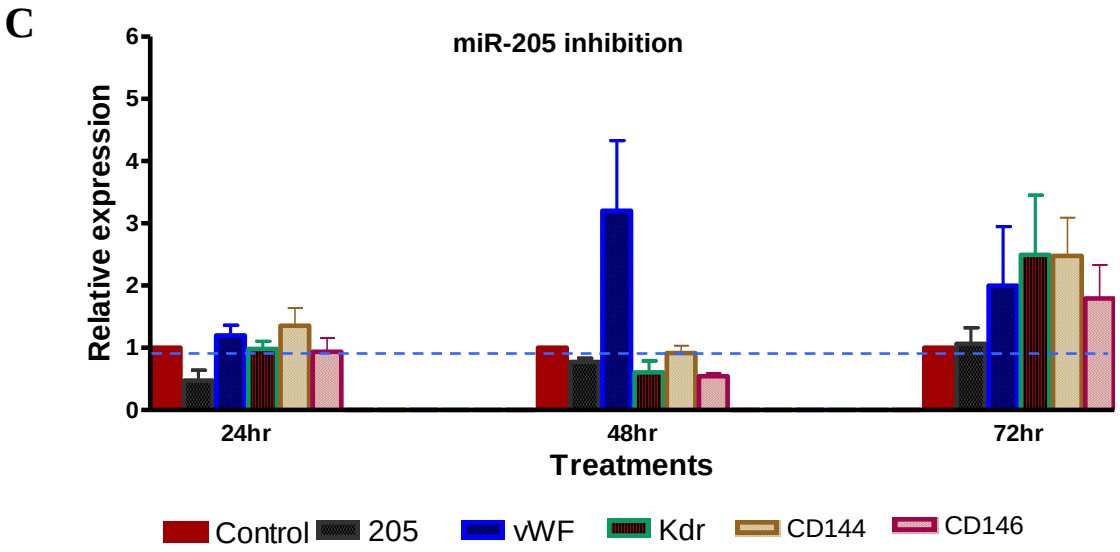

Fig. 32. mirRNAs 1915, 141 and 205 inhibition fail to downregulate the expression of EC markers in day 6 differentiating hESCs

Real-time PCR analysis of EC expression markers after miR-1915, 141 and 205 inhibition. (A) Day 6 differentiating hESCs were transfected with miR-1915 inhibitor and Anti-miR Negative Control. EC mRNA expression levels were analysed at 24, 48 and 72 hours post transfection using real-time PCR as previously described in methods. Each column represent mean ± SEM of three independent experiments (n=3). Data normalized to 5.8s and presented relative to control expression. (B) Day 6 differentiating hESCs were transfected with miR-141 inhibitor and Anti-miR Negative Control. EC mRNA expression levels were analysed at 24, 48 and 72 hours post transfection using real-time PCR as described in methods. Each column represent mean ± SEM of three independent experiments (n=3). Data normalized to 5.8s and presented relative to control expression. (C) Day 6 differentiating hESCs were transfected with miR-205 inhibitor and Anti-miR Negative Control. EC mRNA expression levels were analysed at 24, 48 and 72 hours post transfection using real-time PCR as described in methods. Each column represent mean ± SEM of three independent experiments (n=3). Data normalized to 5.8s and presented relative to control expression.

3.5 ZEB1/TCF8 is identified as the mRNA target for miR-150* and 200c in differentiating hESCs towards the EC lineage

To further investigate the mechanisms by which miR-150* and 200c regulate endothelial biology, potential mRNA targets were searched. Predictions of targets for miR-150* and 200c were carried out using PicTar (http://pictar.mdc-berlin.de), a miRNA target prediction algorithm program tool [159]. Two potential targets, c-Myb and ZEB1/TCF8 were selected based on the high degree of sequence complementarity between the 5' end of the miRNA and the 3'UTR mRNA target.

3.5.1 c-Myb and ZEB1/TCF8 were selected as potential mRNA targets for miR-150 and 200c*

Expression patterns of both c-Myb and ZEB1/TCF8 were further analysed in a 9-day time course study using differentiating hESCs. During the 9-day hESCs differentiation process, real-time PCR analysis demonstrated that mRNA levels of both c-Myb (Fig.33A *Left*) and ZEB1/TCF8 (Fig.33A *Right*) were significantly decreased as compared to day 0 control (undifferentiated hESCs). In determination of whether there is a direct relationship between miR-150* and c-Myb or ZEB1/TCF8, miR-150* was overexpressed in CD146+ cells and mRNA levels of mRNA targets were determined (Fig.33B *Left*). Both mRNA expression of c-Myb or ZEB1/TCF8 were decreased in the miR-150* overexpression study. In a similar experiment, overexpression of miR-200c in CD146+ cells also resulted in the reduction of both mRNA expression levels of c-Myb or ZEB1/TCF8 (Fig.33B *Right*). However, a significant decrease was observed in only ZEB1/TCF8 mRNA expression and not in c-Myb expression for both miR-150* and 200c overexpression studies.

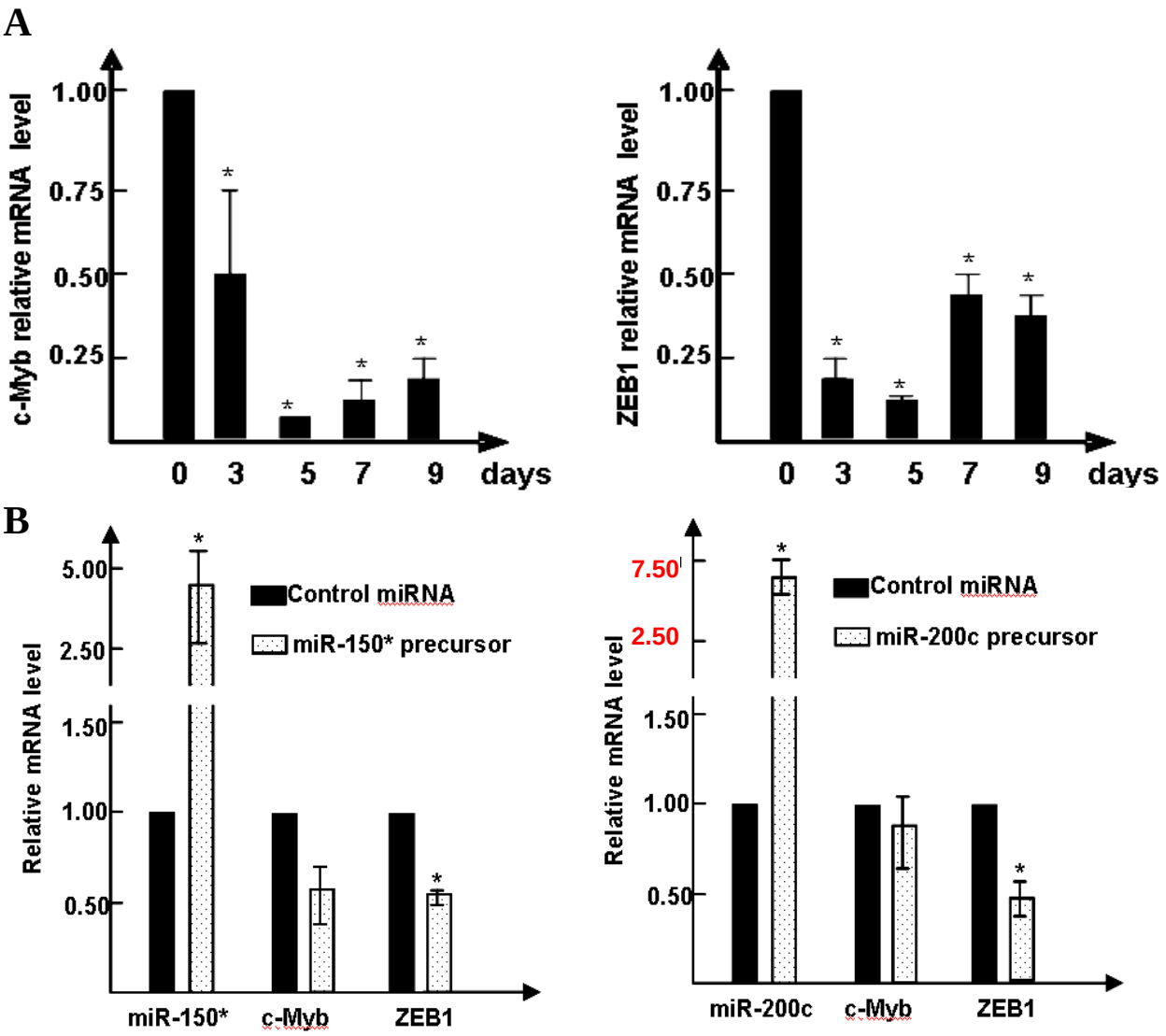

Fig. 33. Identifying miR150* and 200c's target/s

Expression of miR-150* and miR-200c's potential mRNA targets during hESCs-EC differentiation and in miRNA overexpression studies were determined. (A) Clumps of undifferentiated hESCs colonies were seeded on matrigel and cultured in EGM-2 medium for 3, 5, 7 and 9 days. During each respective time-point, RNA was extracted, reversed transcribed to cDNA as previously described and subjected to real-time PCR analysis. *Left* c-Myb mRNA expression. *Right* ZEB1/TCF8 mRNA expression Day 0 (control) samples were obtained from undifferentiated hESCs. Data represent mean ± SEM of three independent experiments (n=3). Data normalized to 18S and presented relative to day 0

expression. * p< 0.05 (vesus control), Paired t-test followed by two tailed test. (B) CD146+ cells **were transfected with** either c-Myb or ZEB1/TCF8 precursors and RNA was extracted 48 hours later. Reverse transcription to obtain cDNA was carried out and subjected to real-time PCR analysis. *Left* miR-150* overexpression. *Right* miR-200c overexpression. Data represent mean ± SEM of three independent experiments (n=3). Data normalized to 5.8s and presented relative to miR control expression.* p< 0.05 (vesus control), Paired t-test followed by two tailed test.

3.5.2 ZEB1/TCF8 functions as the mRNA target for both miR-200c and miR-150 in hESC-derived endothelial cells*

Based on observations from the previous overexpression study (Fig.33B), it is clear that ZEB1/TCF8 is the potential mRNA target for miR-150* and 200c. As shown in Fig.34A, The 3' UTR of human ZEB1/TCF8 contains two highly conserved 7-8-mer binding sites that are perfectly complementary to nucleotides (nt) 1-8 of miR-200c. Interestingly, nt 1-8 of miR-150* also do bind to the 3' UTR of human ZEB1/TCF8 which contains one highly conserved 8-mer binding site (Fig.34A). To further verify if both miR150* and 200c share the same mRNA target *in vitro*, the 3'UTR of ZEB1/TCF8 (Appendix 1) was cloned into a luciferase reporter. Luciferase assay was then assessed after overexpressing miR-150* and 200c. The activity of luciferase from construct that included portion of the ZEB1/TCF8 3'UTR, was significantly decreased upon overexpression of miR-200c at 48 and 72 hours post transfection (Fig.34B). There was also a decrease in the luciferase activity observed in miR-150* overexpression assay at both time points (Fig.34B).

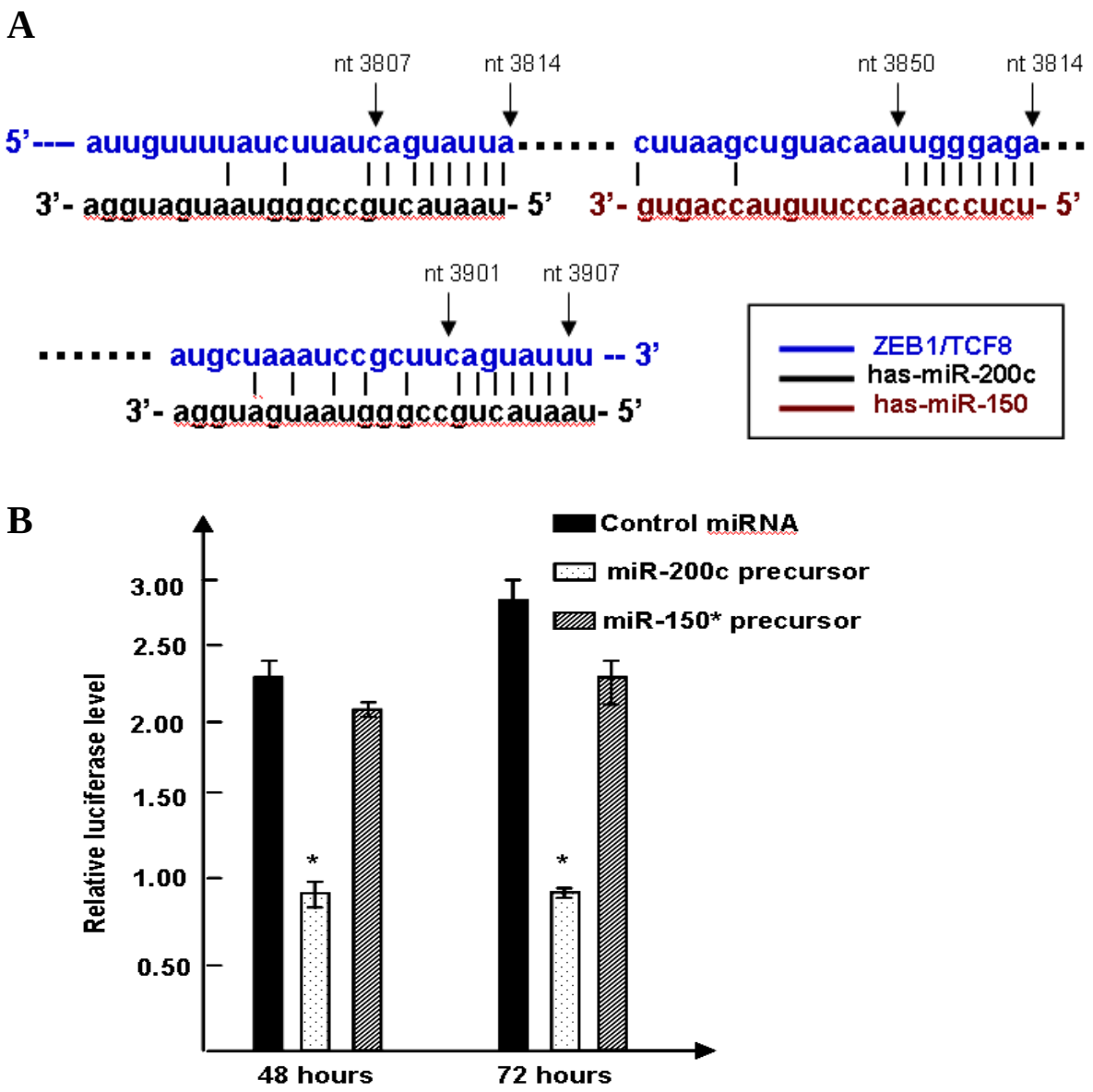

Fig. 34. ZEB1/TCF8 function as a mRNA target for miR-150* and 200c

(A) Complementary sequences of potential miR-150* and 200c that bind to mRNA target, human ZEB1/TCF8 3'UTR are depicted in this illustration. (B) 3'UTR of ZEB1/TCF8 was cloned into a luciferase reporter. Luciferase assay was then carried out as previously described on CD146+ cells after overexpressing miR150* and 200c at 48 and 72 hours post-transfection.

3.6 miRNAs play a role in blood vessel formation in developing chick embryos

Since it was previously shown *in-vitro* that both miR-150* and miR-200c modulate the expression of EC markers in differentiating hESCs, it will be interesting to discern if this phenomenon also occurs *in vivo*. Animal models are valuable tools for testing gene functions and drug mechanisms *in vivo*. As the chick embryo is easy to work with and readily available, an experiment using developing chick embryos was carried out to analyse the functions of miR-150* and miR-200c. Analysis of HH20 chick embyos after treatment with transfection complexes containing miR-150*(Fig.35C) or miR-200c (Fig.35B) inhibitor showed a suppressed number of blood vessels formed as compared to control treated chick embryos (Fig.35A). This observation implies that miRNAs are involved in the formation of blood vessels.

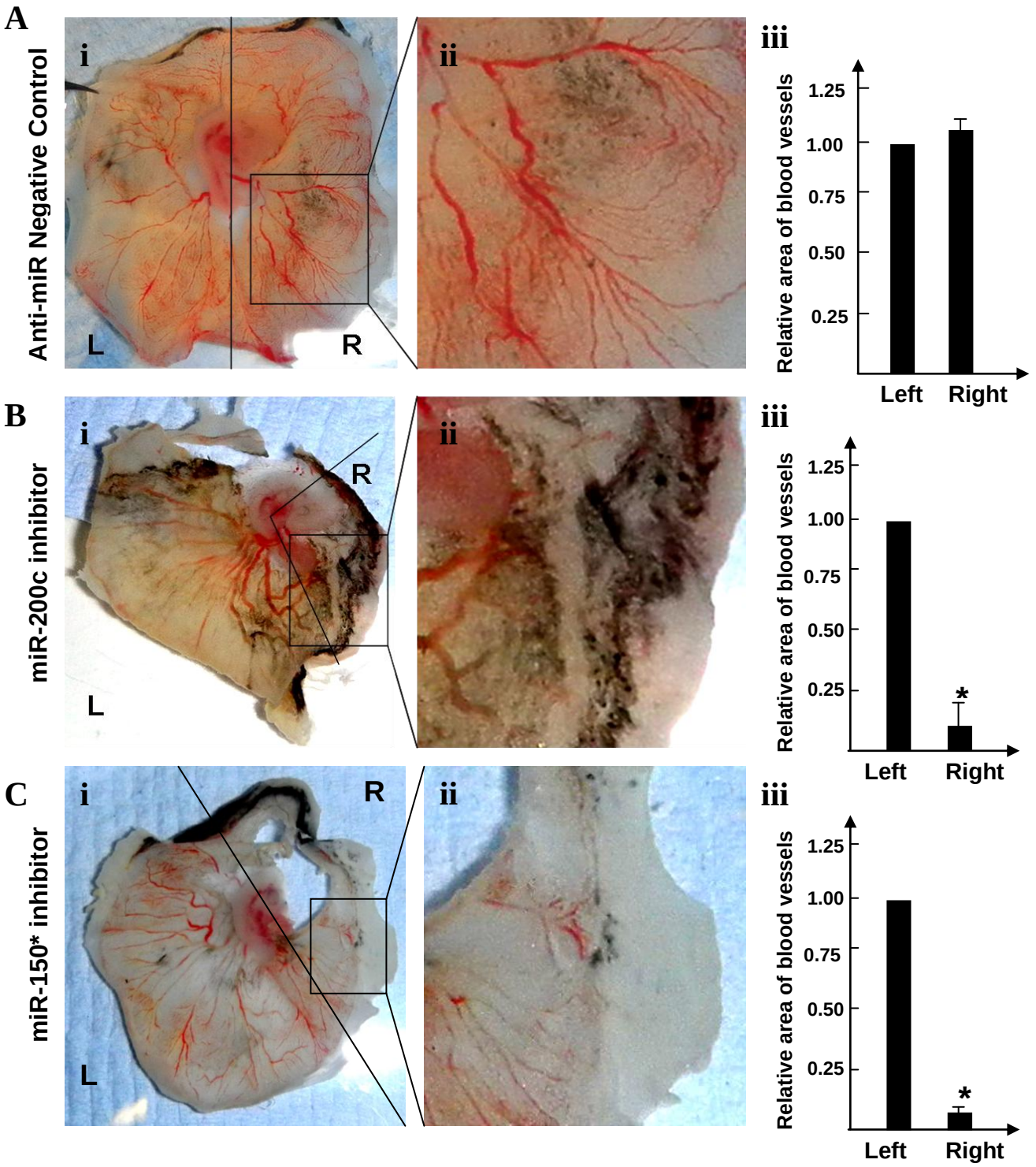
A
Anti-miR Negative Control
i
ii
iii
L
R
Relative area of blood vessels
1.25
1.00
0.75
0.50
0.25
Left
Right
B
miR-200c inhibitor
i
ii
iii
R
L
Relative area of blood vessels
1.25
1.00
0.75
0.50
0.25
*
Left
Right
C
miR-150* inhibitor
i
ii
iii
R
L
Relative area of blood vessels
1.25
1.00
0.75
0.50
0.25
*
Left
Right

Fig. 35 miR-150* and miR-200c play a role in blood vessel formation *in vivo*.

HH10 staged chick embryos were treated with transfection complexes containing Anti-miR Negative Control, miR-150* or miR-200c inhibitor. The relative area of blood vessels formed in these chick embryos were analysed later at HH20 stage. (A) Negative control chick embryo (HH20). i) Transfection complexes containing Anti-miR Negative Control treatment were administered at the right-hand side of the chick embryo (R). No treatment was administered at the left-hand side (L) of the chick embryo. An enlarged image of an area of the control treatment was depicted in ii. iii) A bar graph illustrating an analysis on the number of observed blood vessels at both sides of the chick embryo using a program in photoshop. Each column represent mean $\pm$ SEM of three independent experiments (n=3). (B) miR-200c treated chick embryo (HH20). i) Transfection complexes containing miR-200c inhibitor were administered at the right-hand side of the chick embryo (R). No treatment was administered at the left-hand side (L) of the chick embryo. An enlarged image of an area of the control treatment was depicted in ii. iii) A bar graph illustrating an analysis on the number of observed blood vessels at both sides of the chick embryo using a program in photoshop. Each column represent mean $\pm$ SEM of three independent experiments (n=3). * Relative area of blood vessels with miR-200c inhibition (R) was significantly different from non-treated area (L) at HH20; $P < 0.05$, paired t test followed by one-tail test. (C) miR-150* treated chick embryo (HH20). i) Transfection complexes containing miR-150* inhibitor were administered at the right-hand side of the chick embryo (R). No treatment was administered at the left-hand side (L) of the chick embryo. An enlarged image of an area of the control treatment was depicted in ii. iii) A bar graph illustrating an analysis on the number of observed blood vessels at both sides of the chick embryo using a program in photoshop. Each column represent mean $\pm$ SEM of three independent experiments (n=3). * Relative area of blood vessels with miR-150* inhibition (R) was significantly different from non-treated area (L) at HH20; $P < 0.05$, paired t test followed by one-tail test. (R) Right, (L) Left.

3.7 hESCs differentiate towards the smooth muscle cell lineage

In order to fulfill the potential of hESCs in treating cardiovascular diseases, the understanding of its roles and functional biology in vasculogenesis is pivotal. Henceforth, hESCs differentiation towards the vascular lineage serves as the first step. As shown previously, this project has achieved the derivation of ECs from hESCs. The next objective is to derive SMCs, another component of the vasculature from pluripotent hESCs. SMC differentiation was achieved by culturing undifferentiated hES cell clumps on collagen IV-coated dishes or plates in SMC differentiation medium as previously described in detail for mouse SMC differentiation [160]. Expression of SMC markers was analysed during differentiation to determine whether the differentiation protocol was optimal in deriving vascular SMCs. A set of SMC markers was analysed using real-time PCR (Figs 36-39), western blot (Fig.40) and immunocytochemistry (Figs 41-43).

3.7.1 Collagen IV can drive hESCs differentiation towards SMCs

To induce SMC differentiation from hES cells, undifferentiated hES cells were plated on collagen IV coated dishes or plates and cultured in SMC differentiation medium (DM) for the indicated experimental time-points. Total RNA and protein were extracted and subjected to real-time RT-PCR and western blot analysis, respectively. The mRNA expression of SMA was increased significantly at day 3 and 5 compared to basal control levels (Fig.36). SMA mRNA expression appeared to decrease slightly from days 7-9, but still displayed a sustained high level during the period of differentiation. Following a similar trend, gene expression of Calponin gradually increased from day 0 and its expression at day 3 and 5 were significantly increased compared to control levels (Fig.37). After which there was a gradual decrease of Calponin expression from days 7-9. SM-MHC II mRNA expression was significantly increased compared to control at day 5, which was slightly later than SMA and Calponin expressions (Fig.38). However, platelet-derived growth factor receptor-beta (PDGFR-β) gene expression increased in a time-dependent manner, reaching significance levels at days 7 and 9 (Fig.39). Furthermore, based on

overall relative expression levels, the PDGFR-β gene appeared to be expressed the most with its maximal expression of around 60.0 at day 9, while the expression of the other three SMC markers peaked at day 3 or day 5 which subsequently decrease slightly but stll displayed a sustained high level during the period of differentiation. As the cells differentiated further, the expression of PDGFR-β gene was increased indicating the attainment of an increased functional SMC phenotype.

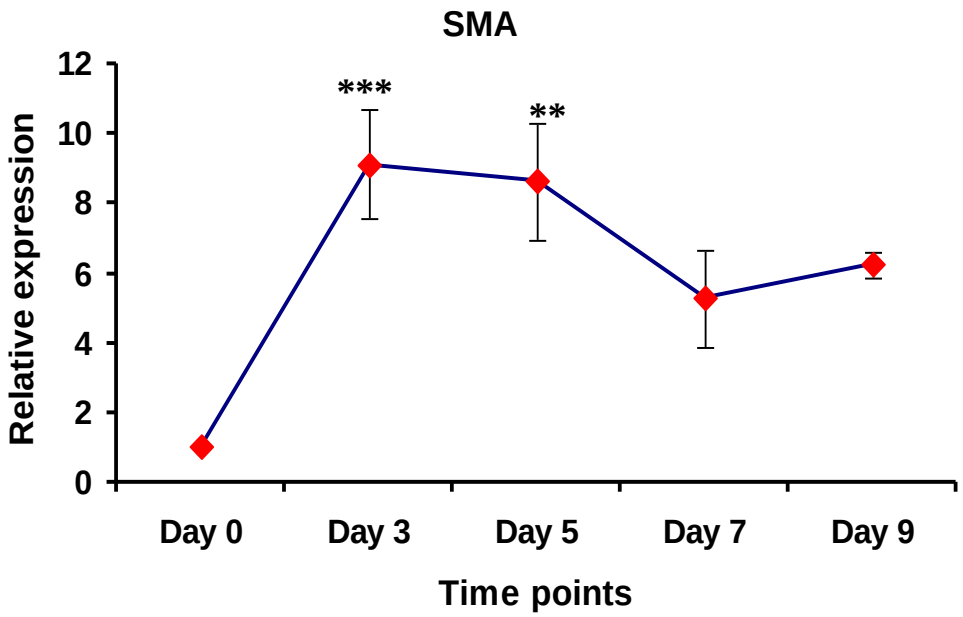

Fig. 36. Gene expression of SMA in differentiating hESCs over a period of 9 days.

Clumps of undifferentiated hESCs colonies were seeded on collagen IV and cultured in SMC differentiation medium for 3, 5, 7 and 9 days. During each respective time-point, RNA was extracted, reversed transcribed to cDNA as previously described and subjected to real-time PCR analysis. Day 0 (control) samples were obtained from undifferentiated hESCs. Data represent mean ± SEM of three independent experiments (n=3). Data normalized to 18S and presented relative to day 0 expression. *** Relative expression of SMA at day 3 was significantly different from day 0; $p < 0.001$. ** Relative expression of

SMA at day 5 was significantly different from day 0; p< 0.01. One-way analysis of

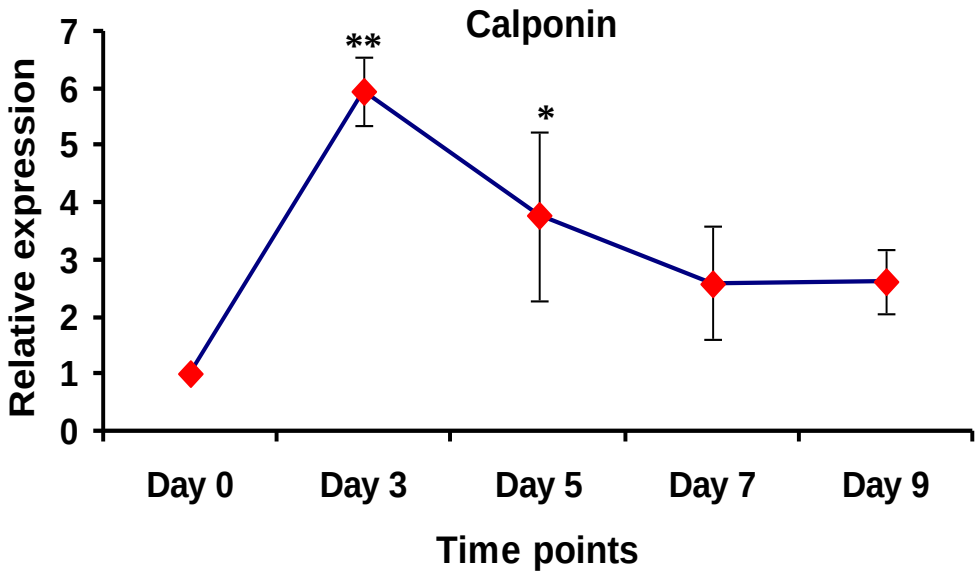

variance (Anova) followed by Bonferroni's Multiple Comparison Test.

Fig. 37. Gene expression of Calponin in differentiating hESCs over a period of 9 days.

Data represent mean ± SEM of three independent experiments (n=3). Data normalized to 18S and presented relative to day 0 expression. ** Relative expression of Calponin at day 3 was significantly different from day 0; p< 0.01. * Relative expression of Calponin at day 5 was significantly different from day 0; p< 0.05. One-way analysis of variance (Anova) followed by Bonferroni's Multiple Comparison Test.

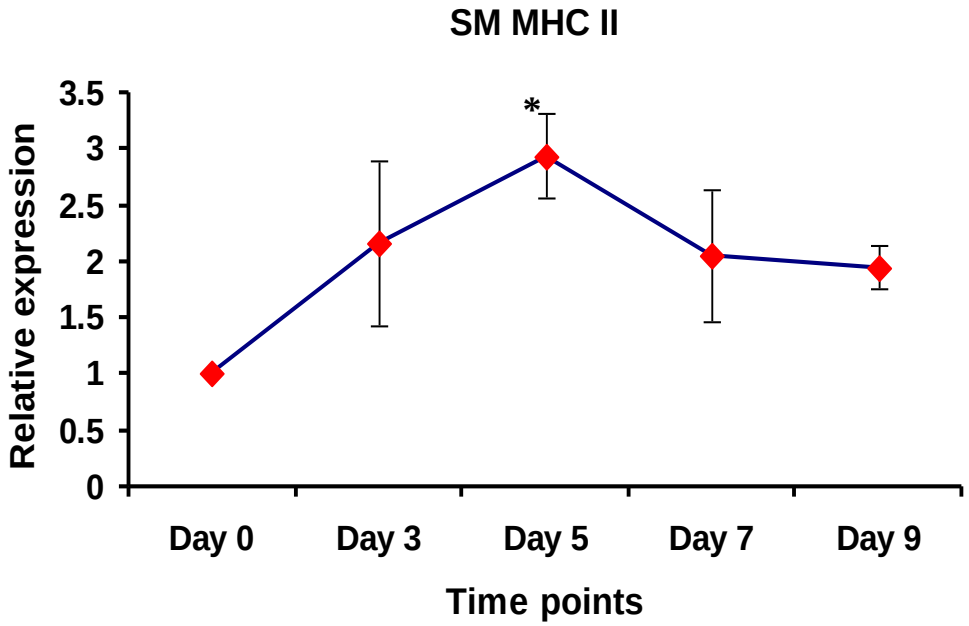

Fig. 38. Gene expression of SM-MHC II in differentiating hESCs over a period of 9 days.

Data represent mean ± SEM of three independent experiments (n=3). Data normalized to 18S and presented relative to day 0 expression. * Relative expression of SM-MHC II at day 5 was significantly different from day 0; $p < 0.05$. Paired t-test followed by two tailed test.

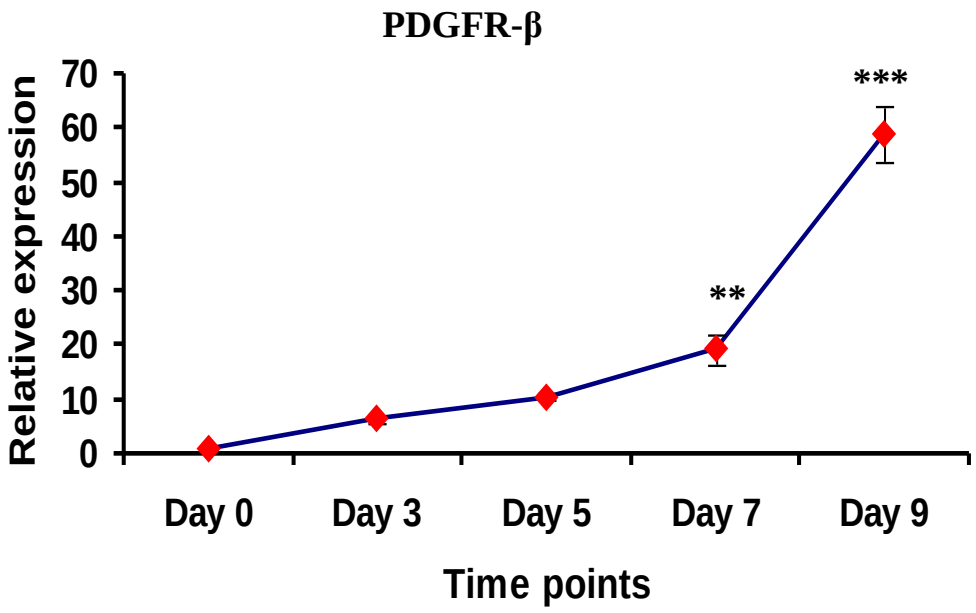

Fig. 39. Gene expression of PDGFR-β in differentiating hESCs over a period of 9 days.

Data represent mean ± SEM of three independent experiments (n=3). Data normalized to 18S and presented relative to day 0 expression. ** Relative expression of PDGFR-β at day 7 was significantly different from day 0; $p < 0.01$. *** Relative expression of PDGFR-β at day 9 was significantly different from day 0; $p < 0.001$. One-way analysis of variance (Anova) followed by Bonferroni's Multiple Comparison Test.

3.7.2 Differentiating hESCs express SMC proteins in western blot analysis

Further confirmation of the previous gene expression data was achieved by carrying out western blot analysis with antibodies against specific SMC markers on protein samples harvested at the indicated time points. As shown in Figure 40, SMA protein appeared at day 3 and peaked at day 9 (Fig.40 *Top*). Another mature SMC marker, SM MHC-II, however appeared slightly later at day 5 of differentiation which persist at day 7 and further increased its expression at day 9 (Fig.40 *Bottom*). As compared to SMA protein expression, it appeared that SM MHC-II protein expression was much lower.

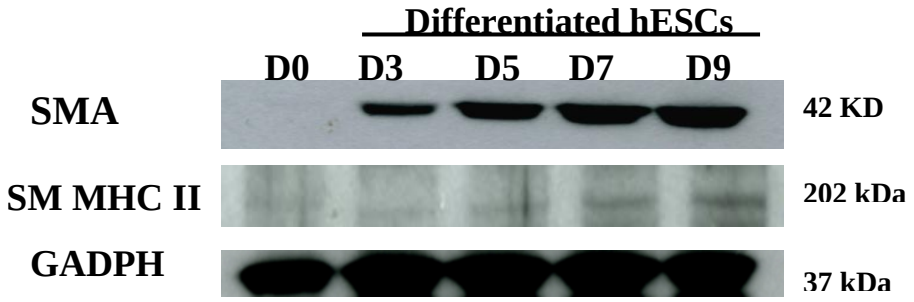

Fig. 40. Western blot analysis of hESCs differentiation towards the SMC lineage over a 9 day period.

Undifferentiated hESCs were differentiated in α -MEM in the presence of FBS and grown over a period of 9 days. As previously described, protein samples were extracted from differentiating hESCs during days 3, 5, 7 and 9. 40µg of each protein sample was loaded into each well, blotted and probed with SMC specific antibodies SMA and SM-MHC II (*Upper panel -Top* to *Bottom*). Each **immunoblot** was reprobed with GADPH, a housekeeping protein to show the total sample loading in each well (*Lower panel*). Day 0 samples were obtained from undifferentiated hESCs which act as negative control. (n=3)

3.7.3 hESC derived SMC-like cells express SMC proteins in immunocytochemistry analyses

Immunofluroscence staining and flow cytometry analysis were conducted to further identify and quantify the SMC population differentiated from hES cells. Day 9 differentiated hESCs were used in both analyses to examine the protein expression levels of SMC-specific markers since most of the SMC protein markers were maximally expressed at that time point as demonstrated by western blots (Fig.40). Calponin which is capable of binding to Actin, Calmodulin, Troponin C and Tropomyosin, could observed in day 9 differentiated hESCs (Fig.41). An appearance of a typical SMC spindle-shaped morphology was observed. Likewise, SMA was also observed in the cytoplasm localised as filaments (Fig.42A). Intriguingly, another population of cells which might represent intermediate SMC was detected as SMA positive, although not displaying a typical SMA staining pattern. These cells displayed a lower level of SMA protein expression which was not localised in distinct filaments (Fig.42B). A mature and late expressing SMC-specific marker SM-MHC II was also observed in the cytoplasm (Fig.43).

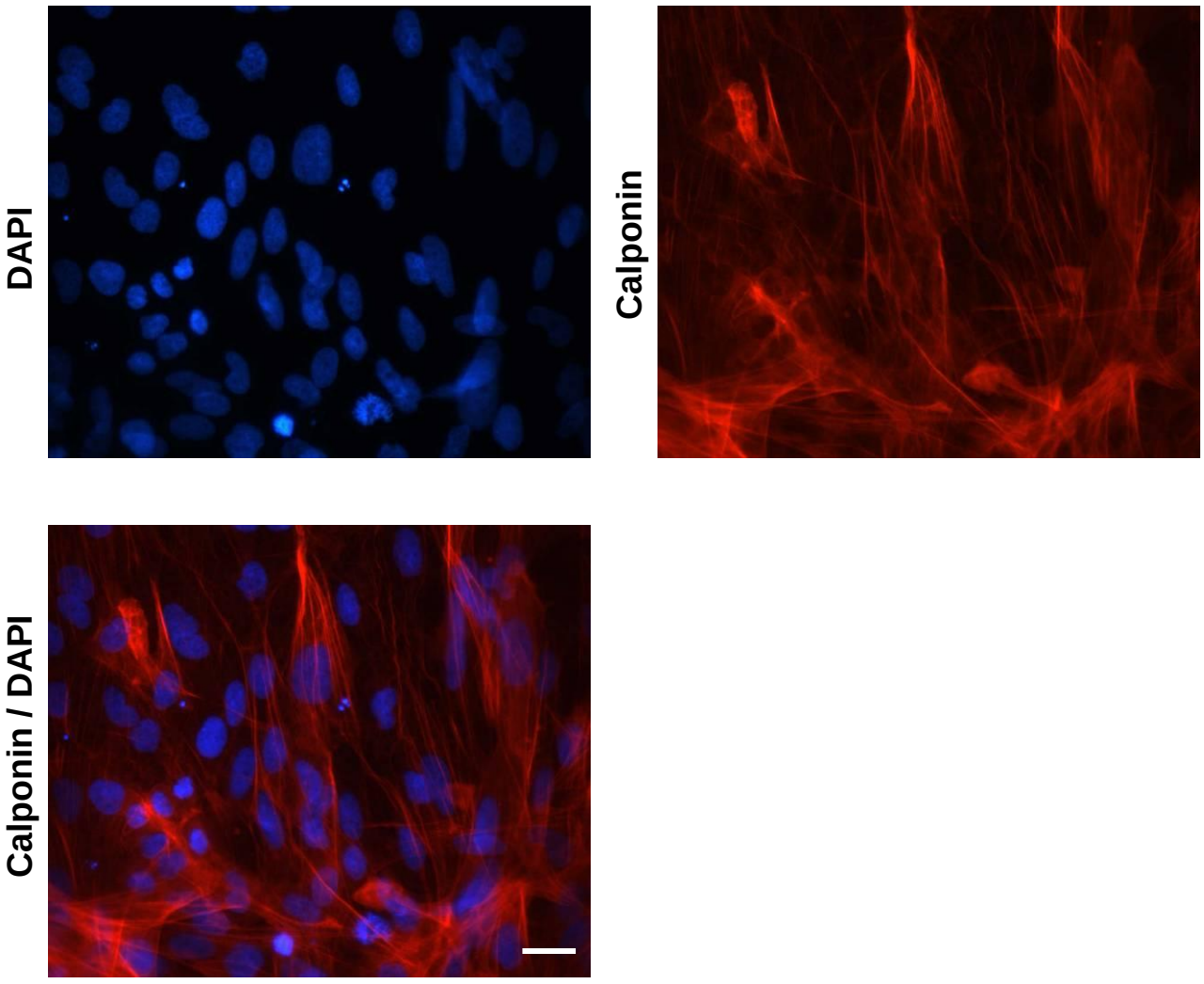

Fig. 41. Expression of calponin in hESCs-derived SMCs.

Day 9 differentiated hESCs grown in SMC differentiation medium were probed with Calponin primary antibody followed by polyclonal goat anti-Rabbit IgG immunoglobulins TRITC. *Anti-clockwise from upper right.* Fluorescent images were captured on calponin positive cells (upper right), nucleic acid stains (DAPI) in individual cell (upper left) and an overlapped image depicting the localisation of both calponin and DAPI. Bar = 20 µm.

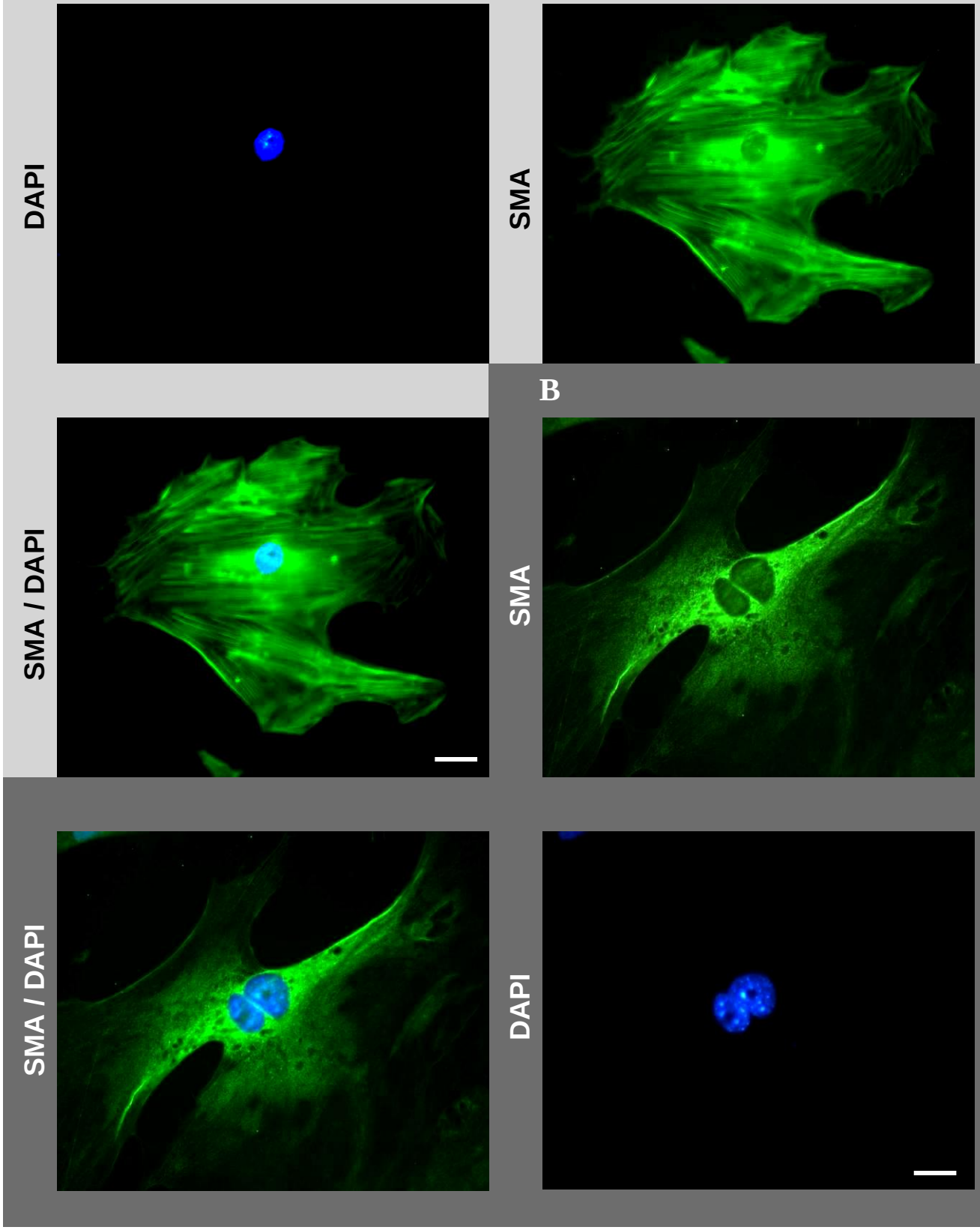
A
DAPI
SMA
B
SMA / DAPI
SMA
SMA / DAPI
DAPI

Fig. 42. Expression of SMA in hESCs-derived SMCs.

Day 9 differentiated hESCs grown in SMC differentiation medium were probed with SMA primary antibody followed by polyclonal goat anti-mouse IgG immunoglobulins FITC. *Anti-clockwise from upper right.* (A) Fluorescent images were captured on a SMA positive cell (upper right), localization of nucleic acid stain (DAPI) (upper left) and an overlapped image depicting the localisation of both SMA and DAPI in the cell (middle left). *Clockwise from middle right.* (B) Fluorescent images were captured on a SMA positive cell (middle right), localization of nucleic acid stain (DAPI) (lower right) and an overlapped image depicting the localisation of both SMA and DAPI in the cell (lower left). Bar = 20 μm

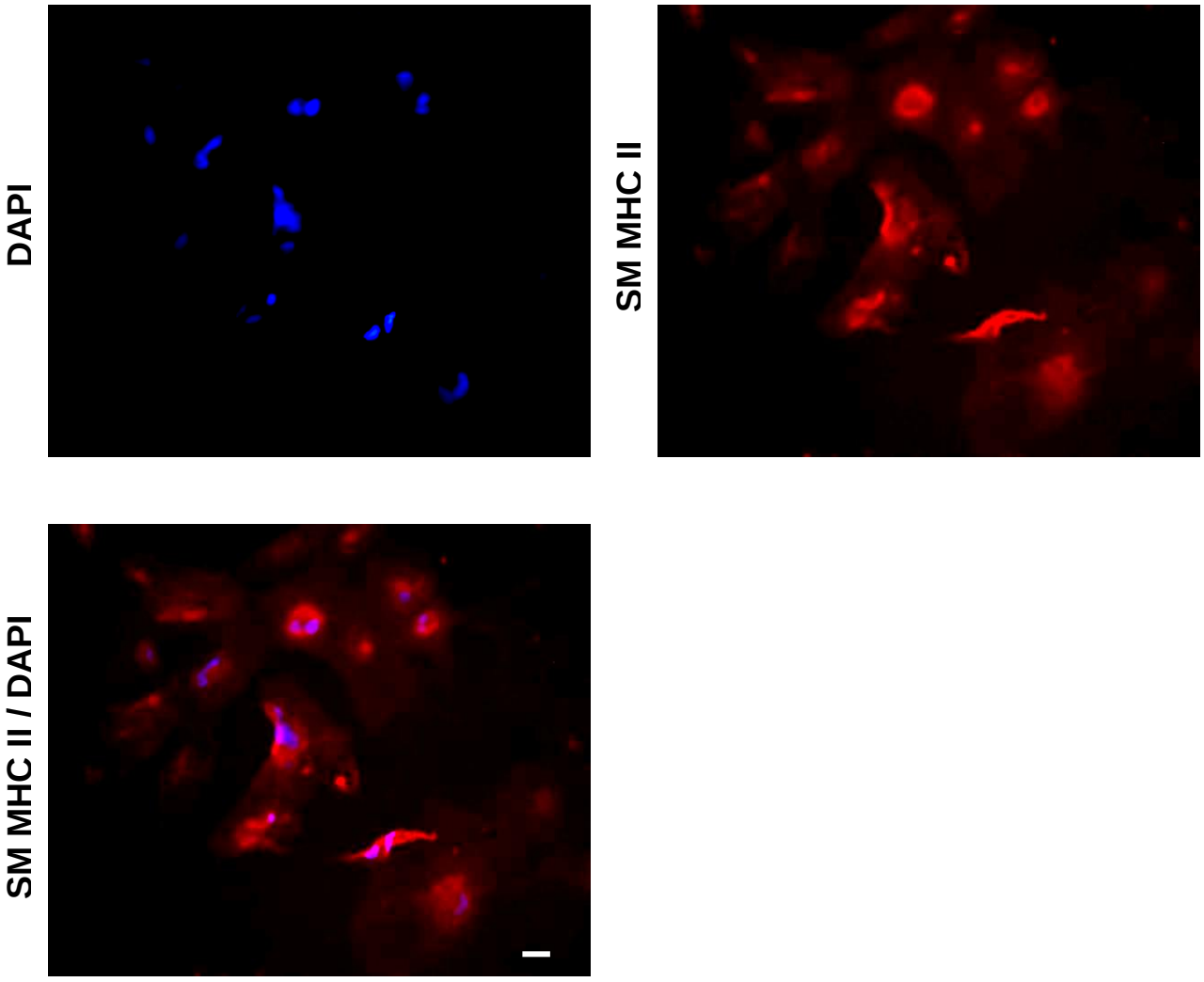

Fig. 43. Expression of SM-MHC II in hESCs-derived SMCs.

Day 9 differentiated hESCs grown in SMC differentiation medium were probed with SM-MHC II primary antibody followed by polyclonal goat anti-Rabbit IgG immunoglobulins TRITC. *Anti-clockwise from upper right.* Fluorescent images were captured on SM-MHC II positive cells (upper right), nucleic acid stains (DAPI) in individual cell (upper left) and an overlapped image depicting the localisation of both SM-MHC II and DAPI. Bar = 20 µm

3.7.4 hESC derived SMC-like cells are capable of contraction when assessed using contractility assay

As it has been well-established that SMCs are able to contract in response to external stimulus such as carbachol and potassium chloride (KCL), a contractibility assay was carried out to assess the function of hESC derived SMC-like cells. 40mM/L of agonist KCL was found to induce contraction in cells. Upon stimulation with KCL, cells underwent contraction as observed by their morphology changes, which showed a contrast from their previous normal resting spindle-shape morphology (Fig.44).

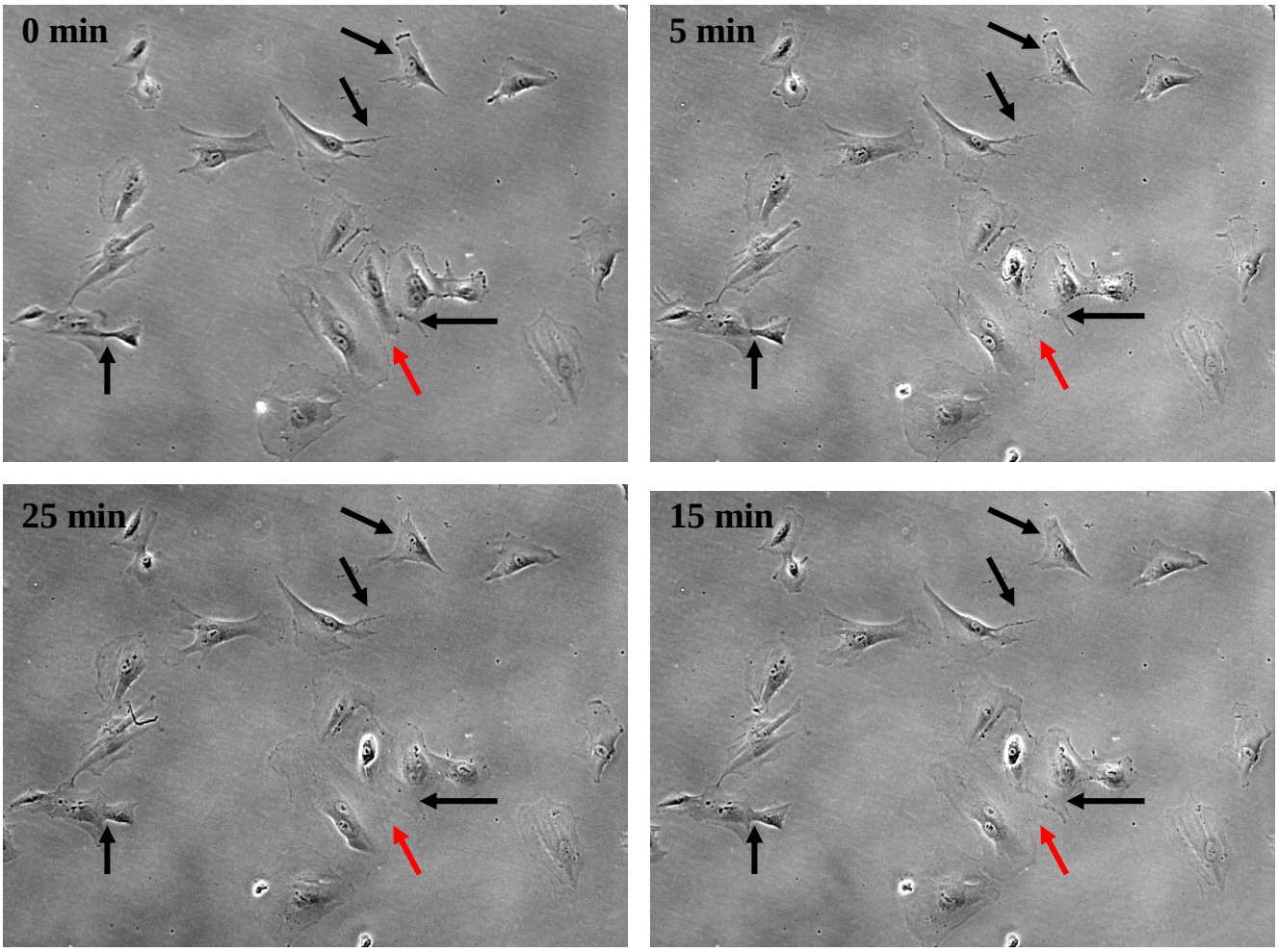

Fig. 44. KCL-induced contraction of hESCs derived SMCs.

Starting clockwise, from top-left hand corner. An image captured before cells were stimulated with 40mM/L of KCL agonist. In here, the cells exhibited elongated and spindle-shaped morphologies. As the duration of agonist stimulation progressed, there was an indication of contraction, with a notable loss of normal resting SMC morphology (shown by arrows). Note that the cell denoted by a red arrow had undergone most contraction, whereby after 5-25 minutes of stimulation resulted in a near rounded morphology, in far contrast to its spindle-shaped appearance before stimulation. Images were taken at 10X magnification.

CHAPTER 4

CHAPTER 4

Discussion

4.1 Determination of pluripotency in cultured undifferentiated hESCs

hESCs were supported on feeder layers of inactivated MEFs which allowed them to grow as undifferentiated colonies [46]. Prior to seeding, MEFs were inactivated with MMC derived from *Streptomyces caespitosus* that crosslinks the complementary double helix strands of the MEFs' DNA. This prevents the separation of the complementary DNA strand, thus resulting in cell cycle arrest [161, 162]. In addition, hbFGF was added to the hESCs culture medium as it is required for maintaining the pluripotent and self-renewal properties of hESCs [163], similar as leukemia inhibitory factor (LIF) is required for the self-renewal of mESCs.

It is vital to determine the pluripotent status of hESCs prior to differentiation as this helps to keep in check with the hESC culture system. Hence, the pluripotent and self-renewal properties of undifferentiated hESCs in culture was initially assessed by detecting activity levels of AP, which resulted in the presence of reddish-purple colonies after staining (Fig.7). AP is a hydrolase enzyme which dephosphorylates molecules such as nucleotides, proteins, and alkaloids under alkaline conditions. An elevated level of AP is associated with undifferentiated and pluripotent stem cells [164, 165]. Differentiated colonies will appear colorless after AP staining, distinguishing the undifferentiated colonies from the differentiated ones. It was reported that undifferentiated hESCs also express pluripotent surface markers such as SSEA4 which is a glycolipid protein carbohydrate epitope as well as keratin sulphate-associated antigens TRA-1-60 and TRA-1-81 [46]. Similarly, undifferentiated hESCs in culture have shown the expression of these pluripotent surface markers and transcription factors OCT3/4 and SOX2 after immunochemistry staining (Fig.8A). Unlike mESCs, undifferentiated hESCs do not express the carbohydrate antigen,

SSEA-1 as shown in Fig.8B, which suggest that differences exist in early development between mouse and human species [166, 167]. Hence the display of pluripotent markers further supports the validity in maintaining pluripotent and undifferentiated hESCs in the cell culture system.

4.2 Establishment of a EC differentiation model for hESCs and their EC expression during differentiation

One of the earliest aims in this project was to establish a model for differentiating hESCs towards the EC lineage. Initial attempts to achieve this were tried and tested using various concoctions of EC growth factors such as VEGF, BMP or FGF in the presence of serum-free medium. It was anticipated that differentiating hESCs in serum-free medium was best approached as serum contained a variety of undefined factors and might not be ideal for future clinical therapeutic application. However, in this project, this type of differentiation model proved fruitless in deriving endothelial-like cells. One possibility was that this particular Shef 3 hESC line requires the presence of certain undefined factors in serum that are not present in serum-free medium which will aid in its vascular differentiation process. Hence modifications were made and the existing endothelial differentiation model was made up of of EGM-2 which contains 2% serum. In addition, Matrigel was chosen as the basement substrate for hESCs differentiation towards EC lineage based on previous reports that showed the ability of ECs to form vascular tubes on the 3-dimensional Matrigel substrate [168, 169]. Moreover, the combination of both EGM-2 and Matrigel closely mimicked the culture environment for growing ECs. Also instead of utilising the formation of embryoid bodies to differentiate hESCs, 200-300 undifferentiated hESC clumps were simply seeded onto the Matrigel matrix. This method ensured that every single hESCs grown as a monolayer were subjected to equal exposure to the differentiation medium. However, this could not be achieved if hESCs were grown as embryoid bodies instead.

Determination in the validity of the hESCs differentiation model towards EC lineage was assessed by detecting a set of EC markers during differentiation. Using real-time PCR, the expression in the majority of endothelial-specific genes such as CD144/VE-cad (Fig.9),

vWF (Fig.11) and Kdr (Fig.12) increased as the number of days lengthened during the 9 days differentiation period. Gene expression for CD144/VE-cad appeared at day 3 (Fig.9), which was slightly earlier as compared to the reported appearance of CD144/VE-cad in day 4 differentiating human embryoid body [67]. CD146 gene expression also appeared at day 3 but subsequently decreased in the later period of differentiation (Fig.10). Gene expressions of CD144/VE-cad, vWF and Kdr at day 9 were significantly elevated as compared to expression at day 0 control levels (Figs. 9, 11, 12). Furthermore, at day 9, both vWF and Kdr gene expression levels were the highest hovering around 4.0, compared to CD144/VE-cad which was at around 2.0. mRNA level of Nanog, which is a key factor in maintaining the pluripotency and undifferentiated state of ESCs, significantly decreased gradually at days 5, 7, and 9 as compared to day 0 (Fig.13.). Overall findings indicated that expression levels of endothelial-specific genes reached its maximum at days 3 or 9, implying a differentiation process towards mature ECs.

Next, protein analysis using western blot, immunocytochemistry and flow cytometry were used to further characterize and quantify differentiating hESCs cultured in EC promoting conditions. The increase in gene expression of CD144/VE-cad and vWF during differentiation correlates with the observation in their increased protein expression in western blot analysis (Fig.14). CD144/VE-cad is a cell adherent protein and mediates cell–cell adhesion (Fig.16) between vascular ECs as part of the adherens junction complex [170]. Western blot analysis showed that protein expression of CD144/VE-cad appeared only at day 9 (Fig.14) whereas as previously shown, its gene expression appeared earlier at day 3 (Fig.9). A probable reason for this discrepancy is that gene expression levels of CD144/VE-cad from differentiation days 3-7 are quite close (< 0.5 fold increase) compared to basal control levels (Fig.9) and this subtle increase is possibly not adequate to detect using western blotting. In contrast, a near 1.0-fold increase was observed at day 9 CD144/VE-cad gene expression level as compared to basal levels (Fig.9), an expression which was sufficient to detect in western blotting (Fig.14).

CD146 is a membrane glycoprotein localized at cell-cell endothelial junction [171] as observed in Fig.17. CD146 protein expression appeared at day 3 and was maximal at day 9 (Fig.14) whereas its gene expression revealed its maximal expression at day 3 which decreased gradually over time (Fig.10). This difference in CD146 gene and protein expression patterns could be due to the late translation of its mRNA and hence the late expression of its protein product. In addition, flow cytometry analysis revealed that 16.4% of the heterogeneous cell population expressed CD146 at day 7 (Fig.21A *Top*). This expression was increased to 34.1% approximately two-fold at day 17 (Fig.21A Bottom).

Previous studies carried out by Levenberg *et al*. and Kaufman *et al*, reported that undifferentiated hESCs express the VEGF receptor, Kdr on their surfaces unlike their mESCs counterparts and increased very slightly during differentiation [67, 172]. In contrary, the undifferentiated Shef 3 cell line which was used in this experiment did not appear to express Kdr and its gene expression increased significantly at day 7 as compared to basal control day 0 (Fig.12). Immunocytochemistry staining of day 9 differentiated Shef 3 hESCs also showed the presence of Kdr (Fig.19) which was otherwise not detected in these undifferentiated hESCs (immunostaining data not shown). This absence of Kdr expression in undifferentiated hESCs was also reported in a study using BG02 and WA09 hESC lines [173]. The hESCs lines used in studies carried out by Levenberg *et al.* and Kaufman *et al.* were H9 and H1 respectively. This showed that differences do exist in different hESC lines and further standardization protocols or cell lines may be required for differentiating hESCs if applied in future clinical therapeutic settings [174, 175].

Several other EC specific markers were also assessed to characterize the differentiating hESCs. vWF protein expression was also detected in flow cytometry analysis (Fig.21B) and western blotting. vWF protein appeared from day 5 and its levels was sustained till day 9 in the western blot analysis (Fig.14). This observation was similar to its gene expression which appeared at day 5 and with a significance increase of expression at day 9 (Fig.11). vWF previously known as Factor VIII related antigen, is synthesized exclusively by ECs and megakaryocytes. It is stored in the intracellular granules or constitutively secreted into

plasma as observed in Fig.20. Immunostaining analysis also showed the presence of CD31/PECAM-1 in differentiated hESCs that is located between EC junction sites (Fig.15). In western blot, CD31/PECAM-1 protein levels showed an increasing time-dependent expression as the differentiation time period lengthened (Fig. 14). Another endothelial specific marker, eNOS or otherwise known as NOS3 in EC, produces nitric oxide which functions as a vasodilator and regulates blood flow and pressure. eNOS is found at cytoplasmic locations in ECs and its protein was detected from days 3 to 9 of hESCs differentiation (Fig.14 & 18).

In general, the overall expression of EC markers during differentiation showed that the differentiation method in deriving ECs from undifferentiated hESCs was successful in achieving mature vWF-expressing ECs at day 9. Further isolation of cells expressing EC markers to obtain a pure EC population was achieved using FACS and their EC function assays will be discussed in the following section.

4.3 Characterisation of CD146+ cells using in vitro *and* in vivo *EC tests*

Next, the heterogeneous population of differentiating hESCs were subjected to FACS for cell sorting to obtain CD146+ cells (Fig.22). The purity of CD146 + cells after sorting was 96.5% (Fig.22A & B). When this population of CD146+ cells was expanded *in vitro* after isolation using FACS, two different cell phenotypes were observed (Fig.23A). The first morphology resembles round endothelial-like cobblestone-shape while the other has a spindle-shaped fibroblast or SMC morphology. It has been reported that the expression of CD146 molecule is not only restricted in EC but also in several other non-malignant and malignant cell types, including smooth muscle cells [176], pericytes [177], follicular dendritic cells [178], lymphocytes [179] and melanoma cells [180]. Since both smooth muscle cells and pericytes share similar spindle-shape fibroblast morphology, it is probable that these cells were also isolated along with the cobblestone cells during CD146+ cell sorting. However, in the later passages of the CD146 cell culture (passage 9), the spindle-shaped fibroblast morphology observed in earlier passages disappeared (Fig.23B), leaving only cobblestone-shaped cells. A likely reason for this phenomenon is that the EGM-2 and collagen-I culture

conditions may only favour EC maintenance and growth while the other cell types die off as the culture period lengthens. This results in the obtainment of only cobblestone-shaped cells as the CD146+ culture gets older. Moreover, flow cytometry analyses for passages 1 and 5 of CD146+ cell population showed that expression levels of EC markers such as CD146, vWF, CD144/VECAD and CD31/PECAM increased in the later passage (Fig 24). This implies that the sorted CD146+ cells that displayed EC morphology and markers can be expanded successfully in the existing culture conditions. Furthermore, immunocytochemistry stainings confirmed that the CD146+ cell population expressed EC protein markers like vWF (Fig.25A), eNOS (Fig.25B), CD31/PECAM (Fig.25C) and CD144/VECAD (Fig.25D) (Fig.25). Next, further tests such as Matrigel assay to assess EC tube formation and Dil-Ac-LDL uptake were carried out to determine the functional capability of these cells.

The uptake of Dil-Ac-LDL is one of the classic hallmarks used to characterize endothelial cells [181]. Firstly, Dil-Ac-LDL is taken up by cells via scavenger receptors. Since Ac-LDL behaves like oxidised LDL, both are degraded within lysosomes by lysosomal enzymes. Later fluorescent lipophilic Dil probes accumulate in the intracellular membrane, labelling the cells [182]. However, smooth muscle cells and pericytes do not possess the scavenger pathway for Ac-LDL metabolism [181]. The CD146+ cell population was capable of Dil-Ac-LDL uptake as evidenced in Fig.26. But since macrophages also take up acetylated-low density lipoprotein [181], co-staining with lectin binding was carried out to distinguish macrophages and endothelial cells. Anti-*Ulex Europaeus*-I (UEA-I) lectin reacts specifically for UEA-I which interacts with α-L fucosyl residues in oligosaccharides present on the membranes of vascular human endothelial cells [183]. Positive stainings of CD146+ cell population for Dil-Ac-LDL and lectin (Fig.26) indictate that these cells are of endothelial origin and not smooth muscle cells, pericytes or macrophages.

Another EC functional test, *in vitro* vasculogenesis assay using Matrigel^{TM} matrix was also carried out to characterise the function of CD146+ cells. The Matrigel^{TM} matrix (BD Biosciences, Bedford, MA) is a soluble basement membrane extract from the Engelbreth-

Holm-Swarm mouse sarcoma. It gels at room temperature [184] and is rich in extracellular matrix proteins. The major components of Matrigel™ matrix are laminin, followed by collagen IV, heparin sulphate proteoglycans and entactin/nidogen [184, 185]. Growth factors such as TGF-β, insulin-like growth factor, fibroblast growth factor as well as collagenases and plasminogen activators are also present [186].

As seen in Fig.27A, CD146+ cells were capable of vasculogenesis in Matrigel™ by forming vascular structures 24 hours after seeding onto Matrigel™ *in vitro*. These cells were also capable of forming complex vascular network *in vivo* in Matrigel™ plugs implanted in SCID mice (Fig.27B). After carrying out a battery of EC characterisation tests, it can be concluded that the population of CD146+ cells are capable of further expansion *in vitro* after FACS cell sorting and display characteristics and functions of ECs *in vitro* and *in vivo*.

4.4 Potential miRNA candidates play a role in hESCs differentiation towards the EC lineage

miRNA has paved a new window in our understanding of gene expression and is one of the most widely applied techniques in biomedical research, especially in the molecular investigation of disease pathogenesis. For instance, it has been reported that miR-1 plays an important role in heart conductivity since miR-1 levels were positively correlated with coronary artery disease and after cardiac infarction. Loss-of-function of miR-1 prevented heart arrhythmia, whereas miR-1 overexpression caused heart arrhythmia in normal and infarcted hearts [187]. Both miR-1 gain- and loss-of-function studies affect the conductivity of the heart through potassium channels was subsequently demonstrated [187]. These results suggest that miR-1 has a prominent effect on the development of cardiac arrhythmia, an irregular electrical activity in the heart. In another study, it was found that the muscle-specific miR-133 is a negative regulator of cardiac hypertrophy, which is an essential adaptive physiological response to mechanical and hormonal stress as well as size of the heart [188]. Taking these studies into consideration, miRNAs are potential therapeutic targets for disease treatments.

In addition, several *in-vitro* evidences have indicated the involvement of miRNA in regulating endothelial cell behavior such as proliferation, migration and the ability to form capillary networks [147-149, 189, 190]. Dicer, an enzyme essential for the biogenesis of most miRNAs is required for embryonic angiogenesis during mouse development [146]. Furthermore, the contribution of miRNA in directing ESCs towards different cell-fates has been suggested in studies using Dicer or Drosha deficient ESCs. These Dicer and Drosha deficient ESCs were unable to generate mature miRNAs which subsequently impeded their differentiation process [191-193]. In addition, miRNA expression profiling analysis in undifferentiated ESCs and differentiating embryoid bodies have identified candidate miRNAs involved in the maintenance of the pluripotent ESC state as well as regulating early mammalian development [194-199]. Besides, accumulating evidences have also demonstrated the crucial involvement of specific miRNAs in the differentiation of ESCs [198-202].

In a recent study, Fish *et al.* showed that miR-126 regulated vascular integrity and angiogenesis in mouse and zebrafish models [152]. However although miR-126 was found enriched in vascular progenitors, it does not control early EC lineage commitment in mESCs [152]. The missing miRNA-link in controlling pluripotent embryonic stem cell fate in differentiation towards the EC lineage is currently undiscovered. Hence the main objective in this project is the determination of which miRNA or miRNAs is/are involved in this crucial process.

To determine which potential miRNAs are involved in embryonic EC development, miRNA array analysis was carried out in hESCs grown in EC differentiating conditions over a 9-day period. From the miRNA array analysis, angiogenic promoting miRNAs such as miR-126 [106, 152] and miR-210 [156] were initially undetected at days 3 and 6 but surfaced at day 9 of differentiation (Fig.28C). In addition, another positive regulator of angiogenesis, miR-130a [156] was found in an increasing trend over the 9-day differentiation period. Moreover, levels of anti-angiogenic miR-221 [149, 156] appeared to decrease over the differentiation time-frame (Fig.28C). miR-145 which has been previously reported to facilitate ESC differentiation by repressing the core pluripotency factors OCT4, sex

determining region Y-box 2 (SOX2), and Kruppel-like factor 4 (KLF4) [201], was induced at day 9 as shown in the miRNA array analysis. These observations clearly demonstrate that our differentiation process of hESCs towards the EC lineage does coincide with previously published miRNA findings.

Five potential enriched miRNAs were selected from the miRNA array analysis and further validated using quantitative real-time PCR. These miRNAs are miR-150* and miR-1915 (Fig.28A) and miR-200 family members, miR-141, miR-200c and miR-205 (Fig.28B). Further examination into the function of miRNAs on hESCs differentiation to ECs, was achieved by carrying out loss-of-function and gain-of-function tests which was transfecting day 6 differentiated hESCs with miRNA inhibitors or precursors respectively. Following which, analyses into whether their inhibition or overexpression would affect EC expression were determined.

Transfection efficiency was monitored using Cy3-labeled Anti-miR Negative Control (Ambion, Applied Biosystems) which has a 5' end fluorescent moiety. Transfection optimization is required to determine optimal conditions required for maximum gene effectiveness. As shown previously, there was a high transfection efficiency of 87.41% after 48 hours transfection with Cy3-labeled Anti-miR Negative Control (Fig.29A) and which dipped slightly to 83.27% at 72 hours post transfection (Fig.29B). This demonstrated that the transfection protocol was optimal and successful in delivering miRNA inhibitors into the cells. The siPORT NeoFX Transfection Agent used in this study utilises an alternative method of transfection called reverse transfection [203]. In reverse transfection, cells are transfected while still in suspension. This saves an entire day , as cells do not need to be plated prior to transfection compared to standard transfection. The lipid-based siPORT^{TM} NeoFX^{TM} Transfection Agent uses liposome-mediated transfection whereby liposomes deliver nucleic acids into the cells [204]. Liposome-mediated transfection has higher efficiency and greater reproducibility than other transfection methods. In addition, siPORT^{TM} NeoFX^{TM} Transfection Agent is a transient transfector giving rise to transient transfection. Transient transfection enables higher copy numbers of foreign nucleic acid

and hence higher levels of gene expression to be present in the cell for a brief period of time. This transient effect can be observed as the effects of miRNA inhibitors and precursors gradually diminish over the 24-72hours post transfection time period (Fig.30-32).

Next, to establish which miRNA is involved in hESCs differentiation towards the EC lineage, EC markers were assayed during real-time PCR. Since all five miRNAs members were selected based on their up-regulated expression during hESCs differentiation to EC, the inhibition of these potential candidates should also influence the downregulation of EC marker expressions. Inhibition studies were carried out using miRNA inhibitors that inhibit endogenous miRNAs. Real-time PCR results in inhibition studies showed that although all five of the selected miRNAs were inhibited, only two out of the five selected miRNAs did downregulate the mRNA expression of specific EC markers as compared to control levels (Fig.30A, 32A-C). At 24 hours post transfection, both miR-150* and 200c were significantly decreased and which downregulated the expression of specific EC markers as compared to control levels (Fig.30A).

Both mRNA levels of miR-150* and 200c were significantly upregulated by transfecting cells with the respective precursors, which are designed to mimic endogenous precursor miRNAs (Fig.31A). mRNA levels of specific EC markers such as vWF, Kdr, CD144 and CD146 were upregulated as compared to control, after the introduction of miR150* precursor (Fig.31Ai) or miR-200c precursor (Fig. 31Aii) into the cells. Further western blot analyses using samples transfected with the same treatments in Fig.31A showed that similar results were obtained (Fig.31B). Taking these findings together, the inhibition of miR-150* and 200c appear to repress EC differentiation from hESCs, whereas their overexpression promote hESCs differentiation towards the EC lineage, suggesting both miRNAs play an important role in endothelial cell differentiation from hESCs.

To provide further evidence on the function of miR-150* and 200c, experiments in inhibiting their expression was carried out in developing chick embryos. It was demonstrated that the number of relative blood vessels were significantly decreased in HH20 chick embyos after treatment with transfection complexes containing miR-150*

(Fig.35C) or miR-200c inhibitor (Fig.35B) as compared to control treated chick embryos (Fig.35A). These observations clearly imply that miR-150* and miR-200c do play a role in EC differentiation during development as shown *in vitro* and *in vivo*. But an intriguing question is how these microRNAs carry out their biological functions and which mechanisms are involved during the EC differentiation process. These questions will form the next set of objectives in the subsequent part of the project.

4.5 microRNAs 150 and 200c target ZEB1/TCF8 during hESCs-EC differentiation*

Ultimately, the function of a miRNA is defined by the genes it targets and how it affects their expression. To understand the mechanisms by which miR-150* and 200c regulate endothelial biology, potential mRNA targets were searched. Predictions of targets for miR-150* and 200c were carried out using PicTar (http://pictar.mdc-berlin.de), a miRNA target prediction algorithm program tool [159]. An important determinant of miRNA target is the high degree of sequence complementarity between the 5' end of the miRNA (seed sequence) and the 3'UTR mRNA target [133, 134]. Another factor is the accessibility of mRNA at the potential binding site [205].

In this study, target prediction using PicTar revealed that potential mRNA targets for miR-150* and 200c were c-Myb and ZEB1. Many reports have also shown that a highly predicted target for miR-150 is the proto-oncogene c-Myb [206-208]. Found highly expressed in hematopoietic progenitor cells, c-Myb expression declines as these cells differentiate [209, 210]. In regard to this study, where the expression of miR-150 appear to promote the differentiation of hESCs towards ECs, it is highly probable that this interaction might also be important during EC development. In addition, overexpressing c-Myb increases the frequency of hemogenic precursors in ESC-derived ECs population [211]. Alternatively, this might imply that an increase of miR-150* expression during the development of embryonic ECs will suppress the expression of its c-Myb target gene and deters differentiation towards the hematopoietic lineage.

miRNA-200c which is a member of the miR-200 family clustered in chromosome 12, has been shown that its overexpression will lead to reduced expression of ZEB1/TCF8 and an increased expression of E-cadherin [212]. Down-regulation of E-cadherin is a crucial event in epithelial-to-mesenchymal transition (EMT) whereas TCF8, a two-handed zinc finger (ZF) homeodomain transcription factor, mediates cell–matrix adhesion and subsequent angiogenesis [213]. EMT facilitates tissue remodelling during embryonic development and has been highlighted in mesoderm formation as well as mesoderm differentiation to diverse tissues or organs during embryogenesis [214, 215]. It also appears that the EMT-activator ZEB1, is expressed in less differentiated cell types like embryonic stem cells [216, 217]. However, the expression of ZEB1 decreases as mESCs differentiate under differentiation-inducing growth conditions [217]. Moreover, Wellner *et al*. also discovered that during mESCs differentiation without the presence of leukaemia inhibitory factor (LIF), levels of stemness-inhibiting miRNAs, miR-200c was upregulated whilst stem cell factors such as KLF4 and Sox2 were decreased [217]. In another seperate study, it was also found that the expression of miR-200c was increased upon differentiation of hESCs [196]. These studies further support our findings that miR-200c which was enriched in our miRNA array analysis study, is present in differentiating ESCs. Taking together the current findings and previously published studies, these strongly suggest that as hESCs differentiate towards the EC lineage, an increase of miR-200c expression contribute to the decline or repression of EMT process, which result in the formation of more differentiated, senescence [218] and less proliferative cells or in this case mature vascular ECs.

In the next part of the study, expression patterns of both c-Myb and ZEB1/TCF8 were further analysed in a 9-day time course study using differentiating hESCs. mRNA levels of both c-Myb (Fig.33A *Left*) and ZEB1/TCF8 (Fig.33A *Right*) were significantly decreased as compared to day 0 control (undifferentiated hESCs). Moreover in miRNA overexpression studies, it was shown that mRNA expressions of both c-Myb and ZEB1/TCF8 were decreased (Fig.33B). These observations demonstrated that c-Myb and ZEB1/TCF8 mRNA expression levels were reciprocally regulated by miRNAs 150* and 200c. However, a significant decrease was observed in only ZEB1/TCF8 mRNA expression but not in c-Myb expression in both miR-150* and 200c overexpression studies. Herein, ZEB1/TCF8 was selected as the preferred mRNA candidate target for miR-150*

and 200c in this study. Interestingly, like miR200c, miR-150* also happen to share a binding site in the 3'UTR of ZEB1/TCF8 (Fig.34A).

Further validation of the ZEB1/TCF8 target site was carried out by cloning the 3'UTR of ZEB1/TCF8 into a luciferase reporter. Luciferase reporter assays were carried out to investigate if miR-150* and 200c directly target the 3' UTR of ZEB1/TCF8. A change in luciferase activity will determine whether a miRNA can bind to the UTR and regulate the expression of the gene [219]. Upon overexpressing miR-200c in CD146+ cells, luciferase activity of 3' UTR of ZEB1/TCF8 was significantly reduced while in miR-150* overexpression, the luciferase activity was moderately reduced (Fig.34B). This demonstrates that both miR-150* and 200c directly target ZEB1/TCF8 and subsequently lead to the differentiation of mature ECs from undifferentiated hESCs.

At this point of time, no other studies have demonstrated or reported the involvement of miRNAs in the development of ECs from hESCs. In this current project, miR-150 and miR-200c were discovered to direct hESCs differentiation into ECs, which is of great clinical use in the future. Patients with atherosclerosis, and especially with cardiac ischemia, treatments such as balloon angioplasty and stenting are frequently used to regain blood perfusion for the local myocardium. However, restenosis, a homeostatic response to vascular injury, leads to the recurrent occurrence of myocardial ischemia. This is due to the loss of the endothelium secondary to the balloon inflation at high pressures and the use of foreign metallic stent. Subsequently, SMCs would be activated and switched on, resulting in the proliferation and secretion of the extracellular matrix. This would lead to luminar narrowing after these interventional procedures were carried out [94, 220]. It has been shown that accelerated reendothelialization by mature ECs effectively inhibits SMC migration, proliferation, and neointima formation, and therefore, preventing the development of the early stages of restenosis after vascular injury [221]. Therefore, the application of these miRNAs discovered in my current experiment can be used for the generation of patient specific ECs and which can also be used to heal the damaged vessel while interventional procedures are being performed in the patient. On the other hand, these miRNAs can also be delivered directly into the coronary arteries and activate the local EC differentiation mechanism so that the vessel damage can be prevented [222].

As miRNA research is still new and has been conducted for only a few years, there are still lots of unknown but exciting and promising findings waiting to be discovered. Most of the miRNA studies have revealed a level of molecular control in human diseases that were beyond the well-accepted regulatory systems such as regulation by transcription factors and signalling proteins [187, 188, 222]. Furthermore, these studies also have implications that, in a cell, a more complex regulatory system, e.g., interactions between miRNAs, cell signaling and transcription factors, is involved in many cellular activities and human diseases. Therefore, it is essential to study the under-lying interactions between miRNAs and cellular regulatory systems and pathways. Hence, this leads to the understanding of gene regulation in a more comprehensive manner and opening up new opportunities in manipulating miRNAs as diagnostic and therapeutic targets.

Other than the determination of applicable miRNAs at the molecular level for the development of new therapeutic strategies, it still remains obscure as to which strategies researchers can use to achieve this goal. Through the understanding of miRNAs is an obvious prerequisite for realizing their rousing promise, which calls for an urgent need to develop suitable technologies for the purpose. Moreover, the ability to efficiently, stably produce and deliver sufficient amounts of miRNAs into the proper cell target, without overt toxicity requires fine tuning of the technology before these can be tried clinically. The pharmacokinetics, cellular safety, and functional stability of miRNA expression in animals needs to be examined, in order to ascertain that the artificial miRNAs are stable, effective, and non-toxic *in vivo*.

4.6 Differentiated SMCs-like cells derived from pluripotent hESCs

Next, VSMCs were derived from pluripotent hESCs as part of the objectives in this project. VSMCs play crucial roles in vasculogenesis and human diseases such as atherosclerosis and hypertension [39]. VSMCs are notoriously known for presenting a wide range of different phenotypes during different developmental stages [35]. Even in adult organisms, VSMCs are not terminally differentiated unlike other muscle cells and can potentially switch between a contractile and a synthetic phenotype [36]. Hence exploring the molecular mechanisms of

early VSMC differentiation will contribute to better understanding of VSMCs and future clinical therapies for vascular diseases.

In this study, differentiation of pluripotent hESCs towards the SMC lineage was achieved. mRNA expressions of most SMC-specific markers, such as SMA (Fig.36) and Calponin (Fig.37), were maximal at day 3 and subsequently decreased slightly over the next following days of differentiation. At day 5, SM-MHC II mRNA expression was maximal and significantly increased compared to control, which was slightly later than SMA and Calponin expressions (Fig.38). However, western blot analyses showed that the specific SMC-markers increased in a time-dependent manner. SMA protein expression was maximally expressed at day 9 and whereas SM MHC-II protein expression only appeared at day 5 and continued to increase over the next few days of differentiation (Fig.40). These time differences in gene and protein expression are possibly due to the late translation of both SMA and SM MHC-II mRNAs and hence the late expression of its protein product. Another possible explanation for the decreased expression levels of some genes at a later stage can be due to the negative feed back pathway upon protein translation and accumulation. Unlike previous observations, PDGFR-β mRNA expression increased in a time-dependent manner, reaching maximal and significance levels at day 9 (Fig.39). PDGF is a well characterised growth factor which has been known for its significant role in angiogenesis [24]. Furthermore, SMCs also secrete PDGF which acts as a major mitogen and chemoattractant [22, 23]. These results imply that during the differentiation process towards the SMC lineage, differentiating cells were attaining increased SMC genes and behaviour as well as expressing the PDBFR-β gene.

Actin is one of the two major cytoskeletal proteins implicated in cell motility, the other being myosin. α-actin being one of the actin isoforms, is found in muscle tissues and a major constituent of the contractile apparatus. SMA has been widely used as a SMC differentiation marker as it is known to express during differentiation of the SMC during development [223]. Immunostaining carried out in day 9 differentiated hESCs showed the

presence of SMA localised in cytoplasmic filaments indicating a contractile SMC phenotype (Fig.42A). A less distinctly stained SMA-positive cell was also observed as shown in Fig.42B. Note that the SMA was not localised as distinct filaments which could imply a possible phenotypic switch to a synthetic morphology and/or represent an intermediate SMC differentiation status. Calponin is a marker of the intermediate stages of SMC differentiation/maturation [8] and is implicated in the regulation of SMC contraction. Like SMA, calponin protein expression was found localised in the cytoplasmic filaments in day 9 hESC-derived SM-like cells (Fig.41). Another mature SMC protein SM-MHC II was also expressed in the cell population (Fig.43). SM-MHC II is a cytoplasmic structural protein which contributes to the contractile function in VSMCs. SM-MHC II is one of the two isoforms identified, the other being designated MHC-I. Since SM-MHC II is a SMC-specific marker of late differentiation or maturation stages [42] and its appearance together with other SMC markers in day 9 hESC-derived SM-like cells imply that the existing differentiation model is successful in deriving VSMCs.

An important characteristic of VSMCs is their ability to contract in response to stimulus [224]. To determine whether the hESC-derived SM-like cells function as normal VSMCs, contractility test using the agoinst KCL was carried out. Upon stimulation with KCL, cells underwent contraction as observed by their morphology changes in contrast with their previous normal resting spindle-shape morphology (Fig.44). In general, the expression of SMC specific marker genes and proteins as well as the ability to contract like VSMC suggest that the differentiated hESCs are most likely to be VSMCs. This also implies that an *in-vitro* differentiation system in deriving VSMCs from hESCs has been successfully established without requiring EB formation. However, further steps such as using cell-sorting will be necessary for obtaining an increased purity and population of SMA and Calponin positive cells. Future work will also focus on determining potential miRNA candidates which play a role in SMC differentiation from pluripotent hESCs.

CHAPTER 5

Conclusion and future plans

Differentiation of hESCs towards both vascular ECs and SMCs has been successfully achieved in this study. hESC-derived ECs express specific EC markers such as PECAM-1/CD31, eNOS, CD144/VE-cad and vWF, while hESC-derived SMCs express specific SMC markers such as SMA, Calponin, SMMHC II and PDGFR-β. Both hESC-derived ECs and SMCs also displayed functional characteristics upon functional analysis.

During hESCs differentiation towards the EC lineage, potential miRNAs that play a role during endothelial differentiation were selected using miRNA array analysis. Enriched miRNAs were identified as miR-150* and miR-200c. The functional roles of miR-150* and miR-200c were demonstrated using loss-of-function and gain-of-function gene experiments. Importantly, it was demonstrated that miR-150* and miR-200c were involved in the *in vivo* vasculogenesis in developing chick embryos. In addition, luciferase reporter assay verified EMT-activator ZEB1/TCF8 as an important mRNA target for miR-150* and 200c during the differentiation of hESCs toward mature ECs.

These findings may suggest that as hESCs differentiate towards the EC lineage, an increase of miR-200c expression contributes to the decline or repression of EMT process. Meanwhile, miR-150* also participates and contributes to the differentiation of hESCs which subsequently result in the formation of more differentiated, senescence and less proliferative cells or in this case, mature vascular ECs. These findings illustrate that miR-150* and 200c can regulate the development of ECs from hESCs, providing new targets for modulating vascular formation and creating novel clinical therapies in future cardiovascular disease applications.

Future work will encompass the following:

1. To further delineate the verification of ZEB1/TCF8 as an important mRNA target for miR-150* and 200c using mutation binding sites assays.
2. To investigate if c-Myb is the mRNA target for miR-150* during EC differentiation process from hESCs.
3. To examine the potential involvement of ZEB1/TCF8 in EC differentiation from hESCs using siRNAs.
4. To identify the potential microRNAs that modulate SMC differentiation from human ES cells.
5. To explore the therapeutic potential of hESC-derived endothelial cells in cardiovascular diseases by using various models, such as vessel injury and hindlimb ischemia.

Publications, Presentations and Abstracts

Presentations and Abstracts

1. **Luo Z**, Xiao Q, Wang W, Xu Q, Differentiation of human embryonic stem cells towards the endothelial lineage and the role of microRNAs (British Atherosclerosis Society Spring Meeting, 13-14 June 2011, Manchester, Poster Presentation)

2. **Luo Z**, Xiao Q, Wang W, Xu Q, The derivation of CD146+ cells from human embryonic stem cells and their endothelial differentiation (UK National Stem Cell Network meeting, 12-14 July 2010, Nottingham, Poster Presentation)

Publications

1. Xiao Q, Wang G, Yin X, **Luo Z**, Margariti A, Zeng L, Mayr M, Ye S, Xu Q, Chromobox protein homolog 3 is essential for stem cell differentiation to smooth muscles in vitro and in embryonic arteriogenesis, Arterioscler Thromb Vasc Biol. 2011 Jun 9

2. **Luo Z**, Wang G, Wang W, Xiao Q, Xu Q, Signalling pathways that regulate endothelial differentiation from stem cells, Front Biosci. 2011 Jan 1:16:472-85

3. Kane NM, Xiao Q, Baker AH, **Luo Z**, Xu Q, Emanueli C, Pluripotent stem cell differentiation into vascular cells: a novel technology with promises for vascular re(generation), Pharmacol Ther. 2011 Jan;129(1):29-49.

4. Zhang L, Jin M, Margariti A, Wang G, **Luo Z**, Zampetaki A, Zeng L, Ye S, Xu Q, Zhu J and Xiao Q, Sp1-dependent activation of HDAC7 is required for PDGF-BB-induced smooth muscle cell differentiation from stem cells, J Biol Chem. 2010 Dec 3;285(49):38463-72.

5. Xiao Q, Wang G, **Luo Z**, Xu Q, The mechanism of stem cell differentiation into smooth muscle cells, Thromb Haemost. 2010 Sep;104(3):440-8.

6. Xiao Q, **Luo Z**, Pepe AE, Margariti A, Zeng L, Xu Q, Embryonic stem cell differentiation into smooth muscle cells is mediated by Nox4-produced H2O2, Am J Physiol Cell Physiol. 2009 Apr; 296(4):C711-23.

Reference list

1. Wikipedia. Capillary. Available at: http://en.wikipedia.org/wiki/File:Illu_capillary.jpg. Accessed 23 June 2009.

2. Fawcett DW. *A Textbook of Histology*. New York: Chapman & Hill; 1994.

3. Li JK-J. *Dynamics of the vascular system.* Vol Vol. 1: World Scientific Publishing Co. Pte. Ltd.; 2004.

4. Rushmer RF. Structure and Function of the Cardiovascular System. Philadelphia: Saunders; 1972.

5. Jaffe EA. Cell biology of endothelial cells. *Hum Pathol.* 1987;18(3):234-239.

6. Pratt BM, Form D, Madri JA. Endothelial cell-extracellular matrix interactions. *Ann N Y Acad Sci.* 1985;460:274-288.

7. Seyer JM KA. *Connective tissues of the subendothelium.* 1st ed. Boston:: Little Brown; 1992.

8. Sage H, Pritzl P, Bornstein P. Secretory phenotypes of endothelial cells in culture: comparison of aortic, venous, capillary, and corneal endothelium. *Arteriosclerosis.* 1981;1(6):427-442.

9. Sage H, Bornstein P. Endothelial cells from umbilical vein and a hemangioendothelioma secrete basement membrane largely to the exclusion of interstitial procollagens. *Arteriosclerosis.* 1982;2(1):27-36.

10. Grant DS, Tashiro K, Segui-Real B, Yamada Y, Martin GR, Kleinman HK. Two different laminin domains mediate the differentiation of human endothelial cells into capillary-like structures in vitro. *Cell.* 1989;58(5):933-943.

11. Mosher DF, Doyle MJ, Jaffe EA. Synthesis and secretion of thrombospondin by cultured human endothelial cells. *J Cell Biol.* 1982;93(2):343-348.

12. Jaffe EA, Mosher DF. Synthesis of fibronectin by cultured human endothelial cells. *J Exp Med.* 1978;147(6):1779-1791.

13. Cantor JO, Keller S, Parshley MS, Darnule TV, Darnule AT, Cerreta JM, Turino GM, Mandl I. Synthesis of crosslinked elastin by an endothelial cell culture. *Biochem Biophys Res Commun.* 1980;95(4):1381-1386.

14. Buonassisi V. Sulfated mucopolysaccharide synthesis and secretion in endothelial cell cultures. *Exp Cell Res.* 1973;76(2):363-368.

15. Oohira A, Wight TN, Bornstein P. Sulfated proteoglycans synthesized by vascular endothelial cells in culture. *J Biol Chem.* 1983;258(3):2014-2021.

16. Bombeli T, Mueller M, Haeberli A. Anticoagulant properties of the vascular endothelium. *Thromb Haemost.* 1997;77(3):408-423.

17. Barnes MJ, Bailey AJ, Gordon JL, MacIntyre DE. Platelet aggregaton by basement membrane-associated collagens. *Thromb Res.* 1980;18(3-4):375-388.

18. Kao KJ, Pizzo SV, McKee PA. Platelet receptors for human Factor VIII/von Willebrand protein: functional correlation of receptor occupancy and ristocetin-induced platelet aggregation. *Proc Natl Acad Sci U S A.* 1979;76(10):5317-5320.

19. Wagner DD, Marder VJ. Biosynthesis of von Willebrand protein by human endothelial cells: processing steps and their intracellular localization. *J Cell Biol.* 1984;99(6):2123-2130.

20. Heldin CH, Wasteson A, Westermark B. Platelet-derived growth factor. *Mol Cell Endocrinol.* 1985;39(3):169-187.

21. DiCorleto PE, Bowen-Pope DF. Cultured endothelial cells produce a platelet-derived growth factor-like protein. *Proc Natl Acad Sci U S A.* 1983;80(7):1919-1923.

22. Nilsson J, Sjolund M, Palmberg L, Thyberg J, Heldin CH. Arterial smooth muscle cells in primary culture produce a platelet-derived growth factor-like protein. *Proc Natl Acad Sci U S A.* 1985;82(13):4418-4422.

23. Grotendorst GR, Seppa HE, Kleinman HK, Martin GR. Attachment of smooth muscle cells to collagen and their migration toward platelet-derived growth factor. *Proc Natl Acad Sci U S A.* 1981;78(6):3669-3672.

24. Battegay EJ, Rupp J, Iruela-Arispe L, Sage EH, Pech M. PDGF-BB modulates endothelial proliferation and angiogenesis in vitro via PDGF beta-receptors. *J Cell Biol.* 1994;125(4):917-928.

25. Heldin CH, Westermark B. Platelet-derived growth factors: a family of isoforms that bind to two distinct receptors. *Br Med Bull.* 1989;45(2):453-464.

26. Clemmons DR. Exposure to platelet-derived growth factor modulates the porcine aortic smooth muscle cell response to somatomedin-C. *Endocrinology.* 1985;117(1):77-83.

27. Muller WA, Ratti CM, McDonnell SL, Cohn ZA. A human endothelial cell-restricted, externally disposed plasmalemmal protein enriched in intercellular junctions. *J Exp Med.* 1989;170(2):399-414.

28. Albelda SM, Oliver PD, Romer LH, Buck CA. EndoCAM: a novel endothelial cell-cell adhesion molecule. *J Cell Biol.* 1990;110(4):1227-1237.

29. Sun QH, DeLisser HM, Zukowski MM, Paddock C, Albelda SM, Newman PJ. Individually distinct Ig homology domains in PECAM-1 regulate homophilic binding and modulate receptor affinity. *J Biol Chem.* 1996;271(19):11090-11098.

30. Buckley CD, Doyonnas R, Newton JP, Blystone SD, Brown EJ, Watt SM, Simmons DL. Identification of alpha v beta 3 as a heterotypic ligand for CD31/PECAM-1. *J Cell Sci.* 1996;109 (Pt 2):437-445.

31. Schimmenti LA, Yan HC, Madri JA, Albelda SM. Platelet endothelial cell adhesion molecule, PECAM-1, modulates cell migration. *J Cell Physiol.* 1992;153(2):417-428.

32. Graesser D, Solowiej A, Bruckner M, Osterweil E, Juedes A, Davis S, Ruddle NH, Engelhardt B, Madri JA. Altered vascular permeability and early onset of experimental autoimmune encephalomyelitis in PECAM-1-deficient mice. *J Clin Invest.* 2002;109(3):383-392.

33. DeLisser HM, Christofidou-Solomidou M, Strieter RM, Burdick MD, Robinson CS, Wexler RS, Kerr JS, Garlanda C, Merwin JR, Madri JA, Albelda SM. Involvement

of endothelial PECAM-1/CD31 in angiogenesis. *Am J Pathol.* 1997;151(3):671-677.

34. Breviario F, Caveda L, Corada M, Martin-Padura I, Navarro P, Golay J, Introna M, Gulino D, Lampugnani MG, Dejana E. Functional properties of human vascular endothelial cadherin (7B4/cadherin-5), an endothelium-specific cadherin. *Arterioscler Thromb Vasc Biol.* 1995;15(8):1229-1239.

35. Owens GK. Regulation of differentiation of vascular smooth muscle cells. *Physiol Rev.* 1995;75(3):487-517.

36. Velican C, Velican D. The precursors of coronary atherosclerotic plaques in subjects up to 40 years old. *Atherosclerosis.* 1980;37(1):33-46.

37. Hao H, Gabbiani G, Bochaton-Piallat ML. Arterial smooth muscle cell heterogeneity: implications for atherosclerosis and restenosis development. *Arterioscler Thromb Vasc Biol.* 2003;23(9):1510-1520.

38. Chamley-Campbell J, Campbell GR, Ross R. The smooth muscle cell in culture. *Physiol Rev.* 1979;59(1):1-61.

39. Owens GK, Kumar MS, Wamhoff BR. Molecular regulation of vascular smooth muscle cell differentiation in development and disease. *Physiol Rev.* 2004;84(3):767-801.

40. Sobue K, Hayashi K, Nishida W. Expressional regulation of smooth muscle cell-specific genes in association with phenotypic modulation. *Mol Cell Biochem.* 1999;190(1-2):105-118.

41. Garrels JI, Gibson W. Identification and characterization of multiple forms of actin. *Cell.* 1976;9(4 PT 2):793-805.

42. Miano JM, Cserjesi P, Ligon KL, Periasamy M, Olson EN. Smooth muscle myosin heavy chain exclusively marks the smooth muscle lineage during mouse embryogenesis. *Circ Res.* 1994;75(5):803-812.

43. Christen T, Bochaton-Piallat ML, Neuville P, Rensen S, Redard M, van Eys G, Gabbiani G. Cultured porcine coronary artery smooth muscle cells. A new model with advanced differentiation. *Circ Res.* 1999;85(1):99-107.

44. Evans MJ, Kaufman MH. Establishment in culture of pluripotential cells from mouse embryos. *Nature.* 1981;292(5819):154-156.

45. Martin GR. Isolation of a pluripotent cell line from early mouse embryos cultured in medium conditioned by teratocarcinoma stem cells. *Proc Natl Acad Sci U S A.* 1981;78(12):7634-7638.

46. Thomson JA, Itskovitz-Eldor J, Shapiro SS, Waknitz MA, Swiergiel JJ, Marshall VS, Jones JM. Embryonic stem cell lines derived from human blastocysts. *Science.* 1998;282(5391):1145-1147.

47. Takahashi K, Yamanaka S. Induction of pluripotent stem cells from mouse embryonic and adult fibroblast cultures by defined factors. *Cell.* 2006;126(4):663-676.

48. Lowry WE, Richter L, Yachechko R, Pyle AD, Tchieu J, Sridharan R, Clark AT, Plath K. Generation of human induced pluripotent stem cells from dermal fibroblasts. *Proc Natl Acad Sci U S A.* 2008;105(8):2883-2888.

49. Maherali N, Sridharan R, Xie W, Utikal J, Eminli S, Arnold K, Stadtfeld M, Yachechko R, Tchieu J, Jaenisch R, Plath K, Hochedlinger K. Directly

reprogrammed fibroblasts show global epigenetic remodeling and widespread tissue contribution. *Cell Stem Cell.* 2007;1(1):55-70.

50. Meissner A, Wernig M, Jaenisch R. Direct reprogramming of genetically unmodified fibroblasts into pluripotent stem cells. *Nat Biotechnol.* 2007;25(10):1177-1181.

51. Park IH, Zhao R, West JA, Yabuuchi A, Huo H, Ince TA, Lerou PH, Lensch MW, Daley GQ. Reprogramming of human somatic cells to pluripotency with defined factors. *Nature.* 2008;451(7175):141-146.

52. Takahashi K, Tanabe K, Ohnuki M, Narita M, Ichisaka T, Tomoda K, Yamanaka S. Induction of pluripotent stem cells from adult human fibroblasts by defined factors. *Cell.* 2007;131(5):861-872.

53. Wernig M, Meissner A, Cassady JP, Jaenisch R. c-Myc is dispensable for direct reprogramming of mouse fibroblasts. *Cell Stem Cell.* 2008;2(1):10-12.

54. Huangfu D, Maehr R, Guo W, Eijkelenboom A, Snitow M, Chen AE, Melton DA. Induction of pluripotent stem cells by defined factors is greatly improved by small-molecule compounds. *Nat Biotechnol.* 2008;26(7):795-797.

55. Yuan X, Wan H, Zhao X, Zhu S, Zhou Q, Ding S. Brief report: combined chemical treatment enables Oct4-induced reprogramming from mouse embryonic fibroblasts. *Stem Cells.* 2011;29(3):549-553.

56. Hanna J, Wernig M, Markoulaki S, Sun CW, Meissner A, Cassady JP, Beard C, Brambrink T, Wu LC, Townes TM, Jaenisch R. Treatment of sickle cell anemia mouse model with iPS cells generated from autologous skin. *Science.* 2007;318(5858):1920-1923.

57. Park IH, Arora N, Huo H, Maherali N, Ahfeldt T, Shimamura A, Lensch MW, Cowan C, Hochedlinger K, Daley GQ. Disease-specific induced pluripotent stem cells. *Cell.* 2008;134(5):877-886.

58. Okita K, Ichisaka T, Yamanaka S. Generation of germline-competent induced pluripotent stem cells. *Nature.* 2007;448(7151):313-317.

59. Lee H, Park J, Forget BG, Gaines P. Induced pluripotent stem cells in regenerative medicine: an argument for continued research on human embryonic stem cells. *Regen Med.* 2009;4(5):759-769.

60. Pick M, Stelzer Y, Bar-Nur O, Mayshar Y, Eden A, Benvenisty N. Clone- and gene-specific aberrations of parental imprinting in human induced pluripotent stem cells. *Stem Cells.* 2009;27(11):2686-2690.

61. Takahashi K, Okita K, Nakagawa M, Yamanaka S. Induction of pluripotent stem cells from fibroblast cultures. *Nat Protoc.* 2007;2(12):3081-3089.

62. Feng Q, Lu SJ, Klimanskaya I, Gomes I, Kim D, Chung Y, Honig GR, Kim KS, Lanza R. Hemangioblastic derivatives from human induced pluripotent stem cells exhibit limited expansion and early senescence. *Stem Cells.* 2010;28(4):704-712.

63. Smith KP, Luong MX, Stein GS. Pluripotency: toward a gold standard for human ES and iPS cells. *J Cell Physiol.* 2009;220(1):21-29.

64. Reubinoff BE, Pera MF, Fong CY, Trounson A, Bongso A. Embryonic stem cell lines from human blastocysts: somatic differentiation in vitro. *Nat Biotechnol.* 2000;18(4):399-404.

65. Levenberg S, Rouwkema J, Macdonald M, Garfein ES, Kohane DS, Darland DC, Marini R, van Blitterswijk CA, Mulligan RC, D'Amore PA, Langer R. Engineering vascularized skeletal muscle tissue. *Nat Biotechnol.* 2005;23(7):879-884.

66. Ferreira LS, Gerecht S, Shieh HF, Watson N, Rupnick MA, Dallabrida SM, Vunjak-Novakovic G, Langer R. Vascular progenitor cells isolated from human embryonic stem cells give rise to endothelial and smooth muscle like cells and form vascular networks in vivo. *Circ Res.* 2007;101(3):286-294.

67. Levenberg S, Golub JS, Amit M, Itskovitz-Eldor J, Langer R. Endothelial cells derived from human embryonic stem cells. *Proc Natl Acad Sci U S A.* 2002;99(7):4391-4396.

68. Levenberg S. Engineering blood vessels from stem cells: recent advances and applications. *Curr Opin Biotechnol.* 2005;16(5):516-523.

69. Levenberg S, Zoldan J, Basevitch Y, Langer R. Endothelial potential of human embryonic stem cells. *Blood.* 2007;110(3):806-814.

70. Pouton CW, Haynes JM. Embryonic stem cells as a source of models for drug discovery. *Nat Rev Drug Discov.* 2007;6(8):605-616.

71. Sartipy P, Bjorquist P, Strehl R, Hyllner J. The application of human embryonic stem cell technologies to drug discovery. *Drug Discov Today.* 2007;12(17-18):688-699.

72. Risau W. Mechanisms of angiogenesis. *Nature.* 1997;386(6626):671-674.

73. Matsumoto K, Yoshitomi H, Rossant J, Zaret KS. Liver organogenesis promoted by endothelial cells prior to vascular function. *Science.* 2001;294(5542):559-563.

74. Vakaet L. *Morphogenetic movements and fate maps in the avian blastoderm*. New York: Alan R. Liss; 1985.

75. Murray P. The development in vitro of the blood of the early chick embryo. *Proc R Soc Lond B Biol Sci.* 1932;11:497–521.

76. Sabin F. Studies on the origin of blood vessels and of red corpuscles as seen in the living blastoderm of the chick during the second day of incubation. . *Contributions to Embryology.* . 1920;9:213–262.

77. Choi K, Kennedy M, Kazarov A, Papadimitriou JC, Keller G. A common precursor for hematopoietic and endothelial cells. *Development.* 1998;125(4):725-732.

78. Chung YS, Zhang WJ, Arentson E, Kingsley PD, Palis J, Choi K. Lineage analysis of the hemangioblast as defined by FLK1 and SCL expression. *Development.* 2002;129(23):5511-5520.

79. Nishikawa SI, Nishikawa S, Hirashima M, Matsuyoshi N, Kodama H. Progressive lineage analysis by cell sorting and culture identifies FLK1+VE-cadherin+ cells at a diverging point of endothelial and hemopoietic lineages. *Development.* 1998;125(9):1747-1757.

80. Huber TL, Kouskoff V, Fehling HJ, Palis J, Keller G. Haemangioblast commitment is initiated in the primitive streak of the mouse embryo. *Nature.* 2004;432(7017):625-630.

81. Oberlin E, Tavian M, Blazsek I, Peault B. Blood-forming potential of vascular endothelium in the human embryo. *Development.* 2002;129(17):4147-4157.

82. Zambidis ET, Peault B, Park TS, Bunz F, Civin CI. Hematopoietic differentiation of human embryonic stem cells progresses through sequential hematoendothelial,

primitive, and definitive stages resembling human yolk sac development *Blood.* 2005;106(3):860-870.

83. Adair TH MJ. *Angiogenesis*: Morgan & Claypool Life Sciences; 2010.

84. Wang L, Li L, Shojaei F, Levac K, Cerdan C, Menendez P, Martin T, Rouleau A, Bhatia M. Endothelial and hematopoietic cell fate of human embryonic stem cells originates from primitive endothelium with hemangioblastic properties. *Immunity.* 2004;21(1):31-41.

85. Kennedy M, D'Souza SL, Lynch-Kattman M, Schwantz S, Keller G. Development of the hemangioblast defines the onset of hematopoiesis in human ES cell differentiation cultures. *Blood.* 2007;109(7):2679-2687.

86. Chadwick K, Wang L, Li L, Menendez P, Murdoch B, Rouleau A, Bhatia M. Cytokines and BMP-4 promote hematopoietic differentiation of human embryonic stem cells. *Blood.* 2003;102(3):906-915.

87. Gimbrone MA, Jr., Cotran RS, Folkman J. Endothelial regeneration: studies with human endothelial cells in culture. *Ser Haematol.* 1973;6(4):453-455.

88. Doetschman TC, Eistetter H, Katz M, Schmidt W, Kemler R. The in vitro development of blastocyst-derived embryonic stem cell lines: formation of visceral yolk sac, blood islands and myocardium. *J Embryol Exp Morphol.* 1985;87:27-45.

89. Vittet D, Prandini MH, Berthier R, Schweitzer A, Martin-Sisteron H, Uzan G, Dejana E. Embryonic stem cells differentiate in vitro to endothelial cells through successive maturation steps. *Blood.* 1996;88(9):3424-3431.

90. Yamashita J, Itoh H, Hirashima M, Ogawa M, Nishikawa S, Yurugi T, Naito M, Nakao K. Flk1-positive cells derived from embryonic stem cells serve as vascular progenitors. *Nature.* 2000;408(6808):92-96.

91. Li Z, Wu JC, Sheikh AY, Kraft D, Cao F, Xie X, Patel M, Gambhir SS, Robbins RC, Cooke JP. Differentiation, survival, and function of embryonic stem cell derived endothelial cells for ischemic heart disease. *Circulation.* 2007;116(11 Suppl):I46-54.

92. Suzuki H, Watabe T, Kato M, Miyazawa K, Miyazono K. Roles of vascular endothelial growth factor receptor 3 signaling in differentiation of mouse embryonic stem cell-derived vascular progenitor cells into endothelial cells. *Blood.* 2005;105(6):2372-2379.

93. Cho SW, Moon SH, Lee SH, Kang SW, Kim J, Lim JM, Kim HS, Kim BS, Chung HM. Improvement of postnatal neovascularization by human embryonic stem cell derived endothelial-like cell transplantation in a mouse model of hindlimb ischemia. *Circulation.* 2007;116(21):2409-2419.

94. Xiao Q, Zeng L, Zhang Z, Margariti A, Ali ZA, Channon KM, Xu Q, Hu Y. Sca-1+ progenitors derived from embryonic stem cells differentiate into endothelial cells capable of vascular repair after arterial injury. *Arterioscler Thromb Vasc Biol.* 2006;26(10):2244-2251.

95. Zampetaki A, Zeng L, Xiao Q, Margariti A, Hu Y, Xu Q. Lacking cytokine production in ES cells and ES-cell-derived vascular cells stimulated by TNF-alpha is rescued by HDAC inhibitor trichostatin A. *Am J Physiol Cell Physiol.* 2007;293(4):C1226-1238.

96. Qian DZ, Wang X, Kachhap SK, Kato Y, Wei Y, Zhang L, Atadja P, Pili R. The histone deacetylase inhibitor NVP-LAQ824 inhibits angiogenesis and has a greater

antitumor effect in combination with the vascular endothelial growth factor receptor tyrosine kinase inhibitor PTK787/ZK222584. *Cancer Res.* 2004;64(18):6626-6634.

97. Li Z, Suzuki Y, Huang M, Cao F, Xie X, Connolly AJ, Yang PC, Wu JC. Comparison of reporter gene and iron particle labeling for tracking fate of human embryonic stem cells and differentiated endothelial cells in living subjects. *Stem Cells.* 2008;26(4):864-873.

98. Kim J, Moon SH, Lee SH, Lee DR, Koh GY, Chung HM. Effective isolation and culture of endothelial cells in embryoid body differentiated from human embryonic stem cells. *Stem Cells Dev.* 2007;16(2):269-280.

99. Levenberg S, Ferreira LS, Chen-Konak L, Kraehenbuehl TP, Langer R. Isolation, differentiation and characterization of vascular cells derived from human embryonic stem cells. *Nat Protoc.* 2010;5(6):1115-1126.

100. Moon SH, Kim JS, Park SJ, Lee HJ, Do JT, Chung HM. A system for treating ischemic disease using human embryonic stem cell-derived endothelial cells without direct incorporation. *Biomaterials.* 2011;32(27):6445-6455.

101. Wang ZZ, Au P, Chen T, Shao Y, Daheron LM, Bai H, Arzigian M, Fukumura D, Jain RK, Scadden DT. Endothelial cells derived from human embryonic stem cells form durable blood vessels in vivo. *Nat Biotechnol.* 2007;25(3):317-318.

102. Yamahara K, Sone M, Itoh H, Yamashita JK, Yurugi-Kobayashi T, Homma K, Chao TH, Miyashita K, Park K, Oyamada N, Sawada N, Taura D, Fukunaga Y, Tamura N, Nakao K. Augmentation of neovascularization [corrected] in hindlimb ischemia by combined transplantation of human embryonic stem cells-derived endothelial and mural cells. *PLoS One.* 2008;3(2):e1666.

103. Gerecht-Nir S, Ziskind A, Cohen S, Itskovitz-Eldor J. Human embryonic stem cells as an in vitro model for human vascular development and the induction of vascular differentiation. *Lab Invest.* 2003;83(12):1811-1820.

104. Oyamada N, Itoh H, Sone M, Yamahara K, Miyashita K, Park K, Taura D, Inuzuka M, Sonoyama T, Tsujimoto H, Fukunaga Y, Tamura N, Nakao K. Transplantation of vascular cells derived from human embryonic stem cells contributes to vascular regeneration after stroke in mice. *J Transl Med.* 2008;6:54.

105. Bai H, Gao Y, Arzigian M, Wojchowski DM, Wu WS, Wang ZZ. BMP4 regulates vascular progenitor development in human embryonic stem cells through a Smad-dependent pathway. *J Cell Biochem.* 2010;109(2):363-374.

106. Kane NM, Meloni M, Spencer HL, Craig MA, Strehl R, Milligan G, Houslay MD, Mountford JC, Emanueli C, Baker AH. Derivation of endothelial cells from human embryonic stem cells by directed differentiation: analysis of microRNA and angiogenesis in vitro and in vivo. *Arterioscler Thromb Vasc Biol.* 2010;30(7):1389-1397.

107. Chen T, Bai H, Shao Y, Arzigian M, Janzen V, Attar E, Xie Y, Scadden DT, Wang ZZ. Stromal cell-derived factor-1/CXCR4 signaling modifies the capillary-like organization of human embryonic stem cell-derived endothelium in vitro. *Stem Cells.* 2007;25(2):392-401.

108. Sone M, Itoh H, Yamahara K, Yamashita JK, Yurugi-Kobayashi T, Nonoguchi A, Suzuki Y, Chao TH, Sawada N, Fukunaga Y, Miyashita K, Park K, Oyamada N, Taura D, Tamura N, Kondo Y, Nito S, Suemori H, Nakatsuji N, Nishikawa S, Nakao K. Pathway for differentiation of human embryonic stem cells to vascular

cell components and their potential for vascular regeneration. *Arterioscler Thromb Vasc Biol.* 2007;27(10):2127-2134.

109. Thorgeirsson G, Robertson AL, Jr. The vascular endothelium-pathobiologic significance. *Am J Pathol.* 1978;93(3):803-848.

110. Garlanda C, Dejana E. Heterogeneity of endothelial cells. Specific markers. *Arterioscler Thromb Vasc Biol.* 1997;17(7):1193-1202.

111. Aird WC. Endothelial cell heterogeneity. *Crit Care Med.* 2003;31(4 Suppl):S221-230.

112. Zhao Y, Samal E, Srivastava D. Serum response factor regulates a muscle-specific microRNA that targets Hand2 during cardiogenesis. *Nature.* 2005;436(7048):214-220.

113. Chen JF, Mandel EM, Thomson JM, Wu Q, Callis TE, Hammond SM, Conlon FL, Wang DZ. The role of microRNA-1 and microRNA-133 in skeletal muscle proliferation and differentiation. *Nat Genet.* 2006;38(2):228-233.

114. Chen CZ, Li L, Lodish HF, Bartel DP. MicroRNAs modulate hematopoietic lineage differentiation. *Science.* 2004;303(5654):83-86.

115. Berezikov E, Guryev V, van de Belt J, Wienholds E, Plasterk RH, Cuppen E. Phylogenetic shadowing and computational identification of human microRNA genes. *Cell.* 2005;120(1):21-24.

116. Lee RC, Feinbaum RL, Ambros V. The C. elegans heterochronic gene lin-4 encodes small RNAs with antisense complementarity to lin-14. *Cell.* 1993;75(5):843-854.

117. Reinhart BJ, Slack FJ, Basson M, Pasquinelli AE, Bettinger JC, Rougvie AE, Horvitz HR, Ruvkun G. The 21-nucleotide let-7 RNA regulates developmental timing in Caenorhabditis elegans. *Nature.* 2000;403(6772):901-906.

118. Lee Y, Kim M, Han J, Yeom KH, Lee S, Baek SH, Kim VN. MicroRNA genes are transcribed by RNA polymerase II. *EMBO J.* 2004;23(20):4051-4060.

119. Lee Y, Ahn C, Han J, Choi H, Kim J, Yim J, Lee J, Provost P, Radmark O, Kim S, Kim VN. The nuclear RNase III Drosha initiates microRNA processing. *Nature.* 2003;425(6956):415-419.

120. Han J, Lee Y, Yeom KH, Kim YK, Jin H, Kim VN. The Drosha-DGCR8 complex in primary microRNA processing. *Genes Dev.* 2004;18(24):3016-3027.

121. Ruby JG, Jan CH, Bartel DP. Intronic microRNA precursors that bypass Drosha processing. *Nature.* 2007;448(7149):83-86.

122. Lund E, Guttinger S, Calado A, Dahlberg JE, Kutay U. Nuclear export of microRNA precursors. *Science.* 2004;303(5654):95-98.

123. Hutvagner G, McLachlan J, Pasquinelli AE, Balint E, Tuschl T, Zamore PD. A cellular function for the RNA-interference enzyme Dicer in the maturation of the let-7 small temporal RNA. *Science.* 2001;293(5531):834-838.

124. Gregory RI, Chendrimada TP, Cooch N, Shiekhattar R. Human RISC couples microRNA biogenesis and posttranscriptional gene silencing. *Cell.* 2005;123(4):631-640.

125. Chiang HR, Schoenfeld LW, Ruby JG, Auyeung VC, Spies N, Baek D, Johnston WK, Russ C, Luo S, Babiarz JE, Blelloch R, Schroth GP, Nusbaum C, Bartel DP. Mammalian microRNAs: experimental evaluation of novel and previously annotated genes. *Genes Dev.*24(10):992-1009.

126. Ghildiyal M, Xu J, Seitz H, Weng Z, Zamore PD. Sorting of Drosophila small silencing RNAs partitions microRNA* strands into the RNA interference pathway. *RNA.* 2010;16(1):43-56.
127. Okamura K, Liu N, Lai EC. Distinct mechanisms for microRNA strand selection by Drosophila Argonautes. *Mol Cell.* 2009;36(3):431-444.
128. Schwarz DS, Hutvagner G, Du T, Xu Z, Aronin N, Zamore PD. Asymmetry in the assembly of the RNAi enzyme complex. *Cell.* 2003;115(2):199-208.
129. Khvorova A, Reynolds A, Jayasena SD. Functional siRNAs and miRNAs exhibit strand bias. *Cell.* 2003;115(2):209-216.
130. Krol J, Loedige I, Filipowicz W. The widespread regulation of microRNA biogenesis, function and decay. *Nat Rev Genet.*11(9):597-610.
131. Davis E, Caiment F, Tordoir X, Cavaille J, Ferguson-Smith A, Cockett N, Georges M, Charlier C. RNAi-mediated allelic trans-interaction at the imprinted Rtl1/Peg11 locus. *Curr Biol.* 2005;15(8):743-749.
132. Yekta S, Shih IH, Bartel DP. MicroRNA-directed cleavage of HOXB8 mRNA. *Science.* 2004;304(5670):594-596.
133. Lewis BP, Burge CB, Bartel DP. Conserved seed pairing, often flanked by adenosines, indicates that thousands of human genes are microRNA targets. *Cell.* 2005;120(1):15-20.
134. Brennecke J, Stark A, Russell RB, Cohen SM. Principles of microRNA-target recognition. *PLoS Biol.* 2005;3(3):e85.
135. Tay Y, Zhang J, Thomson AM, Lim B, Rigoutsos I. MicroRNAs to Nanog, Oct4 and Sox2 coding regions modulate embryonic stem cell differentiation. *Nature.* 2008;455(7216):1124-1128.
136. Lytle JR, Yario TA, Steitz JA. Target mRNAs are repressed as efficiently by microRNA-binding sites in the 5' UTR as in the 3' UTR. *Proc Natl Acad Sci U S A.* 2007;104(23):9667-9672.
137. Maziere P, Enright AJ. Prediction of microRNA targets. *Drug Discov Today.* 2007;12(11-12):452-458.
138. Pillai RS, Bhattacharyya SN, Filipowicz W. Repression of protein synthesis by miRNAs: how many mechanisms? *Trends Cell Biol.* 2007;17(3):118-126.
139. Liu J. Control of protein synthesis and mRNA degradation by microRNAs. *Curr Opin Cell Biol.* 2008;20(2):214-221.
140. Lagos-Quintana M, Rauhut R, Lendeckel W, Tuschl T. Identification of novel genes coding for small expressed RNAs. *Science.* 2001;294(5543):853-858.
141. Lee RC, Ambros V. An extensive class of small RNAs in Caenorhabditis elegans. *Science.* 2001;294(5543):862-864.
142. Lau NC, Lim LP, Weinstein EG, Bartel DP. An abundant class of tiny RNAs with probable regulatory roles in Caenorhabditis elegans. *Science.* 2001;294(5543):858-862.
143. Griffiths-Jones S. miRBase: the microRNA sequence database. *Methods Mol Biol.* 2006;342:129-138.
144. Ambros V, Bartel B, Bartel DP, Burge CB, Carrington JC, Chen X, Dreyfuss G, Eddy SR, Griffiths-Jones S, Marshall M, Matzke M, Ruvkun G, Tuschl T. A uniform system for microRNA annotation. *RNA.* 2003;9(3):277-279.

145. Suarez Y, Sessa WC. MicroRNAs as novel regulators of angiogenesis. *Circ Res.* 2009;104(4):442-454.
146. Yang WJ, Yang DD, Na S, Sandusky GE, Zhang Q, Zhao G. Dicer is required for embryonic angiogenesis during mouse development. *J Biol Chem.* 2005;280(10):9330-9335.
147. Suarez Y, Fernandez-Hernando C, Pober JS, Sessa WC. Dicer dependent microRNAs regulate gene expression and functions in human endothelial cells. *Circ Res.* 2007;100(8):1164-1173.
148. Kuehbacher A, Urbich C, Zeiher AM, Dimmeler S. Role of Dicer and Drosha for endothelial microRNA expression and angiogenesis. *Circ Res.* 2007;101(1):59-68.
149. Poliseno L, Tuccoli A, Mariani L, Evangelista M, Citti L, Woods K, Mercatanti A, Hammond S, Rainaldi G. MicroRNAs modulate the angiogenic properties of HUVECs. *Blood.* 2006;108(9):3068-3071.
150. Bonauer A, Carmona G, Iwasaki M, Mione M, Koyanagi M, Fischer A, Burchfield J, Fox H, Doebele C, Ohtani K, Chavakis E, Potente M, Tjwa M, Urbich C, Zeiher AM, Dimmeler S. MicroRNA-92a controls angiogenesis and functional recovery of ischemic tissues in mice. *Science.* 2009;324(5935):1710-1713.
151. Sabatel C, Malvaux L, Bovy N, Deroanne C, Lambert V, Gonzalez ML, Colige A, Rakic JM, Noel A, Martial JA, Struman I. MicroRNA-21 exhibits antiangiogenic function by targeting RhoB expression in endothelial cells. *PLoS One.* 2011;6(2):e16979.
152. Fish JE, Santoro MM, Morton SU, Yu S, Yeh RF, Wythe JD, Ivey KN, Bruneau BG, Stainier DY, Srivastava D. miR-126 regulates angiogenic signaling and vascular integrity. *Dev Cell.* 2008;15(2):272-284.
153. Harris TA, Yamakuchi M, Ferlito M, Mendell JT, Lowenstein CJ. MicroRNA-126 regulates endothelial expression of vascular cell adhesion molecule 1. *Proc Natl Acad Sci U S A.* 2008;105(5):1516-1521.
154. Landgraf P, Rusu M, Sheridan R, Sewer A, Iovino N, Aravin A, Pfeffer S, Rice A, Kamphorst AO, Landthaler M, Lin C, Socci ND, Hermida L, Fulci V, Chiaretti S, Foa R, Schliwka J, Fuchs U, Novosel A, Muller RU, Schermer B, Bissels U, Inman J, Phan Q, Chien M, Weir DB, Choksi R, De Vita G, Frezzetti D, Trompeter HI, Hornung V, Teng G, Hartmann G, Palkovits M, Di Lauro R, Wernet P, Macino G, Rogler CE, Nagle JW, Ju J, Papavasiliou FN, Benzing T, Lichter P, Tam W, Brownstein MJ, Bosio A, Borkhardt A, Russo JJ, Sander C, Zavolan M, Tuschl T. A mammalian microRNA expression atlas based on small RNA library sequencing. *Cell.* 2007;129(7):1401-1414.
155. Wang S, Aurora AB, Johnson BA, Qi X, McAnally J, Hill JA, Richardson JA, Bassel-Duby R, Olson EN. The endothelial-specific microRNA miR-126 governs vascular integrity and angiogenesis. *Dev Cell.* 2008;15(2):261-271.
156. Wu F, Yang Z, Li G. Role of specific microRNAs for endothelial function and angiogenesis. *Biochem Biophys Res Commun.* 2009;386(4):549-553.
157. Horan PK, Slezak SE. Stable cell membrane labelling. *Nature.* 1989;340(6229):167-168.
158. Hamburger V, Hamilton HL. A series of normal stages in the development of the chick embryo. 1951. *Dev Dyn.* 1992;195(4):231-272.

159. Krek A, Grun D, Poy MN, Wolf R, Rosenberg L, Epstein EJ, MacMenamin P, da Piedade I, Gunsalus KC, Stoffel M, Rajewsky N. Combinatorial microRNA target predictions. *Nat Genet.* 2005;37(5):495-500.

160. Xiao Q, Zeng L, Zhang Z, Hu Y, Xu Q. Stem cell-derived Sca-1+ progenitors differentiate into smooth muscle cells, which is mediated by collagen IV-integrin alpha1/beta1/alphav and PDGF receptor pathways. *Am J Physiol Cell Physiol.* 2007;292(1):C342-352.

161. Szybalski W, Iyer VN. Crosslinking of DNA by Enzymatically or Chemically Activated Mitomycins and Porfiromycins, Bifunctionally "Alkylating" Antibiotics. *Fed Proc.* 1964;23:946-957.

162. Ueda K, Komano T. Sequence-specific DNA damage induced by reduced mitomycin C and 7-N-(p-hydroxyphenyl)mitomycin C. *Nucleic Acids Res.* 1984;12(17):6673-6683.

163. Ding V, Choo AB, Oh SK. Deciphering the importance of three key media components in human embryonic stem cell cultures. *Biotechnol Lett.* 2006;28(7):491-495.

164. O'Connor MD, Kardel MD, Iosfina I, Youssef D, Lu M, Li MM, Vercauteren S, Nagy A, Eaves CJ. Alkaline phosphatase-positive colony formation is a sensitive, specific, and quantitative indicator of undifferentiated human embryonic stem cells. *Stem Cells.* 2008;26(5):1109-1116.

165. Pease S, Braghetta P, Gearing D, Grail D, Williams RL. Isolation of embryonic stem (ES) cells in media supplemented with recombinant leukemia inhibitory factor (LIF). *Dev Biol.* 1990;141(2):344-352.

166. Solter D, Knowles BB. Monoclonal antibody defining a stage-specific mouse embryonic antigen (SSEA-1). *Proc Natl Acad Sci U S A.* 1978;75(11):5565-5569.

167. Solter D, Knowles BB. Developmental stage-specific antigens during mouse embryogenesis. *Curr Top Dev Biol.* 1979;13 Pt 1:139-165.

168. Grant DS, Kinsella JL, Kibbey MC, LaFlamme S, Burbelo PD, Goldstein AL, Kleinman HK. Matrigel induces thymosin beta 4 gene in differentiating endothelial cells. *J Cell Sci.* 1995;108 (Pt 12):3685-3694.

169. Crabtree B, Subramanian V. Behavior of endothelial cells on Matrigel and development of a method for a rapid and reproducible in vitro angiogenesis assay. *In Vitro Cell Dev Biol Anim.* 2007;43(2):87-94.

170. Salomon D, Ayalon O, Patel-King R, Hynes RO, Geiger B. Extrajunctional distribution of N-cadherin in cultured human endothelial cells. *J Cell Sci.* 1992;102 (Pt 1):7-17.

171. Bardin N, Anfosso F, Masse JM, Cramer E, Sabatier F, Le Bivic A, Sampol J, Dignat-George F. Identification of CD146 as a component of the endothelial junction involved in the control of cell-cell cohesion. *Blood.* 2001;98(13):3677-3684.

172. Kaufman DS, Hanson ET, Lewis RL, Auerbach R, Thomson JA. Hematopoietic colony-forming cells derived from human embryonic stem cells. *Proc Natl Acad Sci U S A.* 2001;98(19):10716-10721.

173. Boyd NL, Dhara SK, Rekaya R, Godbey EA, Hasneen K, Rao RR, West FD, 3rd, Gerwe BA, Stice SL. BMP4 promotes formation of primitive vascular networks in

human embryonic stem cell-derived embryoid bodies. *Exp Biol Med (Maywood).* 2007;232(6):833-843.

174. Andrews PW, Benvenisty N, McKay R, Pera MF, Rossant J, Semb H, Stacey GN. The International Stem Cell Initiative: toward benchmarks for human embryonic stem cell research. *Nat Biotechnol.* 2005;23(7):795-797.

175. Adewumi O, Aflatoonian B, Ahrlund-Richter L, Amit M, Andrews PW, Beighton G, Bello PA, Benvenisty N, Berry LS, Bevan S, Blum B, Brooking J, Chen KG, Choo AB, Churchill GA, Corbel M, Damjanov I, Draper JS, Dvorak P, Emanuelsson K, Fleck RA, Ford A, Gertow K, Gertsenstein M, Gokhale PJ, Hamilton RS, Hampl A, Healy LE, Hovatta O, Hyllner J, Imreh MP, Itskovitz-Eldor J, Jackson J, Johnson JL, Jones M, Kee K, King BL, Knowles BB, Lako M, Lebrin F, Mallon BS, Manning D, Mayshar Y, McKay RD, Michalska AE, Mikkola M, Mileikovsky M, Minger SL, Moore HD, Mummery CL, Nagy A, Nakatsuji N, O'Brien CM, Oh SK, Olsson C, Otonkoski T, Park KY, Passier R, Patel H, Patel M, Pedersen R, Pera MF, Piekarczyk MS, Pera RA, Reubinoff BE, Robins AJ, Rossant J, Rugg-Gunn P, Schulz TC, Semb H, Sherrer ES, Siemen H, Stacey GN, Stojkovic M, Suemori H, Szatkiewicz J, Turetsky T, Tuuri T, van den Brink S, Vintersten K, Vuoristo S, Ward D, Weaver TA, Young LA, Zhang W. Characterization of human embryonic stem cell lines by the International Stem Cell Initiative. *Nat Biotechnol.* 2007;25(7):803-816.

176. Shih IM. The role of CD146 (Mel-CAM) in biology and pathology. *J Pathol.* 1999;189(1):4-11.

177. Montemurro T, Andriolo G, Montelatici E, Weissmann G, Crisan M, Colnaghi MR, Rebulla P, Mosca F, Peault B, Lazzari L. Differentiation and migration properties of human foetal umbilical cord perivascular cells: potential for lung repair. *J Cell Mol Med.* 2011;15(4):796-808.

178. Bardin N, George F, Mutin M, Brisson C, Horschowski N, Frances V, Lesaule G, Sampol J. S-Endo 1, a pan-endothelial monoclonal antibody recognizing a novel human endothelial antigen. *Tissue Antigens.* 1996;48(5):531-539.

179. Pickl WF, Majdic O, Fischer GF, Petzelbauer P, Fae I, Waclavicek M, Stockl J, Scheinecker C, Vidicki T, Aschauer H, Johnson JP, Knapp W. MUC18/MCAM (CD146), an activation antigen of human T lymphocytes. *J Immunol.* 1997;158(5):2107-2115.

180. Lehmann JM, Riethmuller G, Johnson JP. MUC18, a marker of tumor progression in human melanoma, shows sequence similarity to the neural cell adhesion molecules of the immunoglobulin superfamily. *Proc Natl Acad Sci U S A.* 1989;86(24):9891-9895.

181. Voyta JC, Via DP, Butterfield CE, Zetter BR. Identification and isolation of endothelial cells based on their increased uptake of acetylated-low density lipoprotein. *J Cell Biol.* 1984;99(6):2034-2040.

182. Pitas RE, Innerarity TL, Weinstein JN, Mahley RW. Acetoacetylated lipoproteins used to distinguish fibroblasts from macrophages in vitro by fluorescence microscopy. *Arteriosclerosis.* 1981;1(3):177-185.

183. Holthofer H, Virtanen I, Kariniemi AL, Hormia M, Linder E, Miettinen A. Ulex europaeus I lectin as a marker for vascular endothelium in human tissues. *Lab Invest.* 1982;47(1):60-66.

184. Kleinman HK, McGarvey ML, Hassell JR, Star VL, Cannon FB, Laurie GW, Martin GR. Basement membrane complexes with biological activity. *Biochemistry.* 1986;25(2):312-318.

185. Kleinman HK, McGarvey ML, Liotta LA, Robey PG, Tryggvason K, Martin GR. Isolation and characterization of type IV procollagen, laminin, and heparan sulfate proteoglycan from the EHS sarcoma. *Biochemistry.* 1982;21(24):6188-6193.

186. Vukicevic S, Kleinman HK, Luyten FP, Roberts AB, Roche NS, Reddi AH. Identification of multiple active growth factors in basement membrane Matrigel suggests caution in interpretation of cellular activity related to extracellular matrix components. *Exp Cell Res.* 1992;202(1):1-8.

187. Yang B, Lin H, Xiao J, Lu Y, Luo X, Li B, Zhang Y, Xu C, Bai Y, Wang H, Chen G, Wang Z. The muscle-specific microRNA miR-1 regulates cardiac arrhythmogenic potential by targeting GJA1 and KCNJ2. *Nat Med.* 2007;13(4):486-491.

188. Care A, Catalucci D, Felicetti F, Bonci D, Addario A, Gallo P, Bang ML, Segnalini P, Gu Y, Dalton ND, Elia L, Latronico MV, Hoydal M, Autore C, Russo MA, Dorn GW, 2nd, Ellingsen O, Ruiz-Lozano P, Peterson KL, Croce CM, Peschle C, Condorelli G. MicroRNA-133 controls cardiac hypertrophy. *Nat Med.* 2007;13(5):613-618.

189. Chen Y, Gorski DH. Regulation of angiogenesis through a microRNA (miR-130a) that down-regulates antiangiogenic homeobox genes GAX and HOXA5. *Blood.* 2008;111(3):1217-1226.

190. Lee DY, Deng Z, Wang CH, Yang BB. MicroRNA-378 promotes cell survival, tumor growth, and angiogenesis by targeting SuFu and Fus-1 expression. *Proc Natl Acad Sci U S A.* 2007;104(51):20350-20355.

191. Kanellopoulou C, Muljo SA, Kung AL, Ganesan S, Drapkin R, Jenuwein T, Livingston DM, Rajewsky K. Dicer-deficient mouse embryonic stem cells are defective in differentiation and centromeric silencing. *Genes Dev.* 2005;19(4):489-501.

192. Murchison EP, Partridge JF, Tam OH, Cheloufi S, Hannon GJ. Characterization of Dicer-deficient murine embryonic stem cells. *Proc Natl Acad Sci U S A.* 2005;102(34):12135-12140.

193. Wang Y, Medvid R, Melton C, Jaenisch R, Blelloch R. DGCR8 is essential for microRNA biogenesis and silencing of embryonic stem cell self-renewal. *Nat Genet.* 2007;39(3):380-385.

194. Houbaviy HB, Murray MF, Sharp PA. Embryonic stem cell-specific MicroRNAs. *Dev Cell.* 2003;5(2):351-358.

195. Morin RD, O'Connor MD, Griffith M, Kuchenbauer F, Delaney A, Prabhu AL, Zhao Y, McDonald H, Zeng T, Hirst M, Eaves CJ, Marra MA. Application of massively parallel sequencing to microRNA profiling and discovery in human embryonic stem cells. *Genome Res.* 2008;18(4):610-621.

196. Bar M, Wyman SK, Fritz BR, Qi J, Garg KS, Parkin RK, Kroh EM, Bendoraite A, Mitchell PS, Nelson AM, Ruzzo WL, Ware C, Radich JP, Gentleman R, Ruohola-Baker H, Tewari M. MicroRNA discovery and profiling in human embryonic stem cells by deep sequencing of small RNA libraries. *Stem Cells.* 2008;26(10):2496-2505.

197. Tripathi R, Saini HK, Rad R, Abreu-Goodger C, van Dongen S, Enright AJ. Messenger RNA and microRNA profiling during early mouse EB formation. *Gene Expr Patterns.*

198. Knelangen JM, van der Hoek MB, Kong WC, Owens JA, Fischer B, Santos AN. MicroRNA expression profile during adipogenic differentiation in mouse embryonic stem cells. *Physiol Genomics.* 2011;43(10):611-620.

199. Wilson KD, Hu S, Venkatasubrahmanyam S, Fu JD, Sun N, Abilez OJ, Baugh JJ, Jia F, Ghosh Z, Li RA, Butte AJ, Wu JC. Dynamic microRNA expression programs during cardiac differentiation of human embryonic stem cells: role for miR-499. *Circ Cardiovasc Genet.* 2010;3(5):426-435.

200. Cordes KR, Sheehy NT, White MP, Berry EC, Morton SU, Muth AN, Lee TH, Miano JM, Ivey KN, Srivastava D. miR-145 and miR-143 regulate smooth muscle cell fate and plasticity. *Nature.* 2009.

201. Xu N, Papagiannakopoulos T, Pan G, Thomson JA, Kosik KS. MicroRNA-145 regulates OCT4, SOX2, and KLF4 and represses pluripotency in human embryonic stem cells. *Cell.* 2009;137(4):647-658.

202. Krichevsky AM, Sonntag KC, Isacson O, Kosik KS. Specific microRNAs modulate embryonic stem cell-derived neurogenesis. *Stem Cells.* 2006;24(4):857-864.

203. Ziauddin J, Sabatini DM. Microarrays of cells expressing defined cDNAs. *Nature.* 2001;411(6833):107-110.

204. Fraley R, Subramani S, Berg P, Papahadjopoulos D. Introduction of liposome-encapsulated SV40 DNA into cells. *J Biol Chem.* 1980;255(21):10431-10435.

205. Kertesz M, Iovino N, Unnerstall U, Gaul U, Segal E. The role of site accessibility in microRNA target recognition. *Nat Genet.* 2007;39(10):1278-1284.

206. Xiao C, Calado DP, Galler G, Thai TH, Patterson HC, Wang J, Rajewsky N, Bender TP, Rajewsky K. MiR-150 controls B cell differentiation by targeting the transcription factor c-Myb. *Cell.* 2007;131(1):146-159.

207. Lin YC, Kuo MW, Yu J, Kuo HH, Lin RJ, Lo WL, Yu AL. c-Myb is an evolutionary conserved miR-150 target and miR-150/c-Myb interaction is important for embryonic development. *Mol Biol Evol.* 2008;25(10):2189-2198.

208. Oh IH, Reddy EP. The myb gene family in cell growth, differentiation and apoptosis. *Oncogene.* 1999;18(19):3017-3033.

209. Westin EH, Gallo RC, Arya SK, Eva A, Souza LM, Baluda MA, Aaronson SA, Wong-Staal F. Differential expression of the amv gene in human hematopoietic cells. *Proc Natl Acad Sci U S A.* 1982;79(7):2194-2198.

210. Gonda TJ, Metcalf D. Expression of myb, myc and fos proto-oncogenes during the differentiation of a murine myeloid leukaemia. *Nature.* 1984;310(5974):249-251.

211. Dai G, Sakamoto H, Shimoda Y, Fujimoto T, Nishikawa S, Ogawa M. Over-expression of c-Myb increases the frequency of hemogenic precursors in the endothelial cell population. *Genes Cells.* 2006;11(8):859-870.

212. Hurteau GJ, Carlson JA, Spivack SD, Brock GJ. Overexpression of the microRNA hsa-miR-200c leads to reduced expression of transcription factor 8 and increased expression of E-cadherin. *Cancer Res.* 2007;67(17):7972-7976.

213. Inuzuka T, Tsuda M, Kawaguchi H, Ohba Y. Transcription factor 8 activates R-Ras to regulate angiogenesis. *Biochem Biophys Res Commun.* 2009;379(2):510-513.

214. Perez-Pomares JM, Munoz-Chapuli R. Epithelial-mesenchymal transitions: a mesodermal cell strategy for evolutive innovation in Metazoans. *Anat Rec.* 2002;268(3):343-351.
215. Wyatt L, Wadham C, Crocker LA, Lardelli M, Khew-Goodall Y. The protein tyrosine phosphatase Pez regulates TGFbeta, epithelial-mesenchymal transition, and organ development. *J Cell Biol.* 2007;178(7):1223-1235.
216. Ben-Porath I, Thomson MW, Carey VJ, Ge R, Bell GW, Regev A, Weinberg RA. An embryonic stem cell-like gene expression signature in poorly differentiated aggressive human tumors. *Nat Genet.* 2008;40(5):499-507.
217. Wellner U, Schubert J, Burk UC, Schmalhofer O, Zhu F, Sonntag A, Waldvogel B, Vannier C, Darling D, zur Hausen A, Brunton VG, Morton J, Sansom O, Schuler J, Stemmler MP, Herzberger C, Hopt U, Keck T, Brabletz S, Brabletz T. The EMT-activator ZEB1 promotes tumorigenicity by repressing stemness-inhibiting microRNAs. *Nat Cell Biol.* 2009;11(12):1487-1495.
218. Magenta A, Cencioni C, Fasanaro P, Zaccagnini G, Greco S, Sarra-Ferraris G, Antonini A, Martelli F, Capogrossi MC. miR-200c is upregulated by oxidative stress and induces endothelial cell apoptosis and senescence via ZEB1 inhibition. *Cell Death Differ.* 2011.
219. van Rooij E. The art of microRNA research. *Circ Res.* 2011;108(2):219-234.
220. Zeng L, Xiao Q, Margariti A, Zhang Z, Zampetaki A, Patel S, Capogrossi MC, Hu Y, Xu Q. HDAC3 is crucial in shear- and VEGF-induced stem cell differentiation toward endothelial cells. *J Cell Biol.* 2006;174(7):1059-1069.
221. Nowak G, Karrar A, Holmen C, Nava S, Uzunel M, Hultenby K, Sumitran-Holgersson S. Expression of vascular endothelial growth factor receptor-2 or Tie-2 on peripheral blood cells defines functionally competent cell populations capable of reendothelialization. *Circulation.* 2004;110(24):3699-3707.
222. Zampetaki A, Kirton JP, Xu Q. Vascular repair by endothelial progenitor cells. *Cardiovasc Res.* 2008;78(3):413-421.
223. Hungerford JE, Owens GK, Argraves WS, Little CD. Development of the aortic vessel wall as defined by vascular smooth muscle and extracellular matrix markers. *Dev Biol.* 1996;178(2):375-392.
224. Lesh RE, Somlyo AP, Owens GK, Somlyo AV. Reversible permeabilization. A novel technique for the intracellular introduction of antisense oligodeoxynucleotides into intact smooth muscle. *Circ Res.* 1995;77(2):220-230.

Appendix 1

NCBI Reference Sequence: NM_030751.5

5′ taa

3481 tc gtttttctag aaggaaaata aattctaatt gataatgaat

3481 ttcgttcaat attatccttg cttttcatgg aaacacagta acctgtatgc tgtgattcct

3541 gttcactact gtgtaaagta aaaactaaaa aaatacaaaa tacaaaacac acacacacac

3601 acacacacac acacacacac acacacaaaa taaatccggg tgtgcctgaa cctcagacct

3661 agtaattttt catgcagttt tcaaagttag gaacaagttt gtaacatgca gcagattaga

3721 aaaccttaat ***gactcagaga gcaacaatac*** aagaggttaa aggaagctga ttaattagat

3781 atgcatctgg cattgtttta tcttatcagt attatcactc ttatgttggt ttattcttaa

3841 gctgtacaat tgggagaaat tttataattt tttattggta aacatatgct aaatccgctt

3901 cagtatttta ttatgttttt taaaatgtga gaacttctgc actacaaaat tcccttcaca

3961 gagaagtata at***gtagttcc aacccgtgct aac***taccttt tataaattca gtctagaagg

4021 tagtaatttc taatatttag atgtcttagt agagcgtatt atcatttaaa gtgtattgtt

4081 agccttaaga aagcagctga tagaagaact gaagtttctt actcacgtgg tttaaaatgg

4141 agttcaaaag attgccattg agttctgatt gcagggacta acaatgttaa tctgataagg

4201 acagcaaaat catcagaatc agtgtttgtg attgtgtttg aatatgtggt aacatatgaa

4261 ggatatgaca tgaagctttg tatctccttt ggccttaagc aagacctgtg tgctgtaagt

4321 gccatttctc agtattttca aggctctaac ccgccttcat ccaatgtgtg gcctacaata

4381 actagcattt gttgatttgt ctcttgtatc aaaattccca aataaaactt aaaaccactg

4441 actctgtcag agaaactgaa acactgggac atttcatcct tcaattcctc ggtattgatt

4501 ttatgttgat tgattttcag aatttctcta cagaaacgaa agggaaattt tctaatctgc

4561 tttatccatg tacttgcatt tcagacatgg acatgctatt gttatttggc tcataactgt

4621 ttccaaatgt tagttattat ggacccaatt tattaacaac attagctgat ttttacctat

4681 cagtattatt ttatttcttt tagtttatag atctgtgcaa cattttgta ctgtatgtct

4741 tcaaacctgg cagtattaat acccttctta ctgacatatg tacttttagt tttagaaaac

4801 ttttatattt atgtgtctta tttttatatt tctttattta ttacacagtg tagtgtataa

4861 tactgtagtt tgtattaata caataatata ttttagtatg aaaatttgga aagttgataa
4921 gatttaaagt agagatgcaa ttggttctcc tgcattgaga tttgatttaacagtgttatg
4981 ttaacattta tacttgcctt ggactgtaga acagaactta aatgggaatg tattagtttt
5041 acaactacaa tcaagtcatt ttacctttac ccagttttta atataaaact taaattttga
5101 aattcactgt gtgactaata gcatgatgct ctgcagtttt attaagaaat cagcctaacc
5161 atacaactct catttcctta gtaagccaaa ttaggattaa cttctataaa cagtgttggg
5221 aacaatgttt aacattttgt gccaatttgt tcctgtattc atgtatgtaa gttacagatc
5281 tgactcttca tttttaagtt ccttgttaca tcatggtcat tttctagttt tttaccagac
5341 tcccatctca caataaaatg catcaacaag cctgaactgc tgtcattctt ttcatcatta
5401 tcagtatttt ctttggaaaa ctgtgaaatg gggtacattg tcatcctgca tttgattcat
5461 cttgagctga atttgggtaa cactaaatgt tttagacatt ctccactaaa ttatggattt
5521 tcttgtggct aaatgtttct ggagaggtca gagttgacaa aacctcttca caggttgctc
5581 cttcttcctg aaatccttaa tcctccgcat ttcatgcttc aggtcatttc agggaagcct
5641 gggtttagat gcctttctga ctctcagctc ctgcacttct gtcatcatac ctctgatact
5701 attatttata ttccttcccc actaggaaca ggaaccacat ttgtcatagt cactctcaca
5761 ttcctcactg cctaacaggg tgcctggcat aagttgggac aacagatatt tgttgaataa
5821 aaatataatt tgcatgttta tggagctcag ctatgttctc actttttttg cttctaattc
5881 cagaatatat gttaaatgat ctaataattt gattattttc ttataagtct tattaaacac
5941 tagtcataat agacacaata aattatgcct tctttttcta ttgccttaaa **aaaaaaaa 3′**

Appendix 1: Sequence of the 3’ UTR of human ZEB1/TCF8. Area shaded in yellow depicts the location of 3’ UTR of human ZEB1/TCF8. Sequences in red are binding sites for miR-200c while the sequence in green is complementary to the 5’ miR-150*.